2014

Multifunctional and Responsive Polyelectrolyte Nanostructures

Astha Malhotra
University of Central Florida

MULTIFUNCTIONAL AND RESPONSIVE POLYELECTROLYTE NANOSTRUCTURES

by

ASTHA MALHOTRA
B.S.: University of Delhi, 2005

A dissertation submitted in partial fulfillment of the requirements
for the degree of Doctor of Philosophy
in the Department of Chemistry
in the College of Sciences
at the University of Central Florida
Orlando, Florida

Fall Term
2014

Major Professor: Lei Zhai

ABSTRACT

A polyelectrolyte complex is formed by mixing two oppositely charged polyelectrolytes in a solution. The electrostatic interactions between partially charged polymeric chains lead to the formation of a stable complex while avoiding the use of covalent cross linkers. Since complex formation can improve the stability of polyelectrolyte and metal ions in polyelectrolyte can provide various functionalities, PECs incorporated with metal ions are promising candidates for manufacturing stable and multifunctional structures. While the coordination of metal ions and polyelectrolytes has been extensively investigated in solutions and multilayer films, to our knowledge, no research has been performed to study the effect of metal ion/polyelectrolyte interactions on PECs structures and properties. The following research demonstrates the impact of different metal ions in controlling PEC structure morphology and applications. These discoveries indicate great potential of metal ions in PECs to fabricate functional PEC nanostructures.

The research investigates the effect of the interactions between different metal ions and polyelectrolytes on the morphology and properties of PECs, explore the fabrication of different structures using embedded metal ions and understand the impact of metal ion/polyelectrolyte interactions on the nanoparticle structures. The research concludes: 1) incorporating metal ions of different valence into PECs introduces metal ion/polyelectrolyte interactions that can tune the morphology of PECs; 2) metal ion/polyelectrolyte interactions can be used to control the PECs swelling properties and stability in aqueous solutions; 3) the release of embedded metal ions

from PECs to aqueous solutions is affected by metal ion/polyelectrolyte interactions; and 4) the embedded metal ions function as a reagent reservoir for various applications to produce functional structures.

Dedicated to my loving family

ACKNOWLEDGMENTS

Words or expressions are not enough to thank my parents, back home for their patience and the sacrifices. Thank you Papa and mummy for your support and understanding; thank you Amit, Swati and Atharav for being there for me and encouraging me.

I am also extremely thankful to Dr. Lei Zhai for being my dissertation advisor. I do not have enough words to describe my respect and gratitude for him. His constant support towards my research and academics in general have improved me. I feel extremely thankful to have him as my mentor and supervisor.

I am also very grateful to Dr. Swadeshmukul Santra, Dr. Jingdong Ye, Dr. Dmitry Kolpashchikov, Dr. Karin Chumbimuni-Torres and Dr. Jiyu Fang for being part of my dissertation committee and for their encouraging and valuable comments and remarks.

I gratefully acknowledge the support provided by the department of Chemistry, Nanoscience and Technology Center (NSTC), and Advanced Materials Processing and Analysis Center (AMPAC).I am also thankful to Ernie, Michel, Kirk, Mikhail and Karen for their help in the usages of instrumentations.

I would also like to thank all my lab-mates Jean Calderon, Matthew McInnis, Joseph Zuyus, Chen Shen; my undergraduate researchers Joyce Thiesen and Natalie Joseph and the colleagues from collaborating labs. It was a pleasure working with them especially Jean who has been very helpful in several occasions. I am also very grateful to Usha Lal for her caring and helping nature had been a great encouragement.

I also express my deepest appreciation to Tanmay for supporting me relentlessly in all these years. I am also immensely thankful to my friends who helped my stay here more enjoyable and my friends in India and around whose encouragement has really been a great support to me here in a foreign land.

I would also like to express my thanks and sincere regards to everyone else whose help, encouragement and prayers must have strengthened me and helped me achieve things in life.

TABLE OF CONTENTS

LIST OF FIGURES:

LIST OF TABLES:

LIST OF ABBREVIATIONS:

CDs: Cyclodextrins

CS: Chitosan

CeNPs: Ceria nanoparticles

ECM: Extracellular matrix

H_2O_2: Hydrogen peroxide

Hap: Hydroxyapatite

NPs: Nanoparticles

MPECs: Metal ion loaded polyelectrolyte complexes

PAA: Polyacrylic acid

PAH: Polyallylamine hydrochloride

PCFs: Polyelectrolyte complex fibers

PDDAC: poly diallyldimethyl ammonium chloride

PE: Polyelectrolyte

PECs: Polyelectrolyte complexes

PPy: Polypyrrole

PSS: Polystyrene sulfonate

PVA: Polyvinyl alcohol

ROS: Reactive oxygen species

SBF: Simulated body fluids

SEM: Scanning electron microscope

CHAPTER 1: INTRODUCTION

1.1 Polyelectrolytes:

Polyelectrolytes are charged polymers with repetitive charge bearing units. The basic architecture of a polyelectrolyte contains a polymeric backbone that carries repetitive units of charge bearing functional group(s). It is these functional groups that dissociate in polar solvents like water to give either positive or negative charge. Polyelectrolytes can be classified as natural (e.g. DNA, proteins or enzymes), natural derived (e.g. cellulose, alginin, heparin, pectin, chitosan (CS), etc.) and synthetic (e.g. poly allylamine hydrochloride (PAH), poly styrene sulfonate (PSS), poly acrylic acid (PAA), poly diallyldimethyl ammonium chloride (PDDAC), etc.).

Molecular structures of some common polyelectrolytes are given in **Figure 1.**Polyelectrolytes have a non-zero charge at near neutral pH and can be divided into polyanions, polycations and polyampholytes, depending on the nature of the charge. The PAH, CS and PDDAC are examples of cationic polyelectrolytes due to the positively charged amine terminals and PAA and PSS anionic due to their negative charged carboxyl and sulfate terminals. Polyelectrolytes that contain both positive and negative charges are not uncommon and are termed as polyampholytes. A special type of polyampholytes that contain both positive and negative terminals in the each repetitive unit has been termed as polybetaines, which are rather rare and are usually synthetic in nature.

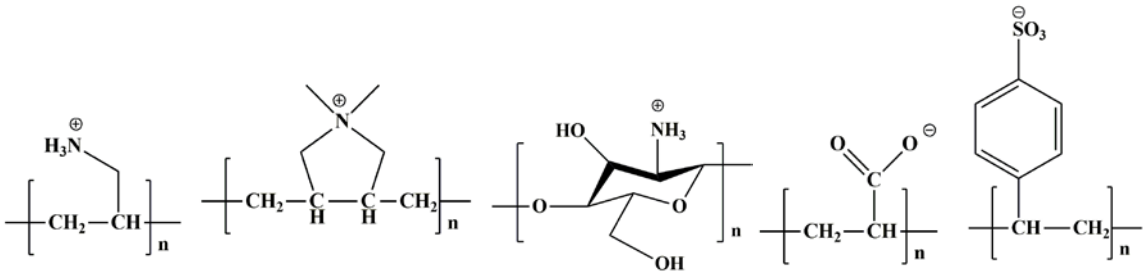

(a) (b) (c) (d) (e)

Figure 1: Molecular structures of common polyelectrolytes: (a) PAH, (b) PDDAC, (c) CS, (d) PAA and (e) PSS. PAA and CS were used in this study.

The dissociation of the functional groups plays a more critical role in the properties and applications of the polyelectrolytes. Polyelectrolytes are classified as week or strong polyelectrolytes on the basis of their dissociation constants. The polyelectrolytes bearing the functional groups that dissociate extensively and are not dependent on the pH of the solution is known as strong polyelectrolytes, similar to a strong acid or base. These polyelectrolytes remain highly charged in most conditions and their surface charge is not easily altered. The PDDAC is good example for strong polyelectrolyte as its quaternary amine bearing functional group retained its positive charge over a wide range of pH. Similarly, PSS is a strong anionic polyelectrolyte. The weak polyelectrolytes on the other hand, have functional groups whose dissociation is pH dependent. Their surface charges can easily be controlled by altering the solution pH and are more amiable to electrostatic tailoring. PAH and CS are weak polyelectrolytes due to the primary amine which is positively charged only at acidic pH (by accepting a proton). The PAA is also weak polyelectrolyte that is ionized only at basic pH when the carboxyl group loses a photon. Likewise to the acids and bases, the pKa plays a critical role in the ionization of weak polyelectrolytes and hence their properties and applications. Presence

of these ionizable groups makes weak polyelectrolytes sensitive to change in environment like pH, ionic strength, electric field and temperature.

Their molecular architecture and nature & extent of charge play an important role in the overall molecular structure and properties of polyelectrolyte. Interestingly, it is the interplay between the electrostatic forces arising from the charged terminal functional groups and the steric effects from the hydrophobic nature of the polymeric backbone that eventually determines the final conformation of these molecules. The conformation of these molecules is inherently linked to their functions. Therefore, in nature this simple principle of polyelectrolyte dissociation and molecular architectures is used to create a vast array of biomolecules. Yet each of them is distinct and different from the other, as it has evolved to function only at a particular environmental condition such as pH or ionic concentrations. The DNA is great example of biological polyelectrolyte that also has complex molecular architecture. Essentially, it has a backbone of phosphate-pentose sugar bearing repetitive units of bases as the functional moiety. Instead of one kind of repetitive functional groups in simple polyelectrolytes, there are four bases in this case, to increase the randomness. The relatively strong nature of dissociations of these bases, along with their specificity of bonding allows the two strands to form a intermolecular complex through hydrogen bonding that eventually results the double helix structure of the DNA. It is the polyelectrolyte nature of each strand that allows them to unzip into two (or zip back) as and when required. This reversible nature is critical for all functions of DNA in any living organism. Like DNA, proteins also function in a similar fashion. In this case too, the balance between the electrostatic forces from the dissociated functional groups of the polyamino acids and the steric forces leads to their final conformations and dictates their functionality. This

protects the active parts or motifs of the molecules and them functional only at a particular condition. At this point it is also noteworthy that the final or quaternary conformation of these biomolecules is a hierarchical structure. This is gradually built upon through simpler primary, secondary and tertiary structures that are formed due to inter- and intra- molecular complexes. The charged functional groups of the polyelectrolytes behave like sticky ends that tend to bind to oppositely charged groups either from the same molecule (intra-molecular) or from neighboring molecules (inter-molecular) forming polyelectrolyte complexes (PECs). This is especially evident for polyelectrolytes with complex molecular structures and/or in highly ionic medium such as buffers.

1.2 Polyelectrolyte complexes:

The importance of polyelectrolytes is often attributed to their ability to form complexes. Several forms and types of polyelectrolyte complexes (PECs) have now been identified in the natural world and we are only beginning to understand their molecular mechanisms. The electrostatic/columbic forces from the charged terminal groups are fundamentally responsible for the complex formation [1-4]. Strong polyelectrolytes having a high charge density generally form insoluble complexes. Similarly, high molecular weights and stoichiometry lead to insoluble and highly aggregated complexes[5]. However, water soluble polyelectrolyte complexes also known as “quasi-soluble” can be formed from weak polyelectrolytes and/or with huge difference in size by mixing in non-stoichiometric ratios.

The dynamic nature of the equilibrium makes PECs versatile in both structure and properties. Simple and small changes in the systems can lead to great thermodynamic alterations in the system, resulting significant variation in its properties. Weak polyelectrolytes are generally more sensitive to the environmental changes and hence are more suitable for applications. Most naturally occurring and naturally derived polyelectrolytes are also weak polyelectrolytes such as amino acids, chitosan, hyaluronic acid, alginin, polysaccharides etc., except for DNA and RNA which are strong polyelectrolytes. By choosing appropriate polyelectrolyte, polyelectrolyte complexes are stable, well tolerated, biocompatible and are more sensitive to changes in environmental conditions**.** The electrostatic interactions between partially charged polymeric chains lead to the formation of a stable polymer hydrogel network while avoiding the use of covalent crosslinkers [6, 7]. Such tunable variations in properties make them suitable for a wide range of applications.

Complex formation can be studied based on the variations in the physicochemical properties (viscosity, pH, and conductivity) of the complex, thus evaluating the complexation reaction. The complexation can be studied in terms of charge neutralization and can be monitored by viscometry, with change in viscosity corresponding to the complexation of one polyelectrolyte with the other. Other methods for monitoring complexation include potentiometry[8] or conductometry[9] with the variations in potential or conductivity corresponding to the presence and the nature of the free ions in solution.

The molecular interactions in PECs may occur at several levels. At the most fundamental level lays the electrostatic interactions between the functional groups and ions present in the environment. This leads to a molecular arrangement to accommodate the change in electrostatic forces due the intra- and inter- molecular conjugation. The steric forces re-configure their secondary structure that often distorts the polymer backbones. In the next level, the secondary structures interact with each other due to hydrophobic and residual electrostatic forces leading to aggregates of PECs that has spatial conformations and orientations. The structural hierarchy of the complexes may continue to escalate to higher levels till it achieves conformational symmetry. It is often a slow and gradual process that eventually seizes when a dynamic equilibrium is achieved. The exact molecular architecture of the poly complexes remains specific to the system, but can be controlled to obtain various shapes and sizes. Different structures can be obtained at different stages of complex by either self-assembly due to primary or secondary interactions or by fabrication[10].

1.3 Polyelectrolyte complex structures:

Hydrogels: A hydrogel is a network of hydrophilic polymers that can swell and hold a lot of water while maintaining their structures. Because of their significant water content, hydrogels possess a degree of flexibility very similar to natural tissue.[11-13] With such unique property, hydrogels have been extensively investigated, and significant progress has been made in designing, synthesizing and employing them in applications such as tissue engineering scaffolds,[11-20] controlled release,[21-23] biomolecular encapsulation, [21, 24, 25] sensing[26-32], nanoparticle synthesis,[29, 33, 34] and molecular imprinting,[35, 36] where facilitating the transport of active materials such as nutrients, ions and drugs are crucial. The kinetics of

swelling and de-swelling of the polymeric components which limits the ion diffusion coefficient ranges from 0.8×10^{-7} to 8×10^{-7} cm^2/s.[37] Therefore, the most significant challenge to make efficient hydrogel devices is the slow response related to low diffusion coefficient. Because hydrogel swelling kinetics are inversely proportional to the square of the dimension,[37] hydrogel fibers with reduced size and larger surface area offer more efficient material transport and faster response than hydrogels.

Nanofibers: Nanofibers are defined as fibers with diameters less than 100 nanometers. Nanofibers have large surface area and are better candidates as a supporting matrix for nanoparticle synthesis. Additionally, these fibers offer the advantages of tunable properties as compared to films. These fibers combine the properties of hydrogel with high surface area [38] [39-45]and smaller size and have been used for a lot of applications like drug delivery, tissue engineering etc. But their use as supporting matrix for nanoparticle synthesis has not been exploited much. There are evidences that polyanion/polycations have similar properties as of extracellular matrix (ECM) of cells and nanofibers resemble the components of ECM and affect the cellular activity because of their nanometer size and geometrical reasons [45]. Cells are able to organize around, attach and proliferate on these fibers as the scaffolds formed of such nanofibers are smaller than the size of the cell [46-49]. Moreover, the bio and cytocompatibility of these fibers can also be modulated through post synthesis modification.

Nanofibers have applications in medicine[50], including artificial organ components[19, 41], tissue engineering[51, 52], implant material, drug delivery[39, 41], wound dressing[53], and bioseparation [54]. Filtration system applications include air, oil, fuel filters for automotive and filters for beverage, pharmacy, medical applications. Energy applications include capacitors[55], Li-ion batteries, electrodes[56], photovoltaic cells, membrane fuel cells[57], and dye-sensitized

solar cells[58]. Other applications include piezoelectric fibers, catalysis [59, 60], air/water purification [61-63].

Among the three common ways of synthesizing fibers: self-assembly, electrospinning and phase separation, electrospinning is the most versatile, simple and cost effective technique. A vast number of polymers can be electrospun into fibers through this technique[38, 39, 43, 44, 48, 51, 53, 57, 58, 64-84]. Briefly, the fibers are fabricated by applying high voltage to polymer solution. As the field strength passes the critical value to overcome surface tension of the polymer solution, a cone-like meniscus is formed (**Figure 2**). From this meniscus, a jet of solution is emitted whose diameter decreases as it approaches the collector electrode, with the evaporation of solvent, leading to the formation of fibers at the collector electrode. The spinning of fibers from polymer solution is controlled by lot of variables: solution properties, instrument parameters and ambient parameters. Solution properties like viscosity[85], conductivity, solubility, molecular weight of the polymer, surface tension, and dipole strength all affect the spinning process. The controllable instrumental parameters are: flow rate of the solution, the distance between the tip of the needle and the collector electrode, field strength, tip design and collector. Environmental (ambient) parameters are temperature and humidity. While spinning fibers, all these parameters need to be optimized for particular polymer to achieve the desired size and morphology of the fibers and their applications[68].

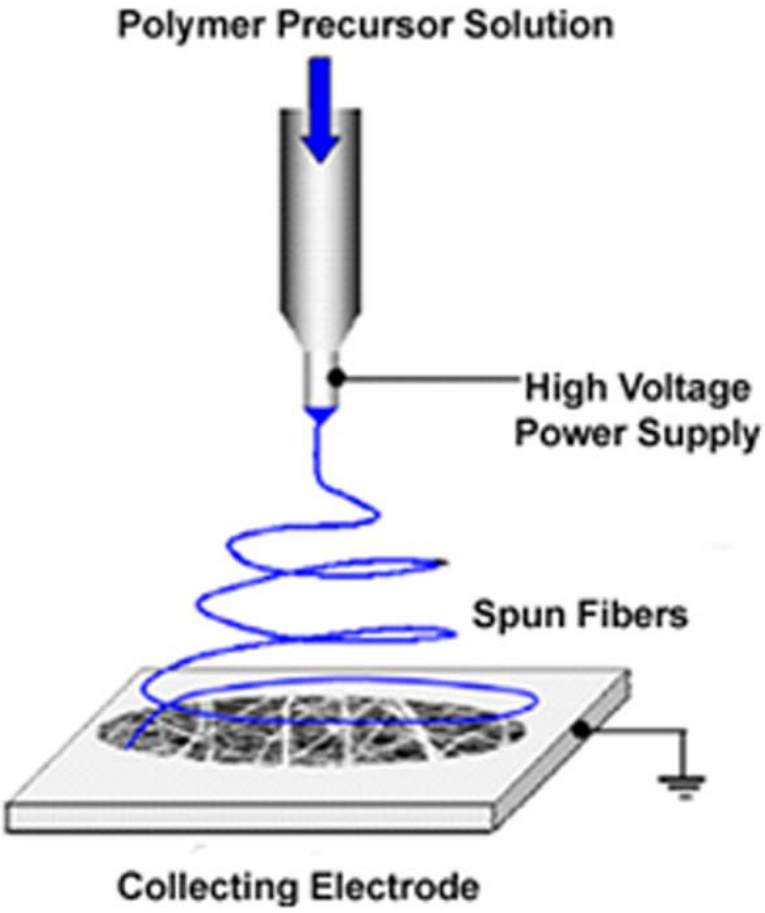

Figure 2: A schematic illustrating the electrospinning phenomenon.

Electrospun polymer fibers though are promising templates to host nanoparticles, functional groups and cross-linking is required for nanoparticle attachment and to obtain stable fibers. These post synthesis modifications can also be of great use for improving the bio and cytocompatibility of these fibers[19]. Post synthesis cross-linking is required to modulate mechanical properties of fibers and make them insoluble in different pH media[86, 87]. Since, electrospinning process requires the fibers to be in liquid phase, cross-linking is done post synthesis. With appropriate functional chemistry, the fibers can be chemically cross-linked by

water based covalent linking. Amine and /or carboxyl groups of the fibers can be utilized for this using carboiimide crosslinkers such as 1-ethyl -3-[3-dimethylaminopropyl] carbodiimide hydrochloride (EDC), leading to amide bond formation. It is difficult to control the cross link density of the fibers using chemical cross-linking. Also, the unreacted cross linkers or chemical initiators or activators can leach and could be toxic for biomedical applications. Thermal[88] and radiation [89] are two other methods for nanofiber cross-linking.

1.4 Applications of polyelectrolyte complexes:

The prospect of tunable properties of the PECs makes them suitable for a wide range of applications the following are some of the most significant and widely used.

1.4.1 Wound healing: Wound healing is a sequential biological process which the government to showcase excepts the whole process of wound healing is usually divided into the four following sequential biological events to which the dominant issue here is itself the whole process of wound healing is usually decided is usually divided into four following sequential biological events: Hemostasis, inflammation, proliferation, maturation and remodeling[90]. As explained above it is primarily in the first two stages that external help is needed to contain and manage the wound healing process the exact nature and needs of this assistance depends on the nature and type of forms.

Although, inflammation is a part of healing process, several reactive oxygen species (ROS) are generated in the process. High concentrations of free radicals from ROS is damaging to cells, causing oxidative modification of biomolecules including nucleic acids, proteins, carbohydrates

and lipids. Oxidative stress has been implicated in various conditions including neurodegenerative diseases, autoimmune diseases and cancer.

Hydrogen peroxide (H_2O_2) is one of the known reactive oxygen species (ROS) together with other reactive molecules such as superoxide radical, hydroxyl radical and nitric oxide. Hydrogen peroxide, reactive oxygen specie, is most commonly associated with oxidative stress causing cytotoxic effects on living cells. It is produced both intracellularly and extracellularly in association with oxidative stress when the normal redox state of a cell is disturbed. It is generated response to various stimuli including cytokines and growth factors. In addition H_2O_2 is produced as a defense mechanism against pathogens, as being released by activated phagocytes. Hydrogen peroxide is also continuously generated under normal physiological conditions, being an inevitable by-product of the aerobic respiration process in cells there are different mechanisms by which $H_2O_2$is generated, facilitating signal transduction in cells; through NOX-system in mitochondria, via singlet oxygen, receptor/ligand interaction or by redox active metal ions.

Both inflammation and infections impair wound healings. In certain situations, like diabetes, they can further cause complications. Therefore, wound dressings with intrinsic antioxidant and antibacterial properties would result in faster recovery of the wound. This is of extreme importance for patients with compromised immune system.

1.4.2 Tissue Engineering: It is a broad area of biomedical research that aims at artificial reconstruction of tissue either completely or partially in a controlled environment. The whole process usually consists of re-creating a matrix similar to the ECM, seeding the cells into it and integrating the whole system together to reconstruct the tissue system.

Polyelectrolytes are often used for these applications for their biocompatibility and functional the chemical, morphological, mechanical and functional properties can easily be controlled by altering the processing nanometers and therefore can be tailored suitably to match the physical, and chemical properties of the ECM. The CS based PECs have found extensive applications in this area primarily due to their biocompatibility. Moreover the NH_2 group allows additional functionalities to be attached to the complex the attachment could be through simple electrostatic interactions or through hydrogen bonding or even through covalent linkage. This gives tremendous control over not just the morphology but also the chemical functionality of the structure which eventually helps to reconstruct the ECM as desired for a particular tissue engineering application.

1.4.3 Antimicrobial applications: Microbial pathogens are one of the biggest menaces to public health and safety the other causes of simple infections to an outbreak of epidemic. In order to maintain the public hygiene, several antibiotic reagents are used every day. Reagents such as alcohols are inexpensive but to the evaporate easily and can be toxic to human helped specially designed antibiotics are more potent for applications but are expensive and can often be placed in harsh conditions moreover these variations are not useful for recording surfaces to keep them sterile.

PECs based on chitosan on the other hand are known for their antimicrobial properties. These PECs have a high density of positive charge amine groups that are known to bind aggressively with the bacterial cell wall and degrade them eventually. CS based PECs being the light from crustaceans that evolved unmatchable microbial resistance retains this chemical property that makes them both antimicrobial and biocompatible at the same time. This advantage has been explored by many researchers in order to construct PECs for antimicrobial applications. Adding

antimicrobial agents such as antibiotic drug molecules can easily be incorporated into the polyelectrolytes tube radius chemical linkages the antimicrobial and thus formed can be applied in various forms such as nanoparticles or nanorods, fibers, emulsions, thin films and hydrogels for a wide range of applications.

1.4.4 Desalination and purification of water: Other than biomedical applications the PEC can also be used for other technological forms such as desalination and water purification. The applications of water purification's use diverse strategies which has different goals. The natural inability of binding bacterial cell walls to electrostatic interactions is exploited to remove pathogens from water. The amine-based functional groups in many polyelectrolytes are often used to correlate and precipitate out heavy metal lines. Similar principles are also used for dissemination of water. The amphiphilic nature of polyelectrolyte makes them excellent emulsifiers. This strategy is simple and effective and efficient because the polyelectrolytes can easily be recovered by changing the conditions such as pH or temperature that dismantles the PEC's. This program technique provides for the bondage of the CDs of polyelectrolytes and their complexes can be synthetic and designed are specifically constructed to remove each of the impurities. Then there they provide a whole spectrum of species that can be used in a simple and effective and convenient manner for water purification and similar technologies.

1.4.5 Actuators and electro-active hydrogels: The applications mentioned so far mostly emphasize and exploit the electrostatic charges produced into the dissociation of the functional groups in the polyelectrolytes. When combined with their stearic properties, the PEC can be used for their viscoelastic properties as well. Such PECs are often known as smart gels that change their shape, structure in response to the external stimuli hence also known as stimuli-, viscoelastic properties values as artificial muscles, which contracted and expanded in response to

the pH and electrical field, giving rise to the concept of stimuli responsive soft matters.

The PECs that response to the externally applied electrical field are referred as electroactive actuators. The charged functional groups produce dipole moments in a polar solvent. These dipoles reorganize themselves under the electric field which eventually leads to the rearrangement of the molecular structure. This manifests itself in a simple 3D structure as a swelling or shrinking behavior. The exact swelling or shrinking behavior depends on the structure, morphology and architecture of the complex; nature of electrical field; functional groups and other parameters like electrolytes.

Most of the early works are on PAA-Na based PECs which formed 3D hydrogels. Later studies were conducted using thin films and fibers which behaved in different manners. In more recent studies highly ionic media, high dielectric functional groups were incorporated into the PEC structures to enhance the viscoelastic properties. In more complicated systems PMACo and/or piezoelectric nanoparticles are incorporated into the PEC resulting into a hydrogel of heterogeneous viscoelastic domains. Such responsiveness would also be achieved for stimuli such as UV and heat radiation. The azo based functional groups (-N=N-) and their modifications are used for the UV responsiveness. The PANI based PECs are used for the heat stimulated applications.

They are now finding increasing applications in many forms of engineering. Electrically activated PAA based gels that used for artificial membranes more biocompatible biopolymers-anchoring sulfate proteoglycans that used for controlled drug delivery systems. The PAA based hydrogels have been made to contract and expand in response to pH and electrical field. The tensile forces generated during this time is similar in magnitude to that of biological muscles,

hence they were termed as artificial muscles. Well cross-linked PVA-PAA based PECs are also used to make actuators that makes the mechanical movement like a fingers in the hand or to able to propel themselves like a movement of a fish. They have been used in soft robotic applications or in artificial heart valves where mechanical actuation is necessary.

1.5 Metal-polyelectrolyte interaction and role of metal ions in PEC formation

Metal ions play essential roles in human body as cofactors, minerals and in enzymes & polypeptides providing structural (zinc fingers) and functional (hemoglobin). Role of metals in biological world for structure stability, catalysis, biomineralization etc. in self-assembly, adhesion and strength has been evident in studies [91-97]. The function of metal ions is in the binding and orienting the molecules and they can take part in redox reactions if the metal is multivalent. The metal ions also take part in complex formation in nature, for example, calcium ions mediates the bridging listerial protein internalin (InlA) of *Listeria monocytogenes*, a food-borne bacterial pathogen and host cell receptor E-cadherin (hEC1).

Metal ions are electrophiles and bind to ligands by coordinate bond or electrostatic interaction. Multivalent metal ions can accommodate many ligands around them at the same time. Binding to the ligand is through the functional groups present on ligands. Some of the common functional groups binding with metal ions are carboxylates, amines, sulphonates, etc. Carboxylates are the most common and well-studied of all the functional groups. Carboxylate ions are far more stable than their free acid counterparts due to the resonance stabilized carboxylate anion. The carboxylate groups of aspartate and glutamate side chains in proteins are a common site for the

binding of a metal ion. Metal ions can form four different types of complexes with carboxylates: ionic, monodentate, bidentate, bidentate bridging.

Metal ions can be incorporated in polyelectrolyte complexes by the functional groups present on the polyelectrolytes. While the coordination of metal ions (monovalent and some divalent) and polyelectrolytes has been investigated in solutions [9, 98-102] and multilayer films, [103-105] to our knowledge, no research has been performed to study the effect of metal ion-polyelectrolyte interactions in PECs on PCF structures and properties. However, not much understanding has been obtained on the formation of complex between two oppositely charged polyelectrolytes and the effect of different salts on the formation of these complexes.

Thus, the goal of this research is to design bioinspired biomimetic metal ion coordinated polyelectrolyte complex nanostructures for various applications.

1.6 Theme of the research:

This dissertation research is focused on the fabrication of different nanostructures from MPECS of nanomaterials towards their diverse applications. Different structures like gels, films and fibers are fabricated from these complexes. Later, their structure and properties are tuned by various surface treatments (covalent and non-covalent functionalization of the surface) to accomplish desired applications. Surface is functionalized by interfacial reactions exploiting the diffusion properties of the structures. The main theme of this research work is to understand interactions between two polyelectrolytes resulting in complex formation and the effect of metal ions on them.

The research includes 1) studying the effect of different metal ions-polyelectrolyte interactions on the complex formation by properties of complex solutions such as viscosity and conductivity, and structure/morphology of PECs, 2) investigating the stability and swelling properties of PEC structures with different metal ions and the diffusion of different metal ions from PECs, 3) functionalization of PCFs using embedded metal ions.

Chapter 3 focuses on the complex formation between PAA and chitosan in the presence of different metal ions. Complex formation was followed by viscosity studies and IR. Based on the observations, a model for complex formation is proposed.

In **Chapter 4** gels are obtained from polyelectrolyte complexes by room temperature crosslinking, thermal treatment and pH change. The swelling and stability of gels in different mediums were also monitored. The morphology of the gels and functionalized gels was studied by SEM.

Chapter 5 focuses on electrospinning of polyelectrolyte complexes. The effect of metal ion on the morphology of electrospun nanostructures was studied. Additionally the effect of other parameters like polymer concentration, voltage etc., was also studied. Nanofabrication of fiber surface through interfacial reactions using the fibers as controlled reservoir of metal ions was also performed.

The focus of **Chapter 6** is the diffusion of molecules across the complex structures. The role of metal ions, crosslinking and dimension was examined.

The potential of structures obtained in previous chapters in different applications was investigated in **Chapter 7**. The gels and fibers show immense potential in biomedical applications.

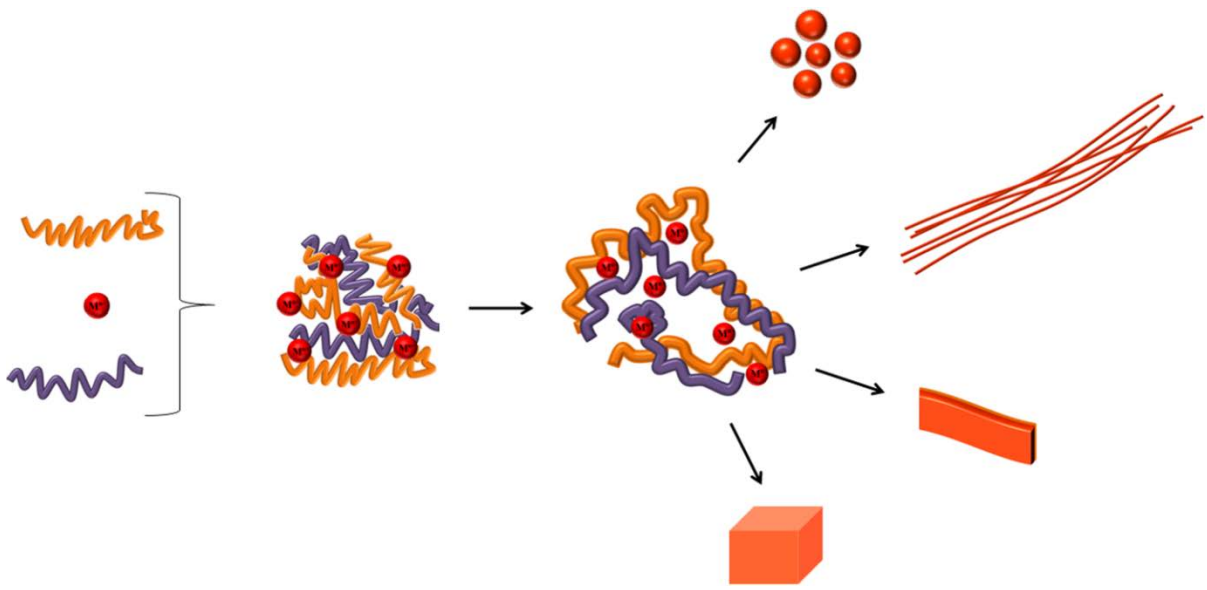

Figure 3: Different dimensional morphologies using metal ion cross linked polyelectrolyte complexes.

CHAPTER 2: EXPERIMENTAL

2.1 PEC formation and characterization:

Preparation of polyelectrolyte complexes: Homogeneous solutions of PAA-CS of varying compositions were prepared. The compositions were varied on the basis of total polymer concentration and PAA: CS ratio. PAA-CS solutions with metal salts were prepared by adding respective metal salt in appropriate concentration. The interaction between the polyelectrolyte complex and metal ions were studied by infrared spectroscopy.

2.2 Gel formation and characterization:

PAA-Cs complexes were allowed to gel at room temperature. The effect of complex composition was (PAA:CS ratio, metal ion, and metal ion concentration) was studied. For temperature dependent gelation, complex solutions were heated to desired temperatures and metal ions were added to it while allowing the solution to stir. Gel formation was followed by viscosity studies.

2.3 Electrospinning of solutions and characterization of nanostructures:

Homogeneous solutions of PAA-CS of varying compositions were prepared. The compositions were varied on the basis of total polymer concentration and PAA: CS ratio. PAA-CS solutions with metal salts were prepared by adding respective metal salt in appropriate concentration. For electrospinning, briefly, 10 mL of respective complex solution was loaded into the syringe with a metal needle, and the needle was connected to a high-voltage power supply. The solution was pumped continuously supplied using a syringe pump. The grounded aluminum foil placed at 27 cm distance was used as collector. All electrospinning was conducted at room temperature. For

characterization purposes, nanostructures were analyzed for structure and morphology with IR, TEM and SEM. TEM and SEM samples were prepared by placing carbon coated copper grids (400 mesh size) and silicon wafers, respectively, directly on the aluminum foil. SEM and TEM images were taken on Zeiss Ultra 55 and JEOL 1011 instrument, respectively.

2.4 Swelling and degradation studies:

In order to examine the swelling ratio of PEC structures the samples with different compositions were weighed and incubated in PBS buffer and different pH solutions at 37°C. The swelling was calculated as the ratio between the weight of the swollen sample and the weight of the dry sample.

Swelling ratio (%) = $(W_s - W_d)/W_d \times 100$

where W_s and W_d are weight of swollen and dry fibers, respectively.

2.5 Nanofabrication/ Functionalization:

2.5.1 Reduction (metal nanoparticles): Ferric ion loaded PAA-CS structures were obtained by electrospinning a homogeneous aqueous solution of PAA-CS (10:1) and 3.57wt% (w.r.t. to polymer wt.) ferric chloride hexahydrate. The fibers were heated overnight at 140°C to obtain sufficient cross-linking. The production of iron nanoparticles in PAA-CS structures was accomplished by subsequently immersing ferric ion loaded PAA-CS fibers in 0.1 M sodium borohydride solution to generate iron nanoparticles in the matrix. The fibers were thoroughly washed with deionized water after each soaking to remove unbound and unreacted metal salt and reducing agent.

2.5.2 Hydrolysis (metal oxide nanoparticles): Cerium ion loaded PAA-CS fibers were heated overnight at 140°C and subsequently treated with 10% ammonium hydroxide solution to produce ceria nanoparticles in the fiber.

2.5.3 Polymerization: PAA-CS fibers loaded with ferric ions were incubated in a solution of 7.0mM pyrrole at 4°C for 24 hrs, where ferric ions in fibers diffused toward the fiber surface and initiated the polymerization of pyrrole.

2.5.4 Biomimetic mineralization: Hydroxyapatite mineralized PAA-CS fibers were obtained by incubating cross linked PAA-CS fibers loaded with calcium ions in serum body fluid at 37°C.

2.6 Diffusion studies:

To perform the diffusion studies across the MPECs, MPECs with preloaded ions were immersed in 0.01 M Arsenazo III solution to form highly colored complexes with metal ions. The formation of the complex was monitored through UV-Vis spectroscopy and the uptake of dye and diffusion of ions across the fibers was studied.

2.7 Biodegradation studies of MPEC structures:

The in vitro degradation of the scaffolds was investigated in phosphate buffered saline (PBS, pH 7.4) and Lysozyme solution (1 mg/mL, pH7.4). The initial weight of the fibers was recorded, and fibers were incubated in PBS and Lysozyme solution at 37°C while continuous shaking, for a period of 6-8 weeks. The fibers were removed from the medium at different time intervals (every

week), rinsed with DI water and then dried. The dried fibers were weighed and compared with the initial weight of the fibers, for the loss of the mass due to degradation.

2.8 Antioxidant studies of ceria nanoparticle loaded scaffolds (with and without cells):

For antioxidant studies, H_2O_2 was used as ROS and Amplex red assay was performed to measure H_2O_2 levels. Amplex Red reagent reacts with H_2O_2 in the presence of horse raddish peroxidase to form resorufin, a fluorophore with excitation and emission at 520 and 590 nm, respectively. Fresh working solutions of Amplex Red (100μM) and HRP (0.2 units/mL) were prepared for each experiment. The antioxidant capacity of the scaffolds (with and without cells) was examined by adding different concentrations of hydrogen peroxide and then read with InfiniteM1000 plate reader (TECAN). Other scaffolds and Ceria nanoparticles in solution were also tested for their cell protecting abilities and to examine difference between the activities of ceria nanoparticles in two different environments.

2.9 Cell seeding and culture on PCFs:

Different cell lines (MG-63, HDF, C2C12, SHSYS5 and PC3) were routinely cultured in 75cm^2 flasks using Dulbecco's modified Eagles' medium (DMEM) supplemented with Ham's F12, 10% Foetal Bovine Serum (FBS)and 1% antibiotic/antimycotic, at 37°C in a humidified atmosphere with 5% CO_2. Cells were detached at 90% confluence, using trypsin-ethylenediaminetetraacetic acid (EDTA) and were seeded onto the respective sterilized scaffolds and incubated at 37°C, 5% CO_2.

2.10 Analysis of cell attachment and spreading:

After 24hrs, samples were washed in PBS and fixed in paraformaldehyde (4% w/v in PBS) for 30 minutes, then rinsed in PBS and dehydrated through a series of graded ethanol (25%, 50%, 75%, 90%, 100%) in distilled water at 5 minute intervals. Finally the samples were sputter coated with palladium and imaged with ZEISS ultra55 SEM to reveal cell attachment and morphology.

2.11 Cell viability

The standard protocol for a commercially available cell assay was used to quantify cell viability (CellTiter 96®, Promega,). Briefly, samples were transferred to 96 well plates, and washed (1x) with phosphate buffered saline (PBS). Solution reagent from kit (120 µl) supplemented with 600µl of DMEM phenol free medium was added to each well. The samples were incubated for 60 minutes at 37°C, 5% CO2, after which the medium above the samples was removed and transferred to microplate reader.

CHAPTER 3: PAA- CS-M^{N+}COMPLEXES

3.1 Introduction:

Polyelectrolytes are charged polymers with an ionizable group on each repeating unit and interesting properties in solutions. Studies have been done on the behavior of polyelectrolytes in solutions and complex formation. Depending upon the nature, size, charge and stoichiometry of the polyelectrolytes, two oppositely charged polyelectrolytes can complex together resulting in variety of structures. By choosing appropriate polyelectrolyte, polyelectrolyte complexes are stable, well tolerated, biocompatible and are more sensitive to changes in environmental conditions **[73, 106-108].** In addition, the polyions in polyelectrolyte complex provide a rich chemical environment to host various molecules **[109].**

The complexes are formed by thermodynamically favorable and dynamic electrostatic interactions between two oppositely charged polyelectrolytes with release of corresponding counterions. Other interactions that may be involved in the process are hydrogen bonding, hydrophobic and Vander wall interactions depending on the environmental conditions. The polyanion/polycations complexes with new and diverse properties and applications are excellent models for understanding interactions and environments in many natural and synthetic materials with similar mechanisms. Some of the applications of these complexes are as tissue engineering scaffolds, encapsulation materials, flocculants, drug or gene delivery, matrices etc. However, not much understanding has been obtained on the formation of complex between two oppositely charged polyelectrolytes and the effect of different salts on the formation of these complexes.

PAA and CS are biocompatible and biodegradable polyelectrolytes with antimicrobial and metal chelating properties and providing functional groups. By combining both PAA and CS, the

system overcomes the disadvantages of both the natural (slow degradation, insufficient mechanical integrity) and synthetic polymers (biodegradation, biocompatibility, etc.).The complex formation between PAA and CS eliminates the need of cross-linking using glutaraldehyde or other cross-linking agents. The system exploits the affinity of both PAA [98, 99, 102, 110] and CS [101, 111-114] for metal ions. The incorporation of metal ions in the complex provided functionality [34, 104] to the system for various biomedical and material applications. Metal ions are also known to form strong crosslinks in aqueous environment.

We demonstrate here incorporation of a range of metals in polyelectrolyte complex to generate a library of functional polyelectrolyte complexes (MPECs). The ability to incorporate diverse metals into polyelectrolyte complexes provides new opportunities for engineering multifunctional systems for various applications. Complex formation was studied with and without metal ions. The complexes formed with metal ions were also compared with metal ion complexes with individual polyelectrolytes. Fifteen Different metal ions including sodium (Na), potassium (K), Lithium (Li),calcium (Ca), nickel (Ni), copper (Cu), zinc (Zn), manganese (Mn)magnesium (Mg), Cerium (Ce), aluminium (Al), vanadium (V), iron (Fe), Titanium (Ti) and zirconium (Zr) were introduced to study their effect on complex formation.

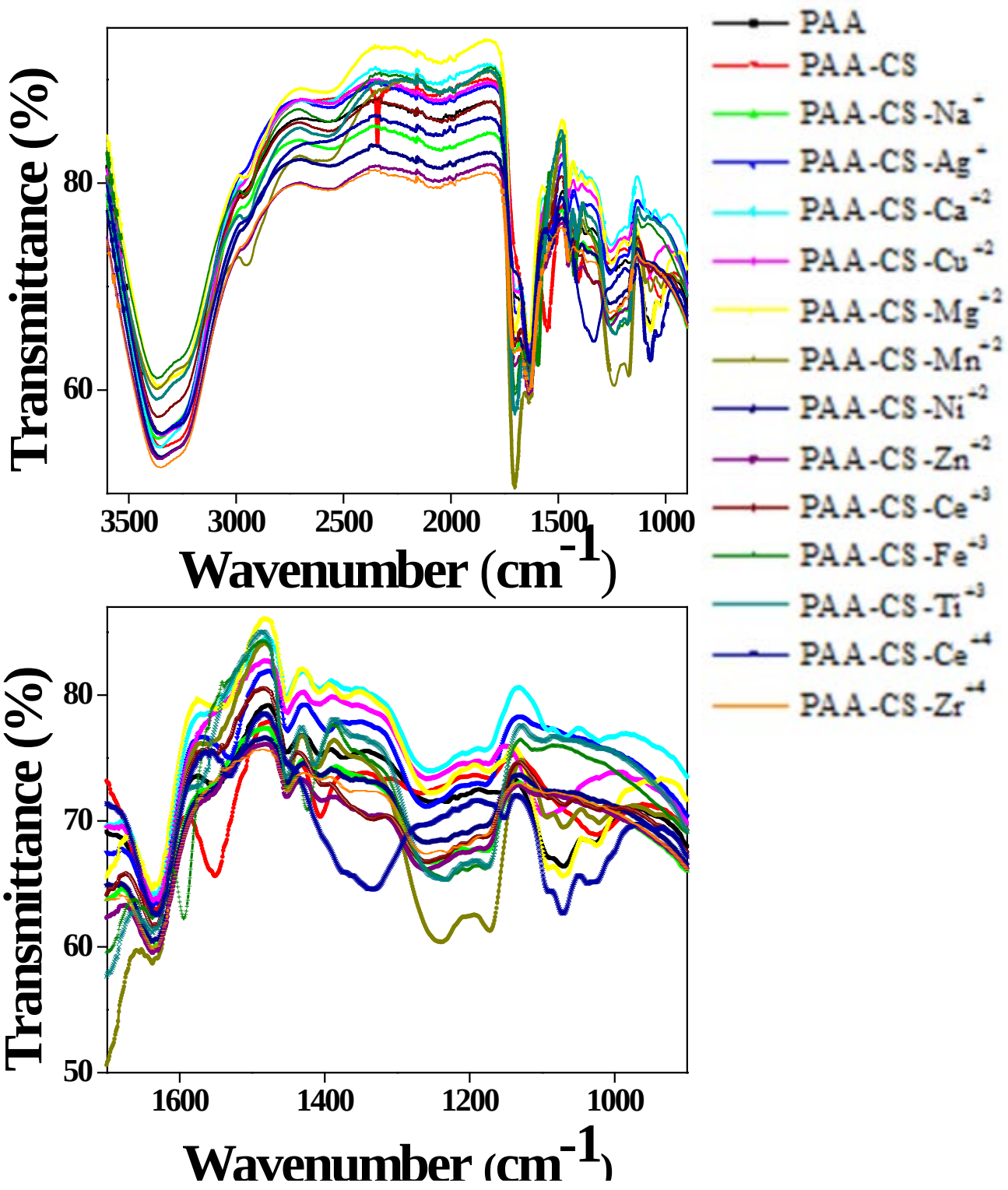

Figure 4: FT-IR spectra of the PAA, CS and their complexes in presence of various metal ions

3.2 PEC formation:

In general, mixing two polyelectrolytes with opposite charges at stoichiometric ratio leads to phase separation and precipitation. However, homogeneous and water soluble complexes can be formed at non-stoichiometric ratio, where concentration of one polyelectrolyte is much excess to the other. The complex formation is a thermodynamically favorable process where the driving force is the entropy decrease during the release of counter ion. The complex formation can take seconds to days to reach equilibrium depending upon the polyelectrolyte concentrations, characteristics, molar ratios, pH, salt concentration, etc. Here, the interactions between chitosan and PAA and their complex formation in the presence of different metal salts were studied and characterized. Functional polyelectrolyte complexes were obtained by incorporating a variety of metal ions into the PAA-CS complex. It was observed that complexes with different metal ions exhibited sol or gel state. The extent to which a liquid character is displayed depends on the charge density, on the nature (presence of hydrophobic groups) of the polyelectrolytes, and on the concentration and nature of ions present in the solution, which all influence the solubility of the components and the complex. **Table 1** presents complexes formed with different ions and their characteristics. It was observed that PAA-CS solutions with different metal ions have different properties and produce MPECs with different structure and morphology.

The difference the behavior of different salts can be attributed to their affinity towards PAA as evident in the IR spectra shown in **Figure 4**. The IR spectra of PAA-CS- metal ion complexes have a clear resemblance with the IR spectra of PAA-M^{n+} in literature [98, 99], indicating that the metal ions bind with PAA and not with chitosan. However, interaction between chitosan and PAA is also evident. Thus, presence of chitosan is necessary for structure stability. The

interaction of chitosan with PAA together with complexation of PAA with metal ions is critical for the structure and functionality. The interaction between different metal ions and carboxylic acids of PAA is different depending upon its charge to size ratio and presence of d orbitals. By assessing the shifts for symmetric and asymmetric stretching of carboxyl (v_{asCOO-} and v_{sCOO-}) the nature of complex formation between the metal cations and the carboxylate ions can be determined. The difference between the symmetric and asymmetric stretch for the carboxylate ion (Δv_{COO-}) suggests the bonding mode[115]. A difference of 105 – 140 cm^{-1} is associated with monodentate bonding, 145 – 185 cm^{-1} could be associated with bidentate chelate bonding and 180 – 200 cm^{-1} is an indication of bidentate bridging bonding[116]. The stretching of the carboxyl group at 1600 cm^{-1} (assymmetric) and 1400 cm^{-1}(symmetric) is dependent on the strength with which it is bound to the metal ion[110, 117]. The free carboxyl has a strong band in the 1735 cm^{-1}. With metal binding there is decrease or disappearance of free carboxyl and appearance of peaks at 1400-1450 cm^{-1}(v_s) and 1600-1500 cm^{-1}(V_{as}). The signal around 530 cm^{-1} and 3400 $cm^{-1}$is probably associated with the metal-N vibrations arising from the coordination of metal ions with nitrogen atoms of the chitosan macromolecules [118, 119].

It is evident from IR data that the metal ion-PAA interactions are more important than metal ion-CS interactions at low pH (~3) since metal ions have negligible interactions with ammonium presented in CS at low pH [111, 114] . While metal ions have negligible interaction with CS at low pH, the protonated amine groups will be deprotonated in aqueous solutions of higher pH. Thus, the function of CS is improving the complex stability is two-fold, forming electrostatic interactions with PAA and generating metal ion-CS interactions at increased pH. IR data suggests the binding constant of transition metals is much larger than earth alkaline and alkaline metals due to the coordination through d orbitals in transition metals. The non-transitional sodium and calcium

interactions with PAA are electrostatic in nature and do not bind strongly. Cerium, copper, zinc, manganese, magnesium, nickel forms bidentate binding, whereas ferric, titanium, aluminium and vanadium ions form bridging complex.

The effect of size to charge ratio on the complexation was also observed. Metal cations with larger size to charge ratio due to the low degree of strain energy associated with a complexed ligand and a large ion were observed to form bidentate complexes. The metal ions with low size to charge ratio attained a less strained bridged complex structure to stabilize larger structural deformation upon formation of a bidentate complex, straining the O-C-O bond angle of the carboxylate group.

Sodium and potassium ions being monovalent shield polyelectrolyte charges, causing shrinking of molecule chains and, decrease in hydrodynamic radius and viscosity. In addition to shielding effect divalent and multivalent ions can cross-link and interconnect the PAA chains influencing the conformation and interaction with chitosan. The cross-linking behavior becomes prominent with increase in valency and overshadows the shielding effect. Both intra chain and inter chain cross-linking takes place in this scenario. Therefore, titanium, vanadium, aluminium and ferric ions exhibit higher viscosities and gel formation than calcium ions.

In conclusion, coordinate of metal with polyelectrolyte complex offers a new intrinsic cross-linking mechanism providing control over complex properties.

Table 1: Complexes of PAA-CS with different metal ions: properties like sol/gel nature of the complex depend on the type of crosslinking of polyelectrolytes with ions. This interaction depends on size to charge ratio and presence of d orbitals.

composition	Sol/gel	Transparency	Ionic radii (pm)	Size to charge ratio	binding
PAA-CS	sol	transparent			
PAA-CS-Na^{+}	sol	transparent	116	116	electrostatic
PAA-CS-K^{+}	sol	transparent	152	152	electrostatic
PAA-CS-Li^{+}	sol	transparent	90	90	electrostatic
PAA-CS-Cu^{2+}	sol	transparent	87	43.5	bidentate
PAA-CS-Zn^{2+}	sol	transparent	88	44	bidentate
PAA-CS-Ni^{2+}	sol	transparent	83	41.5	bidentate
PAA-CS-Mn^{2+}	sol	transparent	81	40.5	bidentate
PAA-CS-Mg^{2+}	sol	transparent	86	43	bidentate
PAA-CS-Fe^{2+}	gel	opaque	75	37.5	bidentate
PAA-CS-Ca^{2+}	sol	transparent	114	57	electrostatic
PAA-CS-Ti^{3+}	gel	opaque	81	27	bridging
PAA-CS-Al^{3+}	gel	opaque	68	22.6	bridging
PAA-CS-Fe^{3+}	gel	opaque	69-	23	bridging
PAA-CS-Va^{3+}	gel	opaque	78	26	bridging
PAA-CS-Ce^{3+}	sol	semi -transparent	115	38.33	bidentate
PAA-CS-Ce^{4+}	sol	opaque	101	25.25	bidentate
PAA-CS-Zr^{4+}	sol	opaque	86	21.5	bidentate

To further understand the role of metal ions in the formation of MPEC formation, the PEC formation with and without metal ions was studied and monitored. A few metal ions (sodium, calcium, cerium, and ferric) were chosen as representative. Complex formation was studied by change in the viscosity of the polyelectrolyte solution upon the addition of metal ions, corresponding to the complete complex formation between two oppositely charged species. The change in the viscosity depended on the metal ion-polyelectrolyte interactions. All the viscosity studies are plotted against time due to the dynamic nature of the process.

3.2.1 Polymer concentration and stoichiometry: Formation of PECS can be monitored by rheological studies. Viscosity and conductivity are important solution parameters affecting electrospinning process too. Both viscosity and conductivity depends on the molar concentrations, pH etc. Viscosity of a polymer depends on its concentration and size. Viscosity of PAA-CS complex with different total polymer content is presented in **Figure 5**. It is known that addition of small amounts of an oppositely charged polyelectrolyte to a polyelectrolyte solution, results in a pronounced increase in viscosity as evident. The increase in total polymer also increases conductivity in a linear manner (**Figure 5**) due to increase in charge density and then get saturated at a concentration where addition of any more polymer does not have any effect on the conductivity because of complete screening of the complex by counter ions. The ratio between the two polyelectrolytes also affects the complex formation and viscosity of the system. The viscosity of the PAA-CS complex solution increased as more chitosan was added. The amount of chitosan in the 5:1 ratio, was too high resulting in the formation of a gel after the first day. The 10:1 ratio formed a gel on day 15. For complexes that did not form a gel, there is an observed spike in viscosity around day 10 and then a gradual decrease in the values. Higher viscosities at higher PAA: CS ratios can be attributed to the formation of non-stoichiometric complex associates (secondary structures). As the chitosan concentration further increases, solutions starts losing its homogeneity and phase separation, eventually precipitating out, does not contribute to the viscosity (decrease in viscosity), with an exponential increase subsequently, resulting in gel-like state. PAA:CS ratio solutions showed a decreasing linear relationship As the amount of Chitosan was increased the conductivity decreased giving the conclusion that PAA is a strong contributor to the values. This is because as more Chitosan is introduced NH_2 groups are converting to NH_3^+ groups limiting the amount of free protons in the complex. As expected the

conductivity decreases with increase in chitosan, as more and more counter ions are involved in screening the charge.

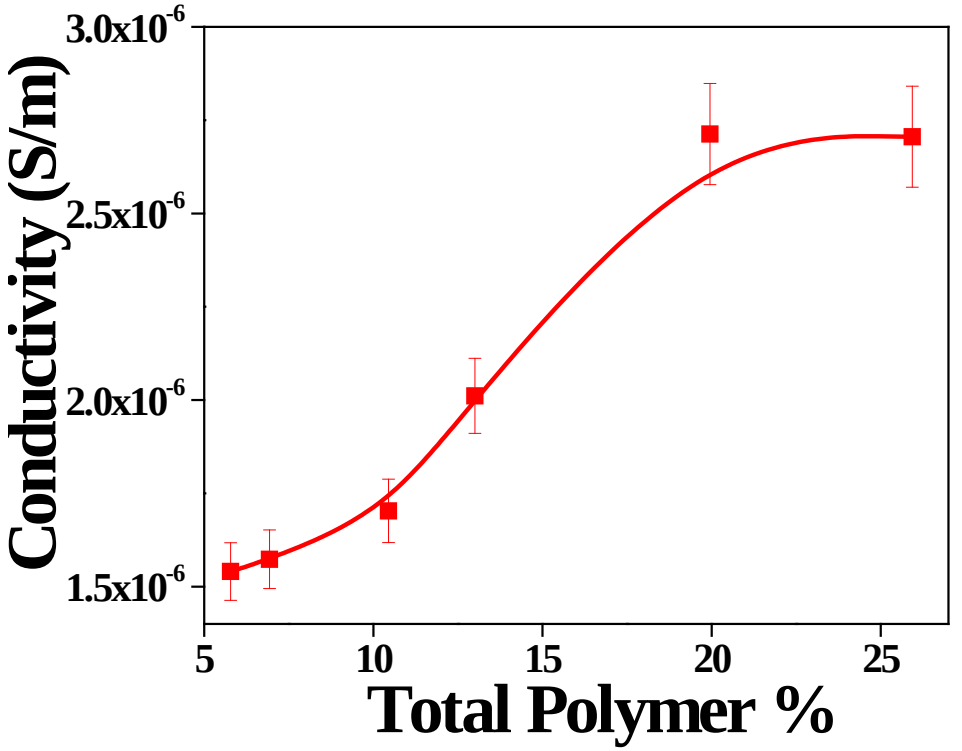

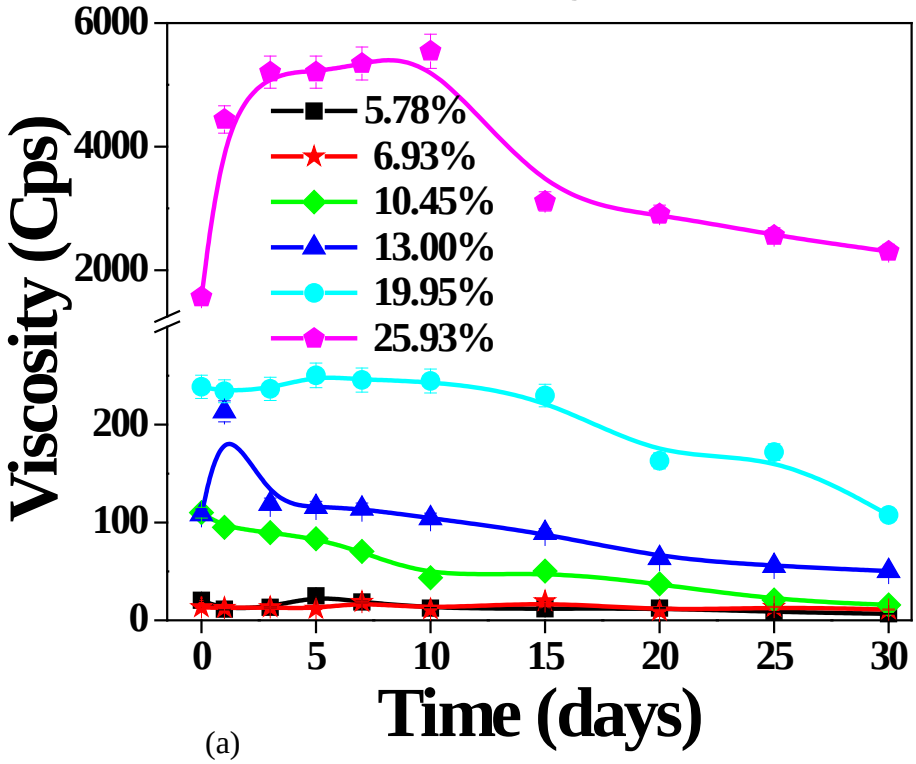

(a)

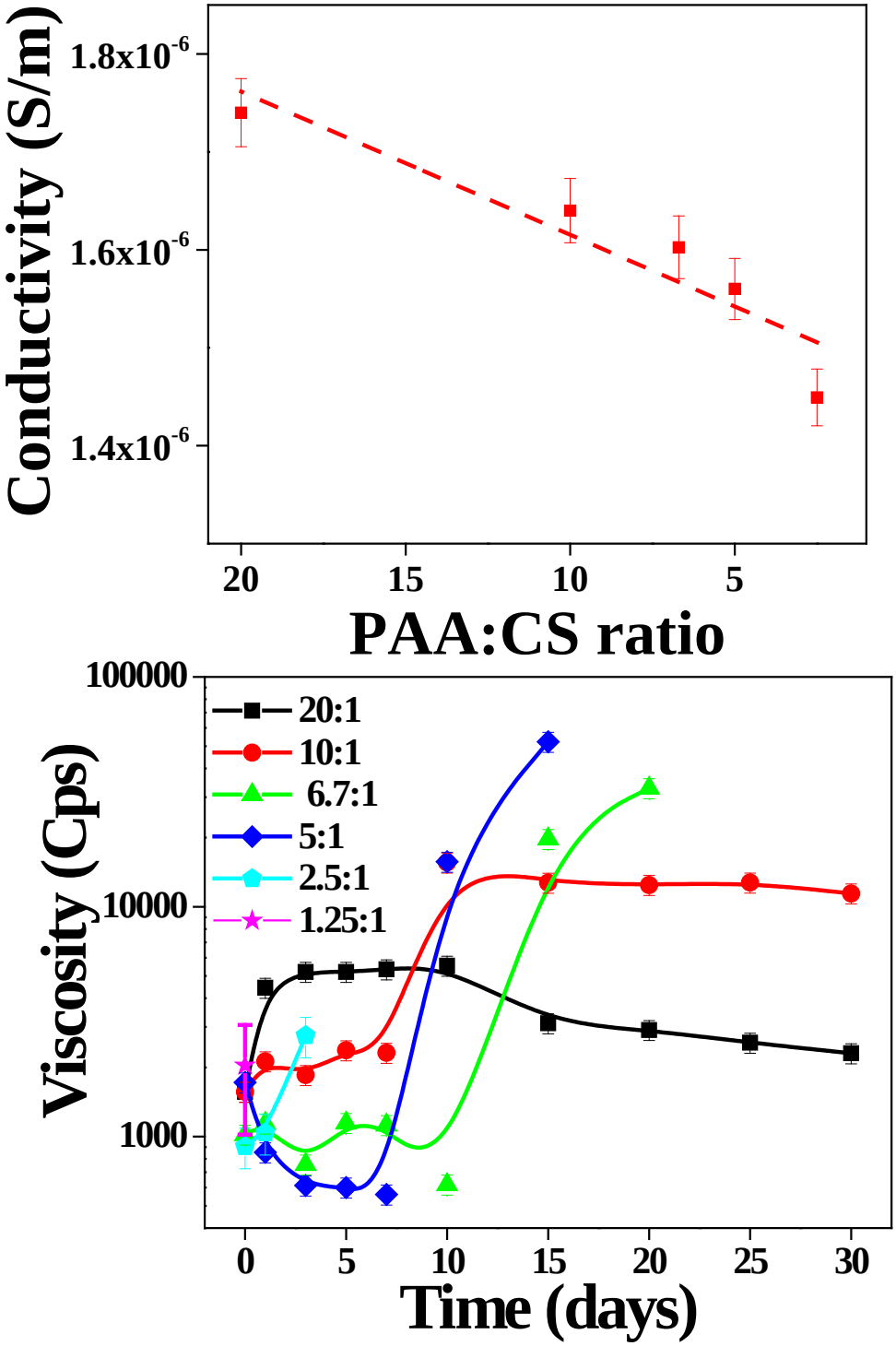

(b)

Figure 5: Conductivity and Viscosity of PAA-CS complexes with **(a)** different total polymer percentage and **(b)** different PAA:CS ratios

3.2.2 Effect of metal salts: In general, addition of salts to the polymer solution increases their conductivity. However, in case of polyelectrolytes, addition of salts results in changing the conformation and chain folding of the polyelectrolyte in the solution, due to the presence of ionic groups.

The polyelectrolyte complexes in which ions were introduced had a similar trend of a spike in viscosity then a gradual decrease in the values. However, the time to reach the spike was less (6-7 days) in as compared to solutions without ions (day 10). The presence of salt promotes rearrangements and shifts the reaction more towards thermodynamic equilibrium. The trend follows the reported polyelectrolyte complex behavior in the presence of salt, where small concentrations of salt decrease the viscosity of the solution due to the screening (**Figure 6**). The concentration for change depends upon the valence and specification of the salt involved.

Change in the conductivity and viscosity of the polyelectrolyte solution upon addition of salt depends on the interaction between the salt and the polyelectrolyte in the solution. It was observed that size to charge ratio and presence of d orbitals dominate the binding. **Figure 7** shows the viscosity of sodium, calcium and cerium ions at equimolar concentrations. Sodium ions, being monovalent, will shield polyelectrolyte charges, and cause the shrink of molecule chains and the decrease in hydrodynamic radius and viscosity. Besides shielding effect, divalent and multivalent ions can interconnect the PAA chains, influencing the conformation and viscosity of PECs. The interconnection of PAA chains becomes prominent when metal ion-PAA interactions overwhelm the shielding effect.

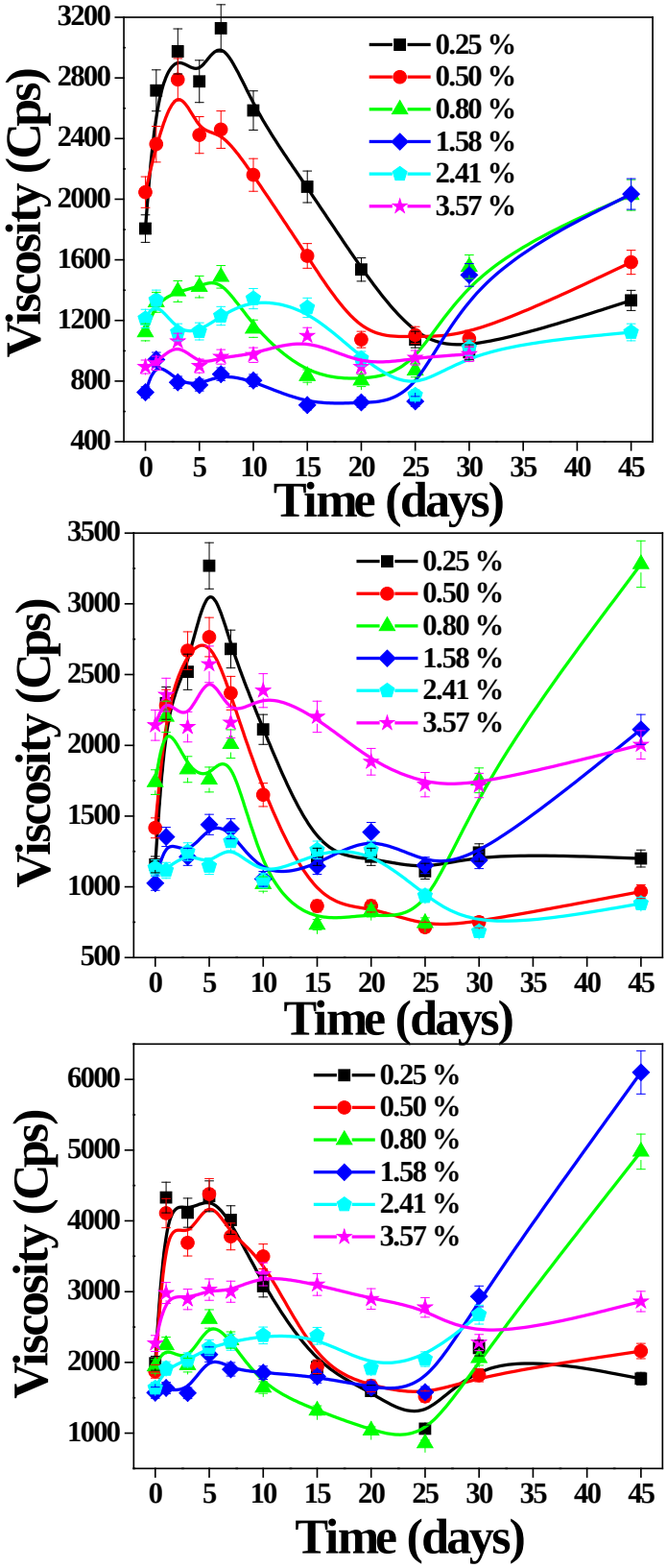

Figure 6: Time dependent viscosity of PAA-CS-M^{n+} complex at different concentrations of: **(a)** Na^{+}, **(b)** Ca^{2}, **(c)** Ce^{3+}

Therefore, it is expected that PECs' viscosity decreases with increased concentration of sodium but increases with increased concentration of metal ions with multiple valence. Metal ions with multiple valence and d orbitals such as cerium ions exhibit more efficient boosting of viscosities. As observed from the results sodium and calcium ion exhibit similar effect with substantial decrease in viscosity with only small amounts. Above 3.57 wt% the PAA-CS complex with cerium ions form gels. Complexes with ferric ions form gels at all concentrations due to its high charge density and strong interactions with PAA resulting in an insoluble complex. The pH of the solution is adjusted to 1 to obtain homogeneous solution. All the studies of ferric salt containing complexes were performed at this pH.

3.2.3 Effect of aging: The time dependence of viscosity can be clearly observed in the plots and can be attributed to slow and dynamic complex formation process. At molecular level, the size and shape of liquid molecules determine the properties of liquid instead structure less liquid with bulk properties and dynamic forces such as viscosity, adhesion etc. at this short range (few nanometers) can be complex and can take really long time to reach equilibrium, appearing to be time-dependent, resulting in "aging" effects. The change in the viscosity with time can be attributed to the continuous counter ion release and rearrangement of polymer chains during complexation due to the weakness of entanglements which change with time and modify internal structure of the complex until equilibrium is reached. Depending on characteristic polyelectrolytes and conditions can lead to different internal structures. The aging effect has its impact on viscosity and in turn electrospinning as explained later. PEC formation is a complex process and occurs in different steps.

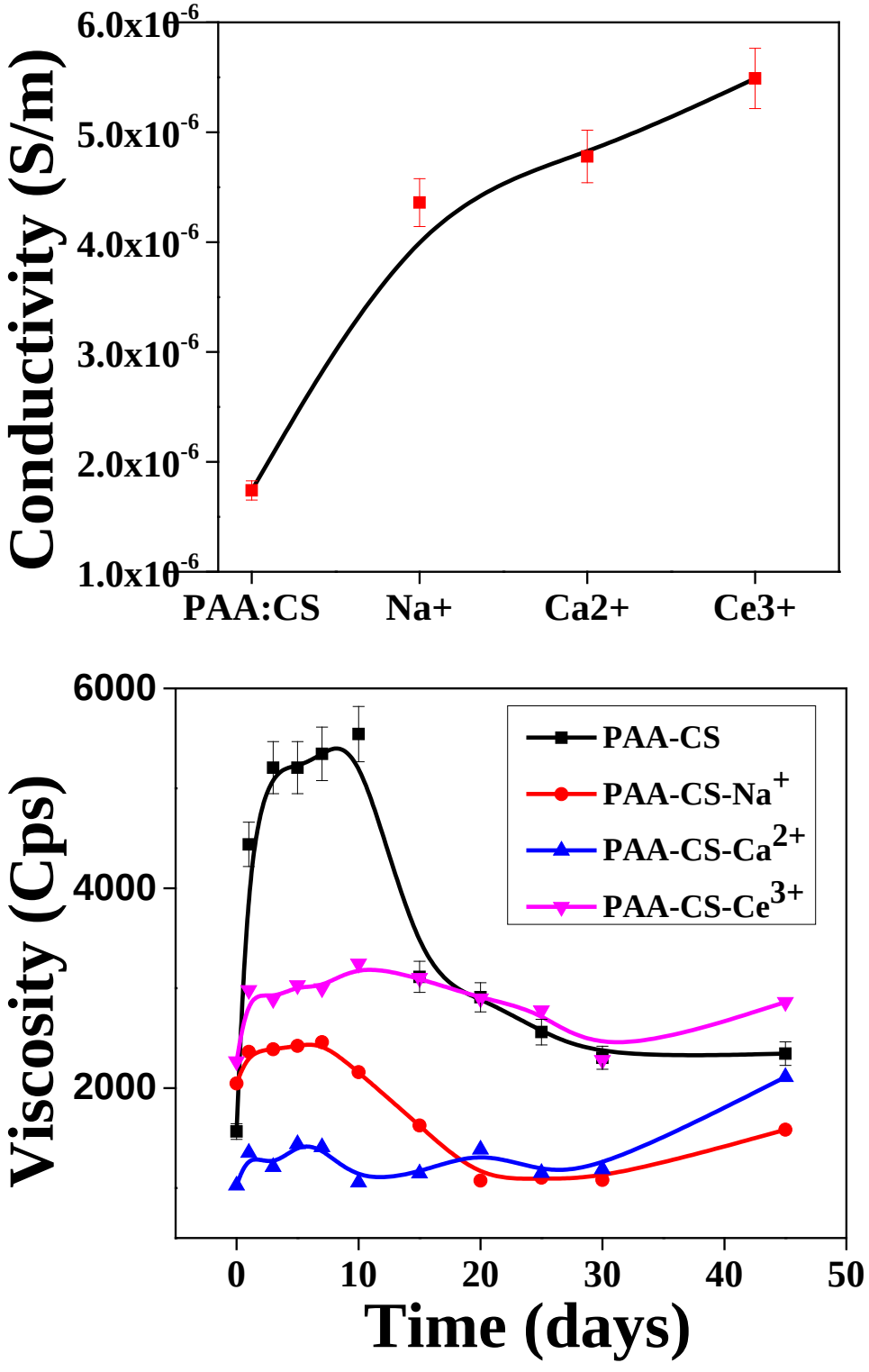

Figure 7: Conductivity and time dependent viscosity of different PAA-CS-M^{n+} complexes at equimolar concentrations.

During the PEC formation P. E. chains collapse due to the columbic screening of P. E. chains by counter ions and there is an initial decrease in the viscosity. This decrease can also be attributed to a more compact coiled up conformation of chains from a more extended conformation due to intramolecular hydrophobic interactions among polymer backbone. In this compact state, viscosity is minimum, where more or less all free polyions have complexed. Other than these intramolecular interactions, certain intermolecular interactions depending upon the long range electrostatic interactions between the P. E. chains also take place. There is always a competition between intramolecular columbic and intramolecular hydrophobic interactions. With more chain entanglement and chain rearrangement with time there is a subsequent increase in viscosity due to intermolecular aggregation in the form of chain entanglement, network or large fibers. Based on the data obtained from viscosity studies and literature, the time dependent complex formation process of PAA-chitosan is proposed.

3.2.4 PAA-CS complex model: The formation of PAA-CS complex starts with the interaction between the aggregates of CS rod-like particles and PAA that leads to an initial increase in the viscosity (II). This increase can also be attributed to a more compact coiled up conformation of chains from a more extended conformation due to intramolecular hydrophobic interactions among polymer backbones. As the CS rods start to stretch and relax into coils, the viscosity decreases as PAA disperse CS coils (III) and forms primary complex. With further chain entanglement of PAA with CS chains, secondary complex formation takes place (networks, fibrils and/or gels) leading to an increase of viscosity (IV).

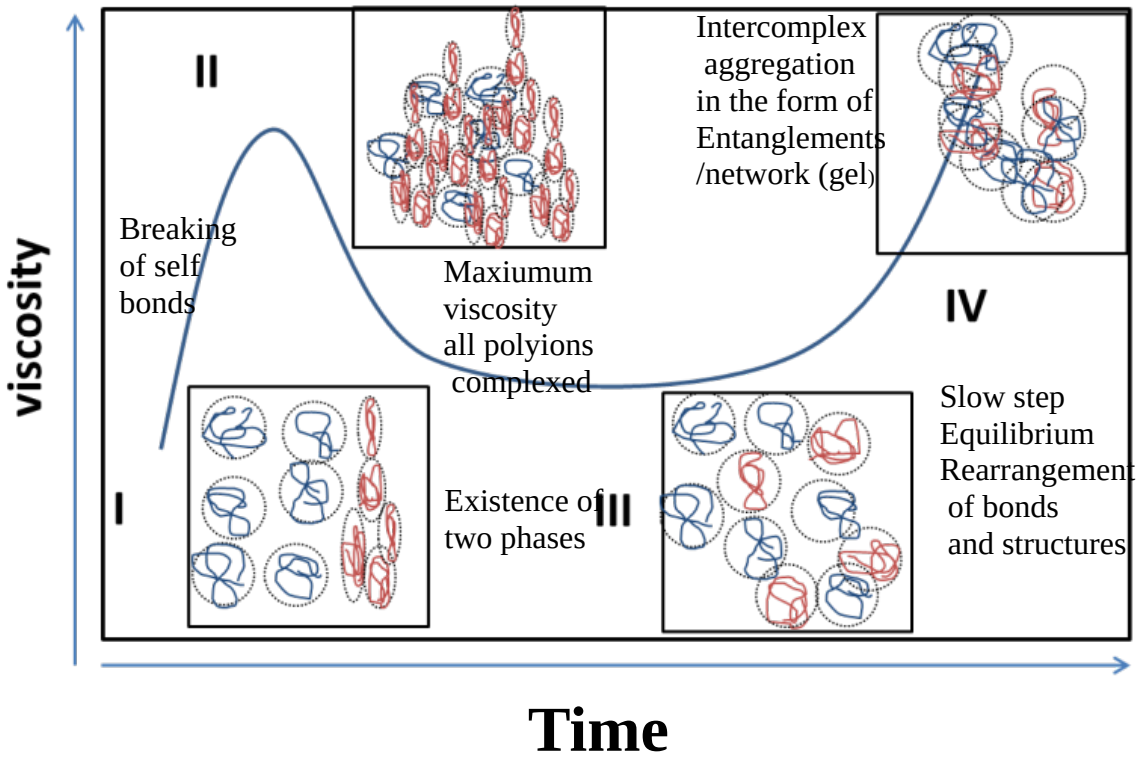

Figure 8: A schematic illustration of the relationship between PAA-CS structures and viscosity.

3.3 Conclusion:

Incorporating metal ions of different valence into PECs introduces metal ion/polyelectrolyte interactions that can tune the morphology of MPECs. The metal ion-PAA interactions are more important than metal ion-CS interactions at low pH. Transition metal ions have much stronger interaction with PAA than main group metal ions due to the availability of d orbitals, which enables the manipulation of PEC morphology through the tuning of solution viscosity. The function of CS is improving the fiber stability is two-fold, forming electrostatic interactions with PAA and generating metal ion-CS interactions at increased pH.

CHAPTER 4: GELATION OF PAA-CS-M^{N+} COMPLEXES

4.1 Introduction:

Hydrogels are three dimensional porous network structures of polymers or polyelectrolytes with high swelling capacity. The formation of these hydrogels can be impacted by a number of varying factors such as polymer concentration, presence of cross linkers and physiochemical conditions like pH and temperature.

The formation of a gel from solution results from either higher degree of crosslinking forming or reduction in the solubility or a combination of both. In a polymer or polyelectrolyte solution in an appropriate solvent, various changes (temperature, pH, addition of a substance) can bring increase cross linking or reduce the solubility resulting in a new phase. Most common way of gel formation is crosslinking. A suitable cross linker, a molecule which at least has two functional reactive sites, interacts with polymer either covalently or ionically forming a 3D network. A critical number of crosslinks per chain is required to allow the formation of a network. The properties of cross linked hydrogels (swelling, stability, elasticity, etc.) depend mainly on the crosslinking density and the type of cross linker.

Most common examples of covalent cross linkers are dialdehydes in particular glutaraldehyde, diacids like tartaric acid and bisamides like methylene bis acrylamide (MBA). Ionic cross linking can be achieved by interaction with oppositely charged components, either ions or molecules, leading to the formation of a network. A special case of ionic cross linking is complexation between two oppositely charged polymers or polyelectrolytes.

In these studies gelation of PAA-CS complexes was studied. However, since these are complexes at non stoichiometric ratios (different PAA:CS ratios) and take lot of time to gel due to secondary complex formation, different metal ions as ionic cross linkers were used to obtain hydrogels. It is shown in Chapter-3 that different metal ions have different interaction affinity which might or might not form gel. These metal ions further provide functionality to these hydrogels for various applications as explained below. Thus, the interactions between metal ions and polyelectrolytes introduce promising opportunities in tuning polyelectrolyte hydrogels, and improving their stability and swelling properties. In addition to the effect of polymer composition and metal ions, the impact of physiochemical properties like temperature and pH on gelation of complexes was examined. The stability of gels at different pH was also assessed.

4.2 Gelation:

The process of conversion of liquid sol into solid phase is known as gel formation of PAA-Cs and PAA-CS-M^{n+} complexes was studied by viscometry and inverted tube test.

4.2.1 PAA:CS ratio: The impact of stoichiometry (PAA:CS ratio) was first to be investigated. It was found that as chitosan concentration increased, gelation time at room temperature decreased (**Figure 9**). For solutions prepared with 2.5:1 ratio, gelation occurred within about 5 days whereas for solutions prepared with 20:1 ratio, gelation occurred after a little bit over a month (34 days). This can be due to the increased complexation between chitosan and polyacrylic acid. For PAA-CS-M^{n+} complexes the gelation time decreased with increased chitosan concentration. The physical appearance of the gels also varied based on chitosan concentrations. The gels went from soft and sticky at lower chitosan concentrations to hard and brittle at higher concentrations, due to the rigid backbone structure of chitosan.

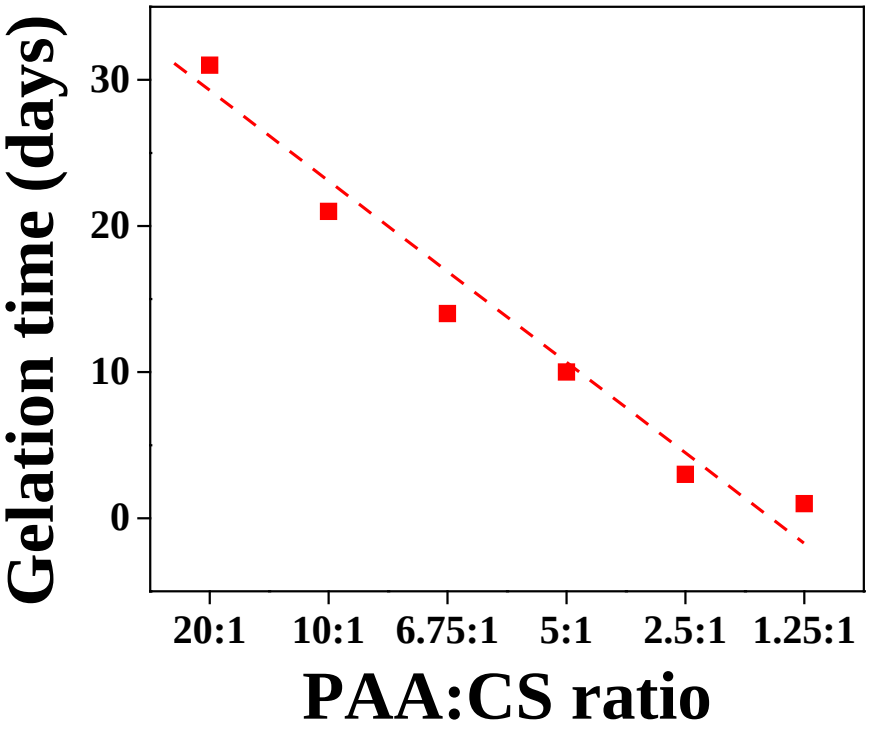

(a)

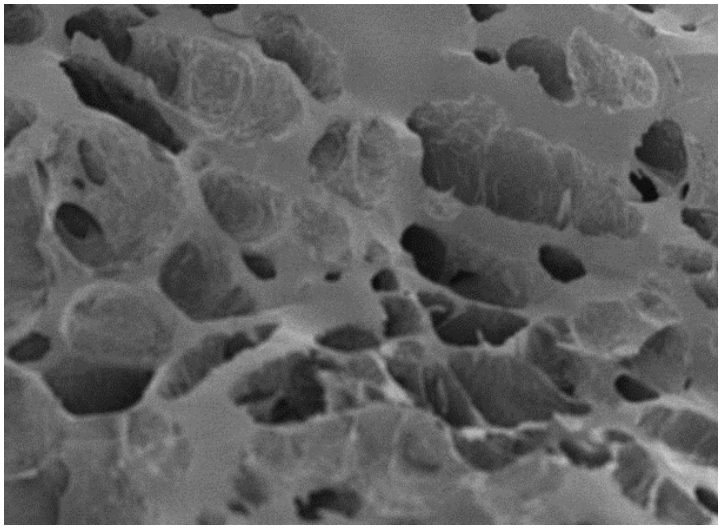

(b)

Figure 9: Dependence of gelation time on PAA:CS ratio and SEM of PAA-CS gel with 10:1 PAA:CS ratio.

4.2.2 Effect of Metal ions: The effect of different ant metal ions, Na^{+}, Ca^{2+}, Fe^{3+}, and Ce^{3+} on gelation of PAA-CS-M^{n+} was clearly evident. For ferric and cerium ions gelling rate was found faster rate than just the two polymers alone. Gelation occurs instantaneously upon addition of ferric ions. However, the gel formed was not homogeneous and a very small amount of acid was added to it and left on stirring to obtain a homogeneous gel. Cerium ions took around a week for gel formation. PAA-CS complexes with sodium and calcium ions, however, did not gel at all at room temperature. This behavior can be explained by different crosslinking of PAA-CS complex by different metal ions as explained in Chapter-3.

4.2.3 Effect of temperature: Several natural (alginin, pectin, etc.) and some synthetic polymers N-isopropyl acrylamide (NIPAM) exhibit temperature dependent gelation. Gelation of complexes close to human body temperature (37°C) is of high significance in several biomedical applications. Therefore we studied the effect of temperature on PAA-CS-M^{n+} complexes. The gelation was studied at three different temperatures (37°C, 45°C and 60°C).

Marked changes in viscosity were observed on thermal treatment of PAA-CS-M^{n+} solutions. It was observed that addition of PAA-CS solutions with calcium ions at 37°C results in dramatic increase in viscosity and gelation. The gelation was observed to occur at as low as 0.25% calcium ions (w/w of polymer concentration). Increased in viscosity of the complex solution in aqueous medium on heating may be due to increased crosslinking by calcium ions through columbic forces leading to distortions in conformations, leading to rearrangement of the complex into more stable conformations. Increase in crosslinking by metal ions is can be due to increased mobility and relaxing of polymer chains at high temperature. It is expected that the complex is further stabilized by a secondary binding force such as hydrophobic interaction in the polymer backbones especially chitosan resulting in formation of more highly ordered structures.

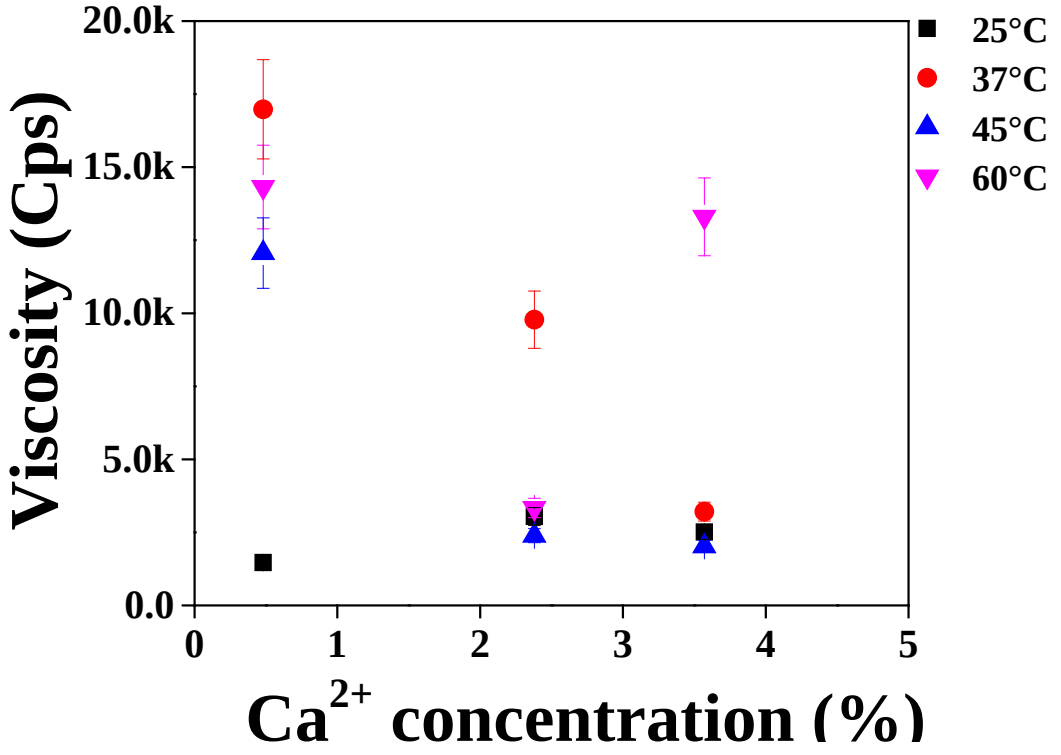

(a)

(b)

(c)

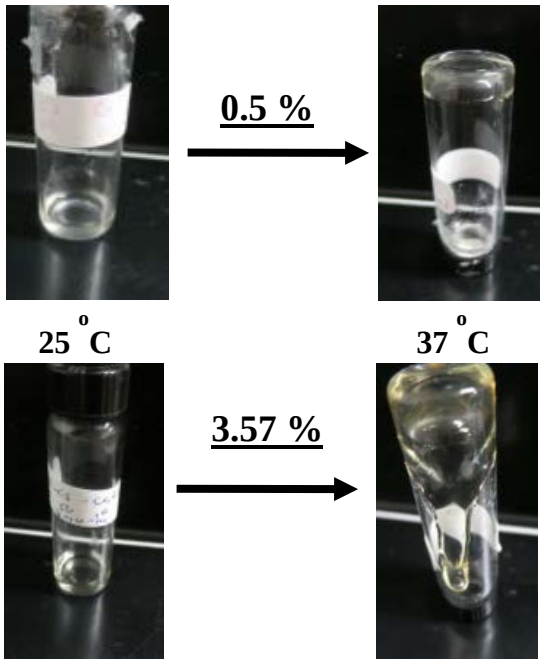

Figure 10: Concentration dependent thermal gelation of PAA-CS complex with calcium ions: **(a)** change in viscosity vs concentration of calcium ions at different temperatures; digital images **(b)** gelation of complex with 0.5% calcium ions at 37°C and **(c)** no gel formation of complex with 3.57% calcium ions at 37°C.

However, it was found that increase in calcium concentration resulted in decrease in viscosity and gelation was not observed beyond 1% calcium ions (w/w of polymer concentration). This can be attributed to increased screening effect overcoming the crosslinking effect. Further increase in temperature (45°C) resulted in decrease in viscosity, however, viscosity increased again at 60°C.Complexes with cerium ions too exhibited gelation at 37°C. The increase cerium ions promoted the thermal gelation, contrary to the case of calcium ions. It is expected as cerium ions have dominating cross linking effect than screening effect. Increase in temperature however did not result in gelation of complexes with sodium ions or PAA-CS complex.

It can be concluded that thermal gelation ability of MPECs is significant as it can reduce gelation time reduced from days or months to a matter of minutes or hours. And gelation can occur at as low as 0.25% of ion concentration (w/w of polymer concentration).

4.2.4 Effect of pH: PAA and CS are both weak polyelectrolytes and the presence of charged functional groups depend on pH. At low pH (3.5), most of the carboxyl and amine groups are protonated, with minimum PAA-CS and polyelectrolyte-meta lion interaction. Hence, at this pH the gelation does not take place for most PAA-CS-M^{n+}. When pH is raised to 7, the amine and carboxyl both get deprotonated and are available for interaction with metal ion leading to enhanced cross-linking. Additionally, the deprotonation of amine groups lead to collapsing of chitosan chains, further contributing to gelation. At further high pH (11), most carboxyl groups are deprotonated, leading to chain repulsion and hence decrease in viscosity (**Figure 12**). The change in interaction of metal ions with PAA is also evident from IR data.

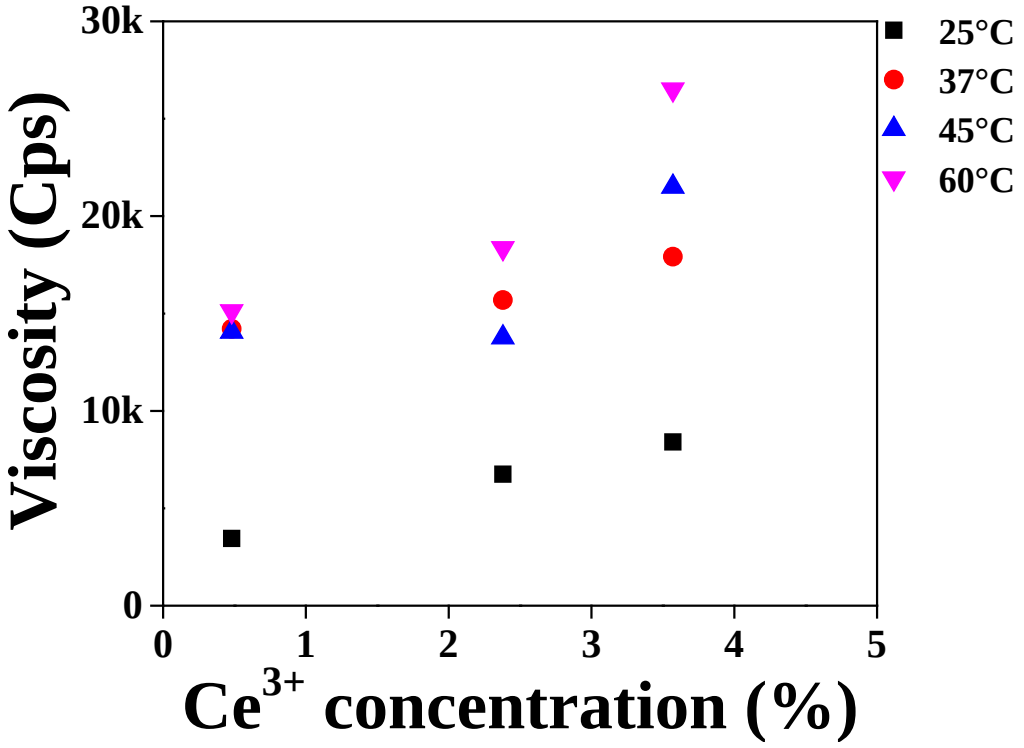

(a)

(b)

(c)

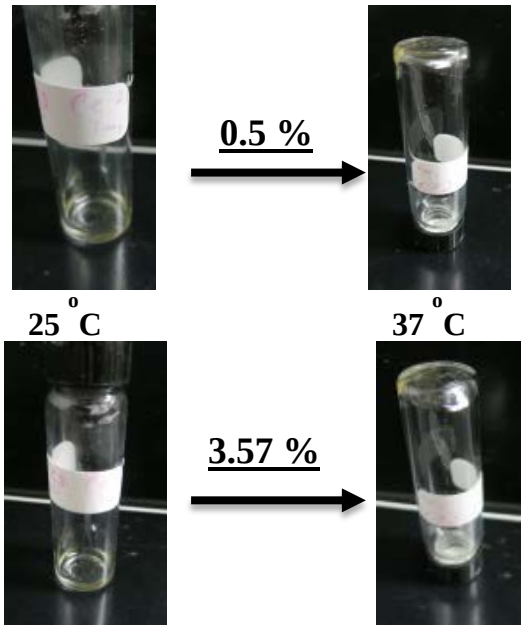

Figure 11:Concentration dependent thermal gelation of PAA-CS complex with cerium ions: **(a)** change in viscosity vs concentration of cerium ions at different temperatures; digital images gelation at 37°C of complex with **(b)**0.5% cerium ions at and **(c)** with 3.57% cerium ions .

4.3 Swelling and Degradation:

As shown in the **Figure 13**, the swelling capacity of hydrogels and free dried gels was measured at different pH. Hydrogels swelled less as expected, compared to their freeze dried because of their pores already being saturated. Gels with metal ions swelled more comparatively to PAA-CS gel. Freeze-dried PAA-CS-Ce^{3+} gel was found to have the greatest swelling ratio. Freeze drying also provided better stability of gels as shown in **Figure 13**. Hydrogels degraded more rapidly at lower and higher pH.

4.4 Stretching and self-healing:

Materials with inherent structural ability to repair damage caused by mechanical usage over time are known as self- healing materials. It occurs by the spontaneous formation of new bonds when old bonds are broken within a material. Self- healing in gels follows the same three steps as in a biological response. The first step immediately after the damage is the triggering followed by the transport of materials to the affected area to form new bond. The third step is the actual repair or healing process in which new bond formation takes place. The third response is the chemical repair process. This process differs depending on the type of healing mechanism and can be affected by environmental conditions like, pH and temperature.

Stretching and self-healing of gels is an important factor because they resemble human tissue and hence can be used in wound dressing, tissue repair and sealants. The 3-D network structure of hydrogels and their ability to absorb large amounts of water via hydrogen bonding, gives rise to firm and elastic nature of gels with self-healing and stretching properties.

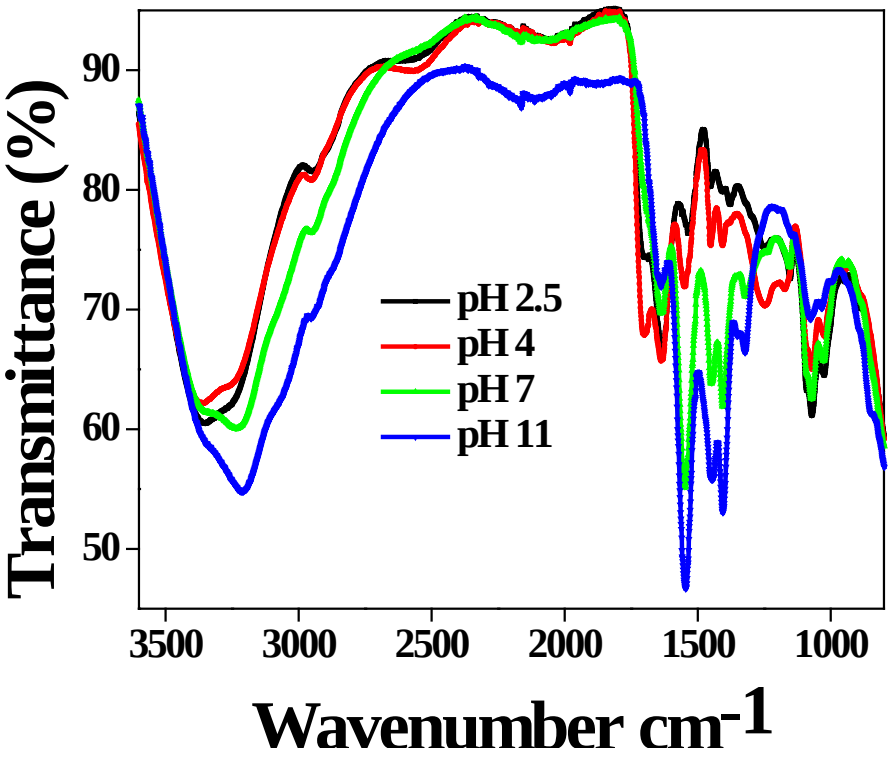

(a)

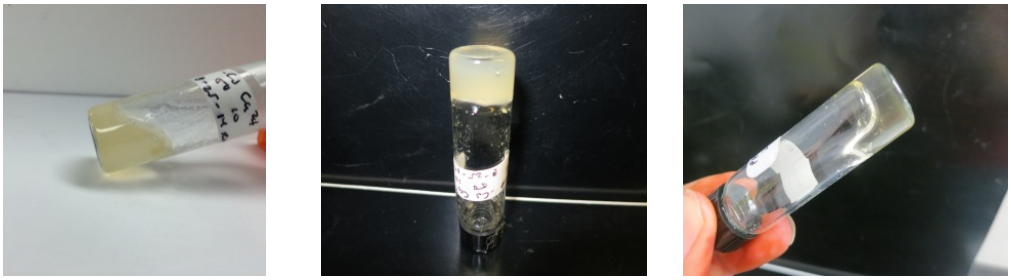

pH 3.5 **pH 7** **pH 10.5**

(b)

Figure 12: Effect of pH on gelation: (a) IR of PAA-CS-Ca^{2+} complex:, **(a)** no gel formation at pH 3.5, **(b)** gel formation on pH 7 and **(c)** highly viscous solution at pH 10.5.

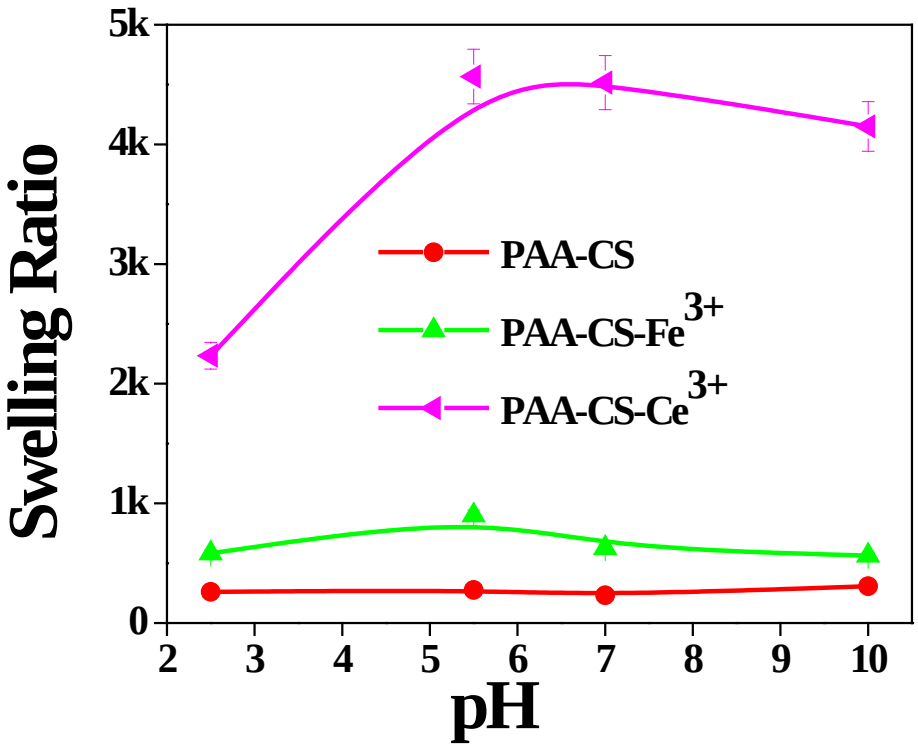

Figure 13: pH dependent swelling and degradation of PAA-CS-M^{n+} gels.

4.4.1 PAA:CS ratio: It was found that increasing chitosan concentration reduced stretching and self-healing ability. This is because of the rigid structure of chitosan and increased disruption of elastic chains of polyacrylic acid by chitosan resulting in brittle gels. It is known that self-healing of hydrogels is known to be mediated through mobility of ions. However, with increase in chitosan, the conductivity decreases (decrease number of ions), hence reduced self-healing. Lower Chitosan concentrations self-healed with ease whereas higher concentrations either took some time or did not heal at all.

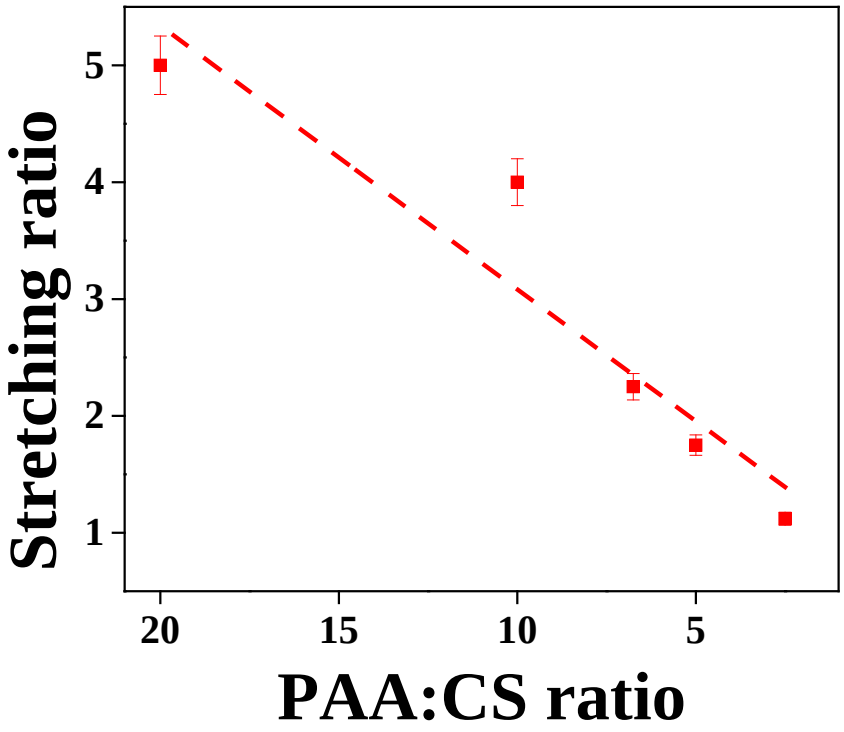

(a)

(b)

(c)

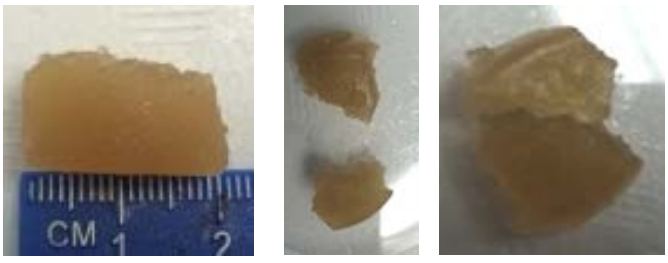

Figure 14: Effect of PAA:CS ratio on stretching and self-healing: **(a)** graph showing PAA:CS ratio dependent stretching properties of PAA-CS hydrogels; digital images of self-healing of PAA-CS hydrogels with PAA: CS ratio **(b)** 10:1 and **(c)** 5:1.

4.4.2 Effect of metal ions: Gels with metal ions exhibited increased stretching and self-healing than gels. Gels cross linked with calcium ions stretched the most followed by gels cross linked by cerium and ferric ions. This can be explained by ease of rearrangement in gels cross linked by calcium ions due to less cross linking. Metal ion concentration also seemed to impact healing and stretching. For ferric ion cross-linked gels, increase in ferric ion concentration increases cross linking and decreased stretching and self-healing resulting in brittle gels. With increase in calcium ions the stability of gels is compromised. For cerium ions dependency on concentration is not that strong, however it follows the ferric ion trend of decrease in stretching on increase in cerium ion concentration. The stretching of metal ion hydrogels can be explained by the breaking and reforming of bonds between the polyelectrolytes and the metal ions to "re-zip" the crack or damage.

4.4.3 Effect of pH: The impact of pH on stretchability and self-healing ability of gels was also tested. The self-healing and stretchability of different metal ion cross linked gels is dependent on the stability and swelling of gels at different pH. **Figure 16** shows the self-healing ability of ferric ion cross linked gels at different pH. The healing ability decreased with pH. It was observed that healing occurred much faster at low pH and is maximum at pH 2 due the decreased cross linking and stability of gel. However, presence of such low pH compromises gel stability. Therefore, for stable self-healing ferric gels, pH 5 is optimum, although pH 7 also exhibit self-healing capacity.

PAA-CS-M^{n+}	Stretching ratio
PAA-CS	5
PAA-CS-Ca^{2+}	30
PAA-CS-Ce^{3+}	13
PAA-CS-Fe^{3+}	10

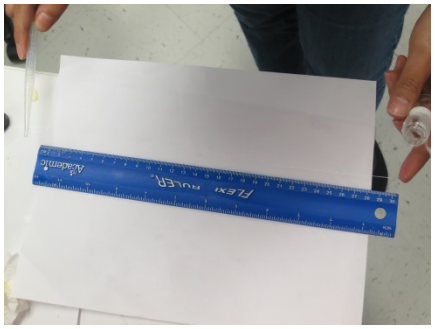

Figure 15: Dependence of stretching ratio on metal ions comparison of stretching ratio of different gels (the blue marking is a foot long ruler); digital images of stretched PAA-CS- Ce3+.

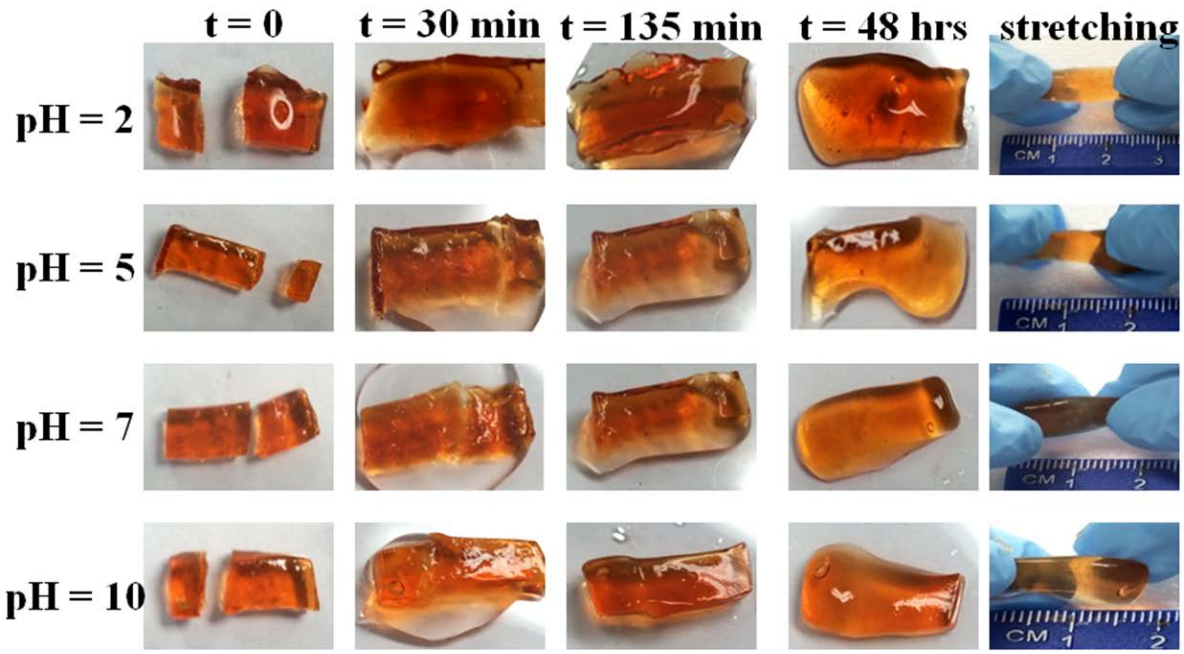

Figure 16: pH dependent self-healing of the PAA-CS Fe^{3+} gels at different time intervals

4.5 Morphology and Functionalization of gels:

Ionically cross linked gels were freeze dried and observed under SEM for morphology and pore size. **Figure17** shows continuous porous structure of gels with inters connectivity, optimal for diffusion of molecules. The ionically cross linked gels can be suitably functionalized for different applications. The calcium, cerium and ferric gels were functionalized with, Hap mineralization, ceria nanoparticles and polypyrrole coating on the surface. **Figure17** shows different functionalized gels.

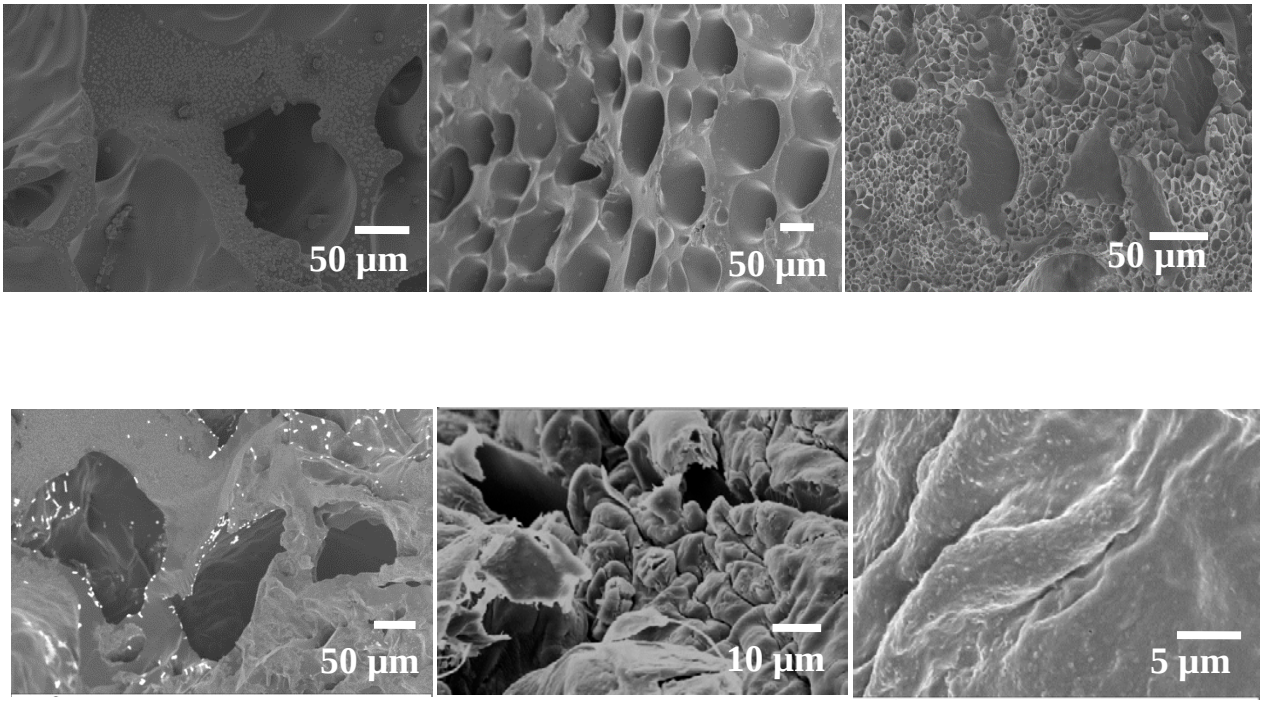

Figure 17:Morphology of the PAA-CS fibers: **(a)**PAA-CS-gel with Ca^{2+}, **(b)** Fe^{3+} and **(c)** Ce^{3+} ions; the bottom row shows their functional application, upon conversion to **(d)** HaP nanoparticles, **(e)** ceria nanoparticles, and **(f)** PPy coating.

Hydroxyapatite (HaP) is a mineral found in human bones and teeth and HaP nanocrystals are grown for bone and dental tissue regeneration and as dental fillers. Hap nanocrystals can be

grown synthesized by several different methods like wet chemical, electro deposition, sol-gel, etc. However, most important method is the biomimetic mineralization of HaP using simulated body fluids (SBFs), fluids with inorganic composition similar to physiological conditions. The HaP grown under these biomimetic conditions is known to highly resemble the structure found in bone. Biomimetic mineralization of Hap is achieved by incubating substrates with saturated solutions of calcium chloride or using HaP nanocrystals as seeds in SBF. Both PAA (carboxyl for Hap mineralization[109]) and CS with its ability to control nucleation and growth during the mineralization process and prevent the interfacial mismatch have shown immense potential for HaP mineralization and bone regeneration. We propose that PAA-CS scaffolds can be used for biomimetic mineralization for bone and tissue regeneration. In this study, PAA-CS scaffolds loaded with calcium ions were incubated in SBF at room temperature, for Hap nanocrystals formation. It is expected that due to hydrogel nature and controlled release of calcium, faster and more controlled growth of Hap nanocrystals would occur.

With free radical scavenging activity, neuroprotective, radioprotective and anti-inflammatory properties, lots of research has been devoted to study the antioxidant property of ceria nanoparticles. Cerium ions exist in two oxidation states +3 and +4. The antioxidant activity is due to the interchange of these two states during a redox reaction. However, there is always a concern regarding the toxicity of these particles, especially when using for biomedical applications. For safer and wider use of ceria nanoparticles, a safe matrix is required. The synthesis of ceria nanoparticles in a solid matrix can meet such requirement. Ceria nanoparticles would be embedded in the matrix so that there is no direct contact between cells and nanoparticles.

Polypyrrole (PPy) is a widely known and investigated conducting polymer with applications in sensing and tissue engineering, actuators and solar cells. It is highly biocompatible and is extensively used in neural regeneration.

4.6 Conclusion

Chitosan and polyacrylic acid can complex together to form gels at room temperature. The gelation time depends upon the polymer concentration and PAA:CS ratio. For non-stoichiometric ratios (high PAA:CS ratio) complex can take days to month to gel. Addition of metal ions as cross linkers decreases the gelation time and also infers properties like stretching and self-healing. The ionic cross linking by metal ions is concentration dependent and varies with the metal ion type. Physiochemical parameters like temperature and pH can also induce gelation in these complexes. The gels thus obtained are stable over a wide range of pH. These gels can be further functionalized for different applications in drug delivery, absorbents and tissue engineering.

CHAPTER 5: ELECTROSPUN PAA-CS-M^{N+} NANOSTRUCTURES

5.1 Introduction:

Role of metals in biological world for structure stability, catalysis, biomineralization etc. in self-assembly, adhesion and strength has been evident in studies [91-97]. Herein we propose biomimetic metal crosslinking for enhanced structure stability and functionality of polymeric systems. Polyelectrolyte complexes (PECs) have been used to produce fibers that are stable in aqueous solutions [49, 79, 107, 120-122]. Fibers with one polyelectrolyte component are water soluble and the crosslinking of these fibers has to be performed in solvent-free [89, 123] or non-aqueous media[78]. We studied the formation of water soluble polyelectrolyte complexes (PECs) of PAA and CS, two biocompatible and biodegradable polyelectrolytes, in the presence of different metal salts (M^{n+}). The homogenous aqueous solutions of these complexes were then electrospun to obtain PAA-CS-M^{n+} nanofibers. Metal coordinated polyacrylic acid-chitosan (PAA-CS) electrospun fibers system act as a reservoir of metal ions for their controlled release.

PAA and CS are biocompatible and biodegradable polyelectrolytes with antimicrobial and metal chelating properties and providing functional groups. The complex formation between PAA and CS eliminates the use of cross-linking fibers using glutaraldehyde or other cross-linking agents modulating the mechanical properties of fibers rendering them stable and insoluble in solutions and at different pH. By combining both PAA and CS, the system also overcomes the disadvantages of both the natural (slow degradation, insufficient mechanical integrity) and synthetic polymers (biodegradation, biocompatibility, etc.). The system exploits the affinity of both PAA and CS for metal ions. The incorporation of metal ions in the fibers provided functionality to the fibers for various biomedical and material applications. While the

coordination of metal ions and polyelectrolytes has been extensively investigated in solutions [9, 98-102] and multilayer films, [103-105] to our knowledge, no research has been performed to study the effect of metal ion/polyelectrolyte interactions in PECs on PCF structures and properties.

Previous studies on effect of metal ion on electrospinning of polymers focused majorly on obtaining defect and bead free smooth electrospun fibers [124, 125]. Here, we demonstrate that metal-ion identity can affect the morphology of electrospun PAA-CS-M^{n+} nanostructures (particles, rods, ribbons and fibers) from aqueous solutions. The incorporated metal ions interact with polyelectrolytes in the solution affecting the conformation of polyelectrolyte molecules and thus molecular entanglement, solution viscosity and conductivity, critical for fiber formation. The metal coordination thereby offers a novel mechanism of controlling electrospinning process of weak polyelectrolytes and the morphology of thus obtained electrospun structures in aqueous environments. The presence of metal ions and metal identity also influence the diffusion of molecules across the fibers. Further, these metal ions may take part in reaction as reactants or precursors and/or as catalyst for the reaction. The confined environment of thus formed fibers allows the controlled synthesis of nanoengineered materials with interesting properties. The size of different nanoparticles synthesized in fibers is approximately 5nm nanoparticles, indicating that the particle size can be controlled by controlling fiber morphology. The application of these new materials include catalysis, biomedical applications, coatings, optics, electronics, water chemistry, etc.

5.2 Electrospinning of PAA-CS nanostructures:

The viscoelasticity, hence, electrospinnabilty of PAA is very high. On the other hand chitosan is a stiff and rigid molecule and difficult to electrospun due to strong intermolecular hydrogen bonding, self-adhesion properties and low solubility in aqueous solutions. The complex formation between PAA-CS in right stoichiometry and presence of salts would result in electrospunable aqueous solution forming nanofibers with properties of both PAA and chitosan.

Generally, mixing two polyelectrolytes with opposite charges at stoichiometric ratio leads to phase separation and precipitation due to the electrostatic interactions between two polyelectrolytes. However, the electrostatic interactions can be reduced or eliminated by manipulating pH of the solution and the stoichiometry. A homogeneous mixture of the two polyelectrolytes is required for the spinning of the fibers. Mixing polyelectrolytes of opposite charges and similar molecular weights often results in water insoluble complexes due to electrostatic interactions between the two polyelectrolytes, hence appropriate solvent has to be chosen. For weak polyelectrolytes, the pH of the system also determines the formation of complex. One such example is PAA- PAH pair system. PAA and PAH are weak polyelectrolytes with pKa of 5.5 and 8.9, respectively. Such weak polyelectrolyte systems can be manipulated by the pH of the medium. PAA has to be completely protonated to avoid interactions between PAA and PAH, in order to make homogeneous mixture of PAA and PAH. At pH 2.1, PAA is completely protonated, although PAH is fully charged. Therefore, homogeneous mixture would be obtained at pH 2.1 by dissolving PAH in PAA at 2:1 molar ratio.

In our studies, homogeneous PAA-CS mixtures were obtained by dissolving CS into a 25% aqueous solution of PAA with PAA:CS molar ratios 20:1, 10:1, 6.75:1 and 5:1, at pH~ 3. **Figure 18** shows polyelectrolyte complex fibers (PCFs) electrospun from polyelectrolyte complex solutions with size around 200 nm. The effect of parameters like concentration (total polymer, PAA: CS ratio and ion concentration), voltage and flow rate on electrospinning of PAA-CS was studied.

(a)

(b)

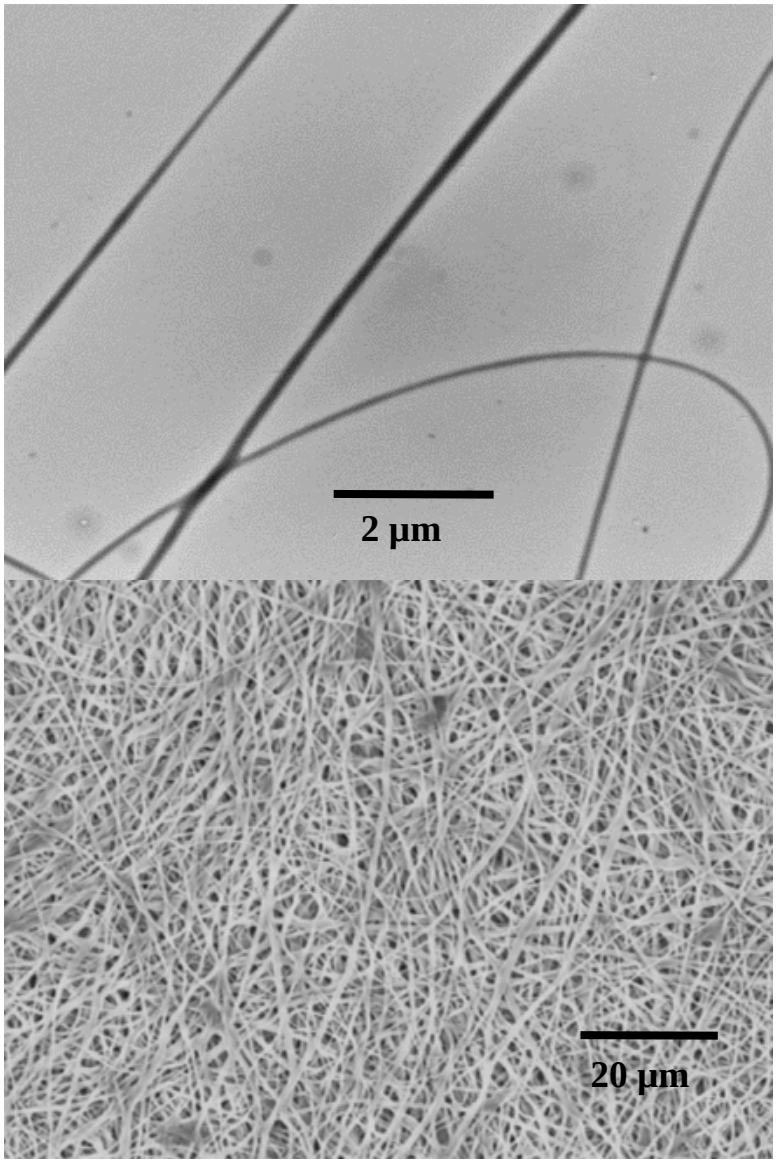

Figure 18: Electron micrographs of PAA-CS fibers: **(a)** TEM and **(b)** SEM. The fibers are about 200 nm in width.

PMFs were also electrospun from polyelectrolyte complexes loaded with metal ions. **Figure 19** shows the TEM and SEM images of electrospun fiber from cerium and ferric ion loaded PAA-CS complexes. The fibers were obtained by electrospinning homogeneous solution of PAA-CS with calcium, cerium and ferric salts in water, respectively. The fibers obtained were smooth and similar to the ones obtain from complexes without the ions.

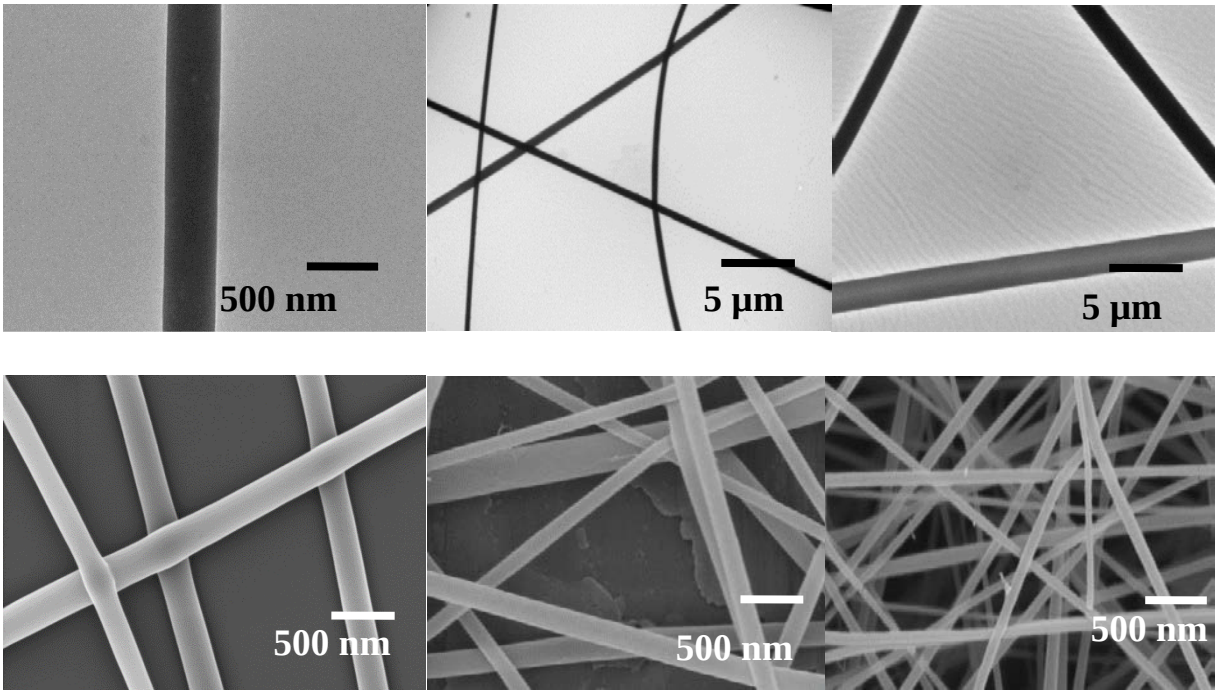

Figure 19::Electron micrographs of PAA-CS-M^{n+} fibers (top row TEM and bottom row SEM images) **(a)** PAA-CS-Ca^{2+}, **(b)** PAA-CS-Ce^{3+} and **(c)** PAA-CS-Fe^{3+}**.**

5.2.1 Effect of total polymer concentration and viscosity: The concentration of a polymer solution should be at least 2-2.5 times above the entanglement concentration (c_e) to produce a continuous polymer fiber via electrospinning. With increase in total polymer concentration, the chain entanglement between polymer chain increases, leading to jet stretching and fiber formation and the morphology changes from beads to fibers (**Figure 20**). Large viscosity at higher concentration disrupts the solution flow due to increased cohesion forces or drying of the solution and decreases the solution electrospinnabilty and with further increase in concentration,

solution turns into gel. At lower concentration within the optimum range, nanofibers along with bundles, junctions and some beads are found due to incomplete stretching before reaching the collector. Lower polymer concentrations lead to the fragmentation of jet and formation of droplets under the effect of surface tension and constant applied voltage.

At lower concentrations and viscosities viscoelastic forces were not sufficient enough to prevent fragmentation of the jet due to the repulsive forces of charge, resulting in droplets. The viscoelastic forces become more prominent with increase in viscosity and compete with the surface tension, resulting defect free fibers, however, the diameter of the fiber increases due to less competent repulsive forces from the charge. At lower concentrations within the optimum range, nanofibers along with bundles, junctions and some beads are found due to incomplete stretching before reaching the collector. In the upper range, nanoribbon formation along with fibers resulted due to incomplete drying of the solvent before reaching the collector.

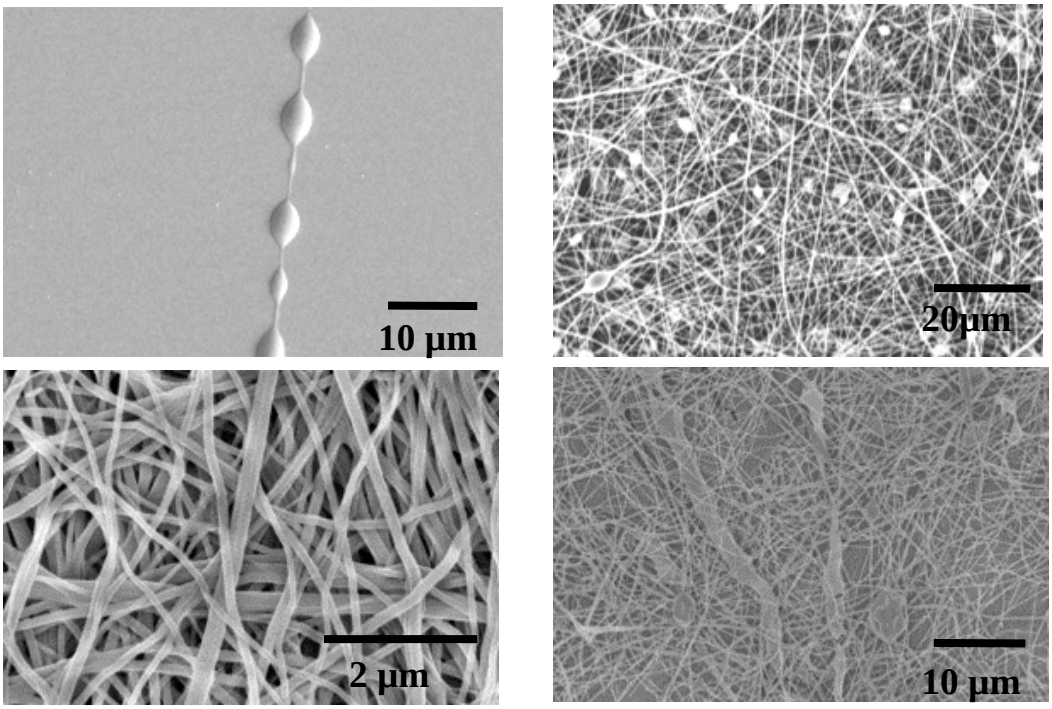

Figure 20: Effect of increasing polymer concentration on PAA-CS fiber formation

5.2.2 Effect of PAA:CS ratio: Increase in chitosan concentration decreases the electrospinnability of solution since CS is a rigid molecule. Decreasing PAA:CS ratio also decreases the conductivity with because of consumption of protons in solutions by CS through the formation of NH_3^+ groups. Hence, higher voltage for electrospinning is required at higher concentration of chitosan. Increase in number of electrostatic interactions with increase in PAA:CS ratio, increases the viscosity of the solution and hence increases the fiber diameter(**Figure 21**). Phase separation between PAA and CS can also been seen in the images, with chitosan forming clusters in PAA matrix. The size of the cluster increases with increase in chitosan concentration. Solutions with very high concentrations of chitosan resulted in precipitation or gel formation, hence could not be electrospun.

5.2.3 Effect of applied voltage and flow rate: An appropriate external voltage is required for initiating and sustaining jet formation for electrospinning. The optimum range of voltage for PAA-CS system was found to be between 8- 11 KV. It was observed that higher voltages were required to electrospun solutions with higher polymer concentrations due to high viscosity of the solutions. At higher voltages the jet became unstable and droplets are observed. At very low voltages, the jet formation is not there. In the range 6-8 KV, few short fibers along with beads and spindle shaped defects were observed. Due to high charge density of the solutions causing repulsive forces and lower voltages not enough for jet stretching, the jet breaks into short fibers. The length of some fibers was also found to be shorter, due to incomplete stretching of the jet. At voltage 8-10 KV, there is little change with jet still ejecting from the bottom of the Taylor cone. Fibers are found to be homogeneous with smaller diameter and defect free in this range (**Figure 22**). At higher voltage, jet is ejected at the end of the tip of the needle and more beads were

observed with the fibers. The fiber morphology also changed from cylindrical to flattened and increased diameter size due to increased flow of solution from tip to collector at higher voltages, resulting in incomplete drying of the solvent before reaching the collector.

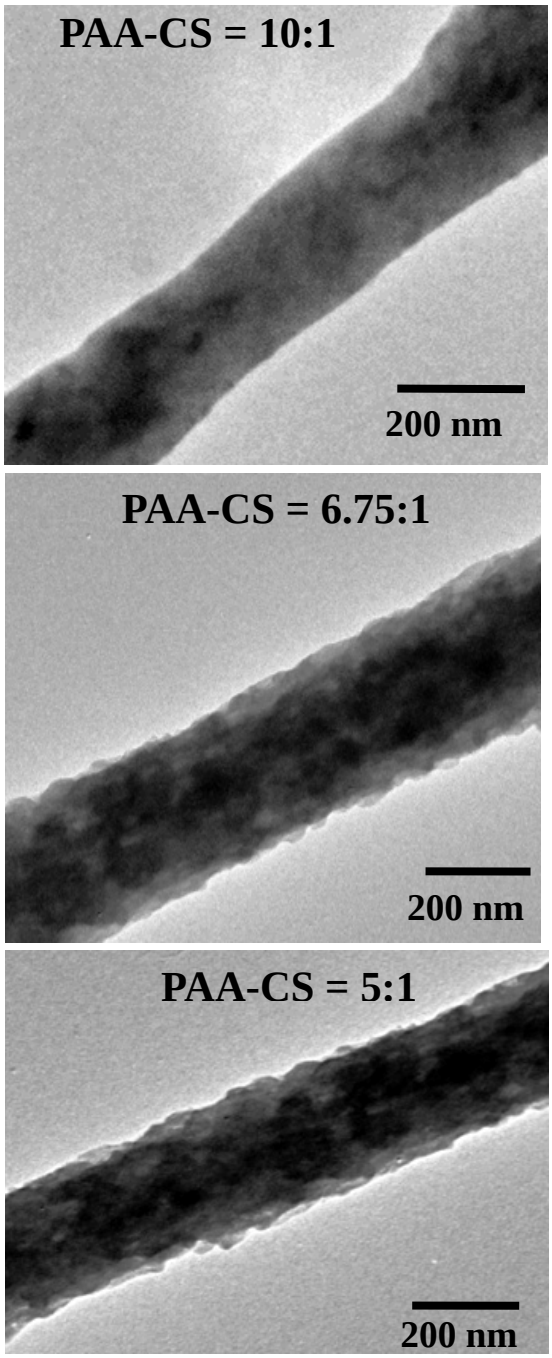

Figure 21: TEM images of PAA-CS fibers electrospun at different PAA:CS ratios **(a)** 10:1 **(b)** 6.75:1 and **(c)** 5:1.

The voltage required to sustain jet was found to be dependent on the concentration of the solutions. It was observed that higher voltages were required to electrospun solutions with higher polymer concentrations due to the high viscosity of the solutions. Higher voltage was also required to produce smooth fibers from solutions without the metal salts as compared to solutions with salts.

The flow rate of the solution through the needle is another important electrospinning parameter influencing the nanofiber diameter, porosity, and geometry and defects. It is found that increase in applied voltage increases the flow rate from tip to collector, increasing the total flow rate. Therefore, external flow rate is inversely proportional to the applied voltage. However, increase in voltage also results in decrease in volume of the drop at tip, disrupting the jet. Therefore, a minimum flow rate is required to maintain the Taylor cone and sustain the jet by replacing the lost solution from the tip as jet is being continuously ejected. Optimum flow rate was also observed to be dependent on the conductivity of the solution. The minimum and maximum flow rate for PAA-CS solutions without metal ions was found to be 0.3 and 0.5 mL/hr., respectively. For solutions with ions the optimum flow rate was found between 0.1-0.3 ml/hr. For solutions containing ferric ions (pH adjusted), due to low viscosity and high conductivities, jet was found to be stable at lower flow rates (0.07 ml/hr.). Jet stability of solutions with higher solution conductivity at lower flow rates could be due to the increased electric current and decreased the surfaces charge density with an increase in flow rate. At higher flow rates, there was an increase in bead defects, bead size and fiber size. Nanoribbons were also observed due to the incomplete drying and flattening of the surface.

5.2.4 Effect of salt: Salts are added to the PECs to improve the complex formation and prevent any aggregation as explained above. Another advantage of salt addition is increased conductivity, although polyelectrolytes have some intrinsic conductivity of their own as compared to the polymer solutions. As compared to other additives like surfactants, added to increase conductivity for smooth fiber formation, the viscosity and surface tension of the solution does not increase on addition of salts, whereas conductivity and charge density increase significantly. It is known that the radius of the nanofiber jet is inversely related to the cube root of the conductivity of the solution, hence increase in solution conductivity results in smaller fiber diameter. Addition of salts increase the net charge density of the solution resulting in increased elasticity and less resistance to fiber formation.

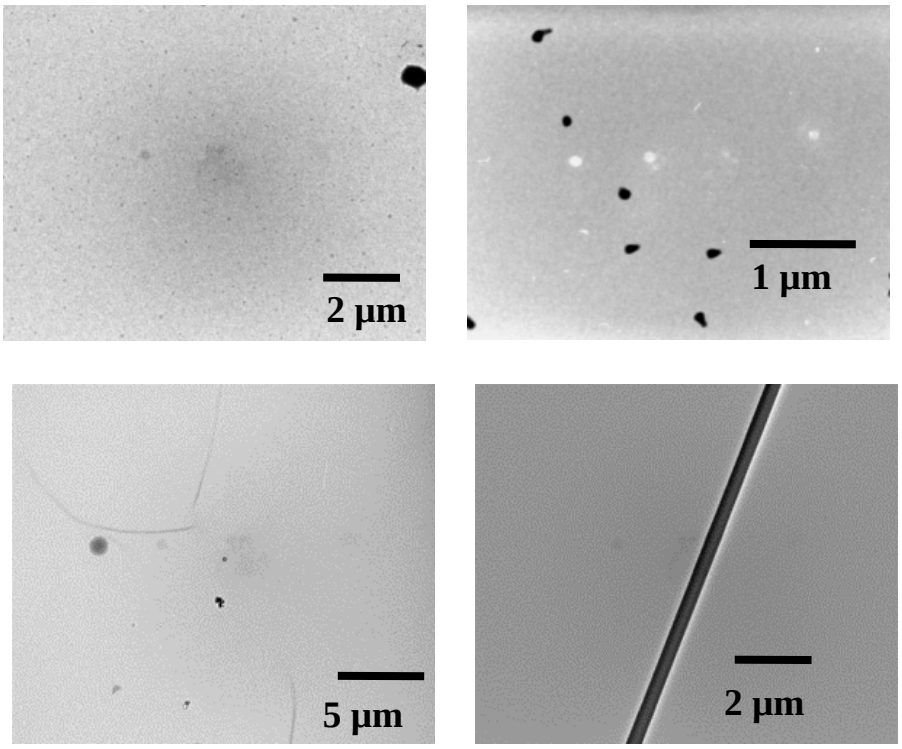

Figure 22: Effect applied voltage during electrospinning on PAA-CS fiber formation

The size, valence, specific ion and the concentration of ions was found to have an effect on the nanofiber morphology. The valence and the size of the ion determine the net charge density of the ion. In general, higher the charge density of the ion, greater is the stretching of jet resulting in smooth fibers. However, in case of ferric ions the higher charge density results in stronger interactions with PAA and immediate gel like formation. Fibers from solution containing ferric ions could be electrospun only after breaking those interactions by adjusting the pH of the solution to 1. The solution, thus obtained has much lower viscosity and much higher conductivity, as compared to other solutions and required low flow rates for Taylor cone formation and defect free fiber formation. PAA-CS solutions containing sodium chloride and calcium chloride have very similar viscosity and conductivity. Though, calcium chloride containing solutions exhibited little higher conductivity and less viscosity due to higher charge density of calcium ions as compared to sodium ions.

The morphology and diameter of the nanofibers also varied for different salts. Fibers electrospun from cerium ion containing solutions showed maximum diameter, and were more loosely packed, suggesting increased pore size, followed by calcium and ferric ions. Nanoribbons were observed along with nanofibers in case of ferric ions and some concentrations of cerium ion solutions. Higher concentration of cerium ion containing solutions and ferric ion turned into gel and could not be electrospun.

Interestingly, in addition to fibers other morphologies were also obtained from electrospinning at different concentration of metal ions and for different type of ion. For calcium solutions nanorods were observed. Fibers obtained from solutions with higher concentrations of calcium

chloride were observed to have re-crystallized nanocrystals on the surface of the fibers. Solutions containing cerium and ferric salts produced nanoparticles, nanorods and nanofibers when electrospun at different metal ion concentrations.

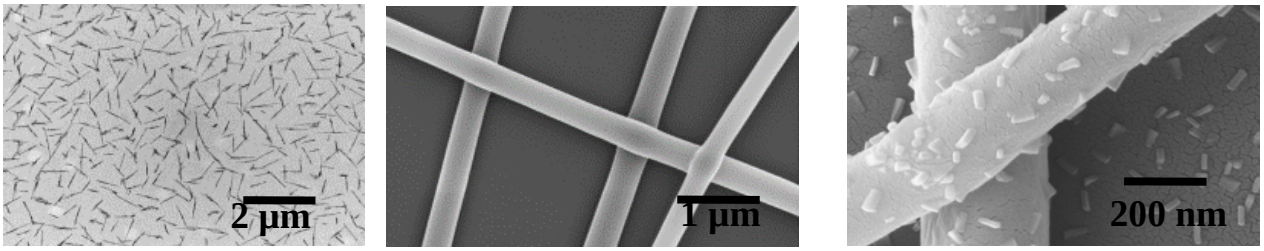

Figure 23: The effect of Ca^{2}+ ion concentration on the surface morphology of the PAA-CS-Ca^{2+} fibers.

Different electrospun morphologies can be explained as a result of coulomb fission because of the high conductivity of these PAA-CS-M^{n+} complexes. At low concentrations of ions, the solutions are conductive causing repulsive forces but the crosslinking is not enough for chain entanglements and jet stretching, the jet breaks into nanoparticles (electrospraying) for cerium and ferric ions due to high size to charge ratio. Nanoparticles formed from electrospinning or electrospraying of PAA-CS- cerium solutions were found to be 15 nm in size and were highly monodisperse (**Figure 24**).

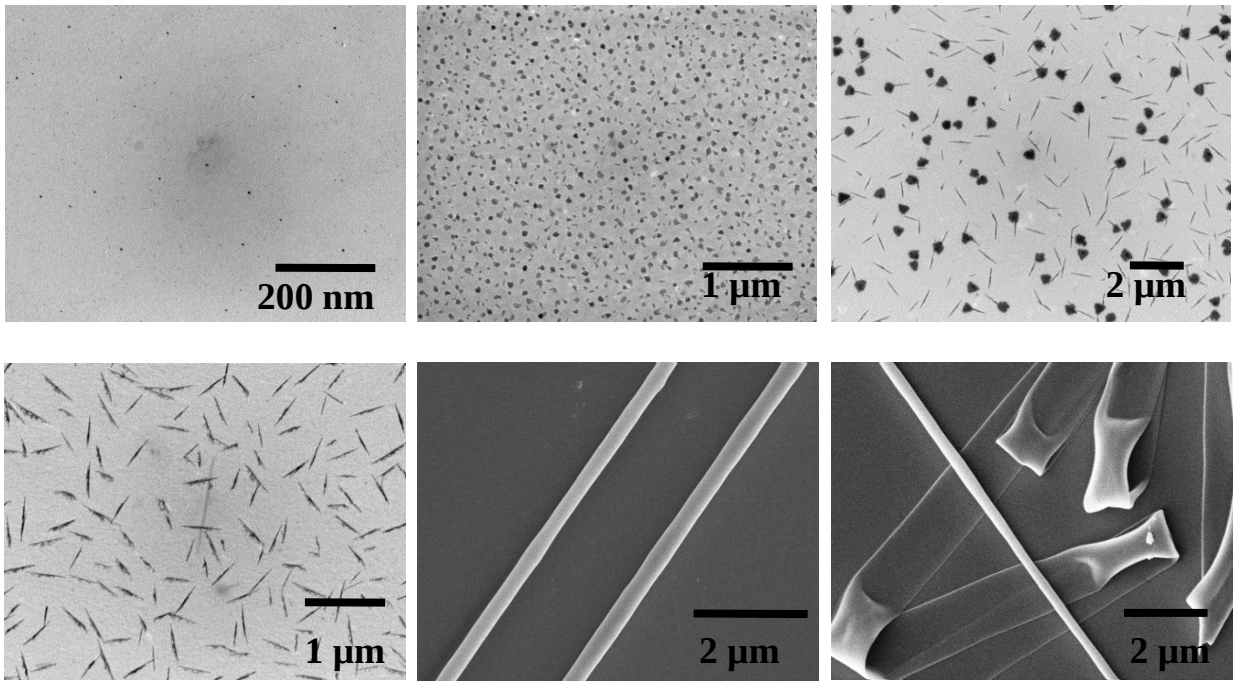

Figure 24: The effect of Ce^{3+} ion concentration on the surface morphology of the PAA-CS-Ce^{3+} fibers.

Due to the exceptionally high conductivity of ferric solution (because of addition of acid), the jet splits and secondary jet results in binary distribution of particles with primary particles of 10 nm in diameter and secondary jet resulting in 2-3 nm size particles as seen in **Figure 25**. With further increase in ion concentration, crosslinking also increases along with the conductivity, resulting in nanorods (25nm in diameter and 500nm in length). For calcium at lower concentrations, solution is conductive, but there are no entanglements for electrospraying or electrospinning. At little higher concentration, some cross linking is there, but not enough charge density for coulomb fission, hence resulting no nanoparticles were observed, only nanorods of 25 nm in diameter and 400-500nm in length were obtained. At optimal concentration and viscosity nanofibers are obtained for all the ions. Fibers are found to be homogeneous with smaller

diameter (100-200 nm) and defect free in this range. At further higher concentrations of cerium and ferric ions, the fiber morphology changed from cylindrical to flattened (nanoribbons) with increased diameter size due to high viscosity and/or increased flow of solution (high conductivity) from tip to collector, resulting in incomplete drying of the solvent before reaching the collector.

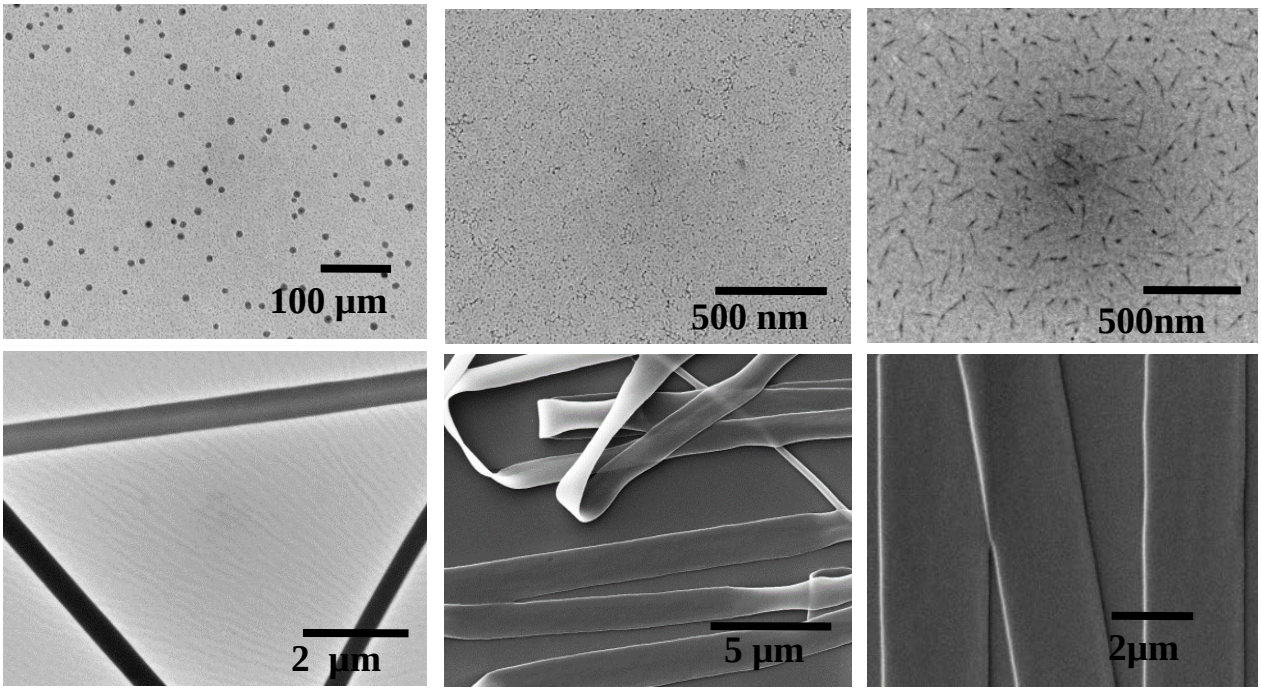

Figure 25: The effect of Fe^{3+} ion concentration on the surface morphology of the PAA-CS-Fe^{3+} fibers.

The morphology dependence of ions seems to be interplay between shielding and crosslinking ability of the ion. Sodium ions, being monovalent, shield polyelectrolyte charges, cause shrinking of molecule chains and decrease in hydrodynamic radius and viscosity. In addition to shielding effect, divalent and multivalent ions can crosslink and interconnect the PAA chains, influencing the conformation and interaction with chitosan. The crosslinking behavior becomes prominent with increase in valency and overshadows the shielding effect. Both intra chain and

inter chain cross-linking takes place in this scenario. Therefore, it is expected that cerium and ferric ions exhibit higher viscosities and gel formation than calcium ions. The stronger interactions of ferric ions with PAA than cerium ions can be explained due to higher charge density of ferric ions due to comparatively smaller ion size of ferric ions. PAA-CS solutions containing sodium chloride and calcium chloride exhibited similar properties. The little difference in viscosity and conductivity can be attributed to better shielding effect of calcium ions than sodium ions due to stronger binding of calcium ions with PAA and ability of calcium ions to penetrate into the cylindrical symmetry of the polyelectrolyte chains than sodium ions.

5.3 Swelling and Stability:

PCF density (chitosan concentration and extent of thermal crosslinking), the interaction between ions and polyelectrolytes and the pH of the solutions play important roles in affecting the swelling ratio of the fibers. The swelling of these fibers leads to polymer-solvent interaction, dilution of the counter ions, electrostatic interactions between the polyion charges, the polyelectrolyte elasticity and the diffusion of molecules across the fibers along with the solvent (water in most cases).The hydrogen bonding and polar interactions within water molecules and water-polyelectrolyte dictates the swelling and subsequent diffusion through these fibers. The swelling of PAA-CS PCFs can be attributed to electrostatic forces due to the ionized group and since PCFs have free PAA molecules (depending on CS concentration) and their degree of ionization depends on the pH of solutions, the PCFs will have pH dependent swelling behavior. In other words, at high pH, the repulsion among the negatively charged carboxylate ions on PAA molecules increases the free volume, thus expanding its capability in taking water.

(a)

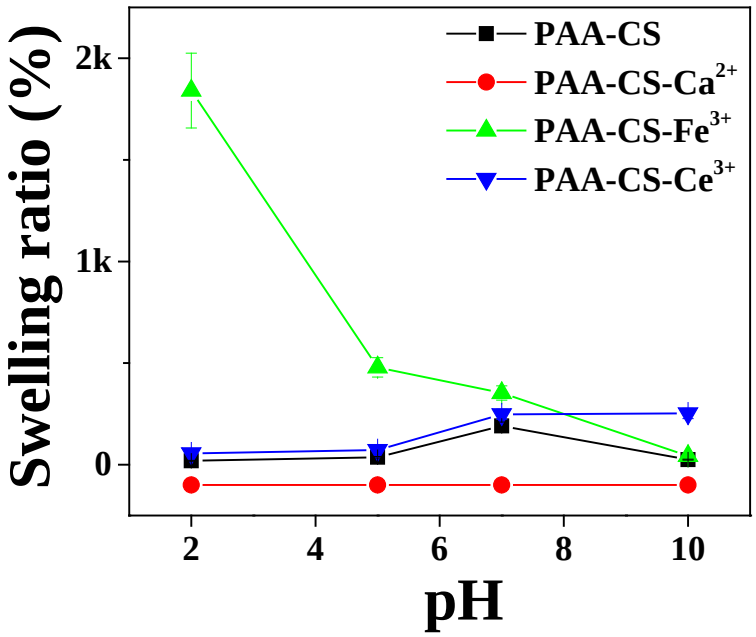

(b)

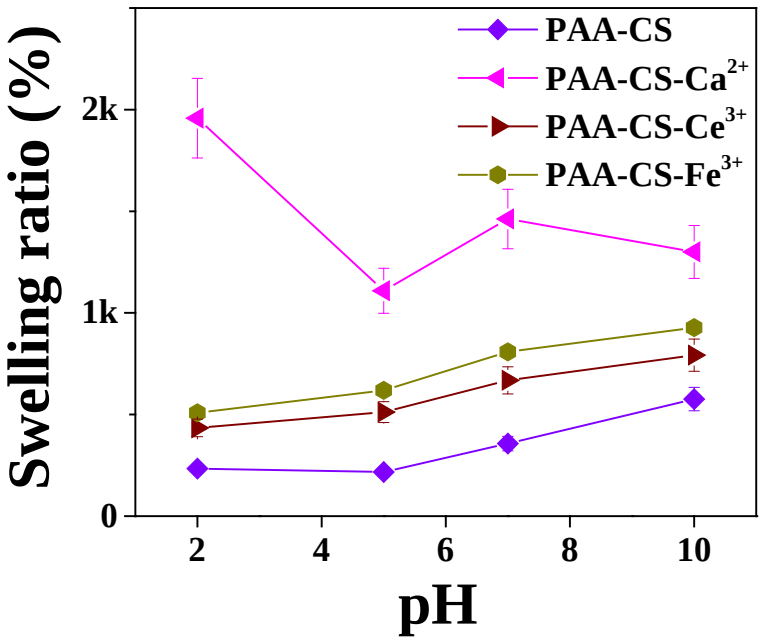

Figure 26: Swelling ratio of **(a)** non cross-linked and **(b)** cross-linked fibers.

For PAA-CS-M^{n+} fibers the size to charge ratio of M^{n+} and cross-linking of PAA-CS complex at particular pH by M^{n+} determines the swelling of the fibers. It is observed that PAA-CS-M^{n+} fibers have higher swelling ratios than PAA-CS fibers and fibers with cerium ions have higher swelling ratio than ferric and calcium ions. With smaller size to charge ratio, as in case of ferric ions, the interaction with carboxylates of PAA is very strong resulting in high metal ion based crosslinking and less swelling. Figure demonstrates the swelling behavior of PAA-CS-M^{n+} fibers at different pH.

The degree of ionization of PAA and CS is pH dependent in solutions, and the metal ion-polyelectrolyte interactions vary with the solution pH, leading to a pH dependent stability and swelling behavior. We hypothesize that at low pH (i.e. 3), since most carboxyl and amine groups are protonated, the metal ion-PAA interactions are mainly through d orbital coordination. Therefore, it is expected that the PCFs with sodium and calcium ions are less stable than the PCFs with transition metals. When the solution pH increases, the concentration of carboxylate and amine groups increases, and promotes the PAA-CS and metal ions-carboxylate electrostatic interactions, and metal ion-amine (CS) d orbital coordination. At high pH, PAAs are fully ionized and most amine groups in CS are neutral, the fiber stability depends on the competition between metal ion-OH interactions and metal ion-carboxylate interactions plus metal ion-CS d orbital coordination.

The effect of crosslinking with chitosan and pH on the swelling of fibers is also quite evident from the data presented here. The enhanced crosslinking between PAA and chitosan reduces the number of PAA carboxylate interaction with metal ions, thus more metal ions are free for water uptake. However, according to the swelling ratio data, the non cross-linked fibers have less

swelling than cross-linked fibers. This can be attributed to the less stability of non cross-linked fibers than cross-linked fiber at low and high pH.

5.4 Interfacial reactions of PCFs:

The large surface area with interconncectivity, functional groups to anchor molecules and permeability to molecules ensures continuous flow of molecules for chemical/biological processes. With hydrogel like structure, controlled release of the reactant or molecular precursors can be achieved. The rate of reaction can be altered by controlling diffusion through density (PAA: CS ratio), cross-linking (electrostatic and/or covalent) and metal ion concentration. The reaction can also be controlled by other reactant concentrations, reaction time and conditions. Thus, PCFs have great potential in nanofabrication, catalysis and as nanoreactors, with their large surface area, rich carboxylate and amine groups, stability in different solvents and the ability to swell to facilitate the diffusion of reactants in and out the fibers. The metal ions can further take part in different reactions as catalysts, reducing agents, oxidants etc. As a proof of concept of metal ions loaded PCFs for nanofabrication four different types of reactions are presented here: reduction, hydrolysis, polymerization and hydroxyapatite formation. Depending on the reaction conditions, the polymerization can be achieved in the solution, on fibers or on other substrates, thus providing a control over the reaction.

5.4.1 Reduction or hydrolysis (metal or metal oxide nanoparticles): The electrostatic interaction between the metal cations and anionic groups of one of the polyelectrolytes drives the incorporation of metal cations into the fibers. Subsequent reduction/ hydrolysis lead to the formation of metal and metal oxide/hydroxide nanoparticles, respectively. Current approaches include *in situ* fabrication where nanoparticles are added to polymer solutions before

electrospinning and post fabrication where nanoparticles are introduced onto fibers via reactions in solutions. Post fabrication approaches are not sufficient in obtaining uniform and controlled functionalization in large scale while the amount of nanoparticles in fibers is limited by the dispersity of nanoparticles in polymer solutions in *in situ* fabrication approaches. [50, 51, 54, 59, 62, 88, 123, 126-130]

The rich environment of PAA-CS fibers further ensures the particle confinement into the matrix. The fabrication of nanoparticles on the polyelectrolyte fiber matrix eliminates the surface modification step which is often necessary in solution based synthesis to obtain particles without aggregation. The recovery and purification of the nanoparticles after the surface modification is also difficult and leads to loss of products. Synthesis of nanoparticles in these fibers also has the advantages of easier removal of impurities, byproducts and excessive reactants, protection of molecule precursors by the functional group of the matrix. As a proof of concept, we synthesized iron (reduction) and ceria nanoparticles (hydrolysis) in PAA-CS fibers. The size of both iron and ceria nanoparticles obtained was of 5 nm, however, iron nanoparticles were embedded in matrix (**Figure 27**), whereas ceria nanoparticles were present at the interface (**Figure 28)**.

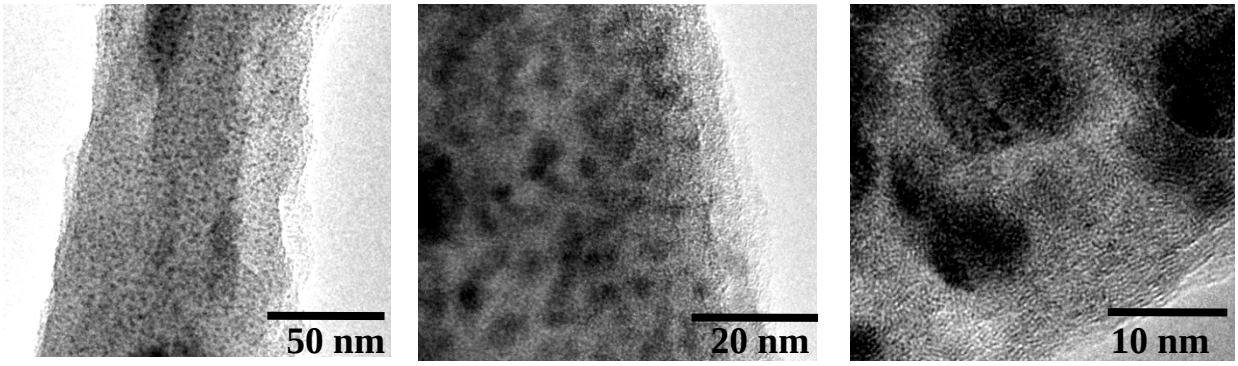

Figure 27: TEM images of iron nanoparticle loaded fibers synthesized from reduction of PAA-CS-Fe^{3+} fibers.

This difference can be explained by diffusion of molecules across the fibers. The diffusion of nascent hydrogen produced from sodium borohydride into the fibers from solution is much faster than the diffusion of ferric ions outside the fibers because of the small size of hydrogen radical, thus the reaction takes place in the matrix and particles synthesized are embedded in the matrix. In case of ceria nanoparticles synthesis, the diffusion of hydroxyl ions inside fibers s faster than the diffusion of cerium ions outside the fibers, with reaction taking place at interface.

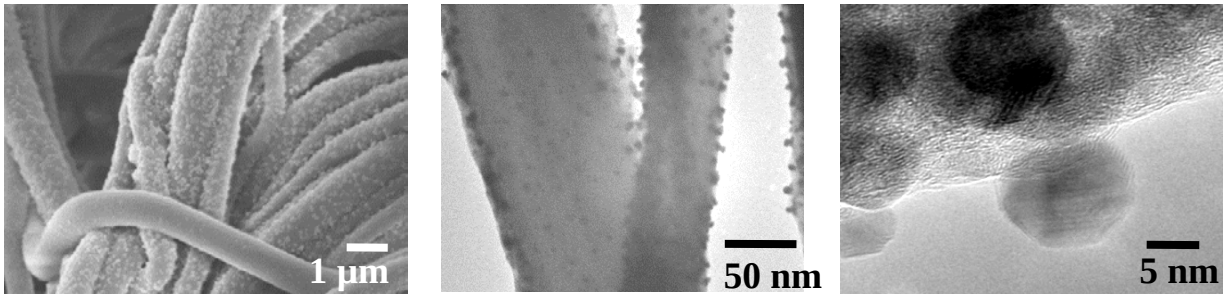

Figure 28: Electron micrographs of ceria nanoparticle loaded fibers synthesized from hydrolysis of PAA-CS-Ce^{3+} fibers: **(a)** SEM, **(b)** TEM and **(c)** HRTEM

5.4.2 Polymerization:

In this study, ion loaded PCFs for polymerization reactions were demonstrated through the pyrrol polymerization. Polypyrrole (PPy) is a widely known and investigated conducting polymer with applications in sensing and tissue engineering, actuators and solar cells. It is highly biocompatible and is extensively used in neural regeneration. In our studies, oxidation polymerization of pyrrole on fiber surfaces was obtained by incubating ferric ion loaded fibers in a solution of pyrrol. The ferric ions in fibers diffused toward the fiber surface and initiated the polymerization of pyrrole. Pyrrole was polymerized, on the fiber surfaces as conducting shells and the color of the fibers changed to black as a result of the PPy deposition. As shown in Figure 7, a layer of polypyrrole was conformly deposited on the PAA-CS fibers.

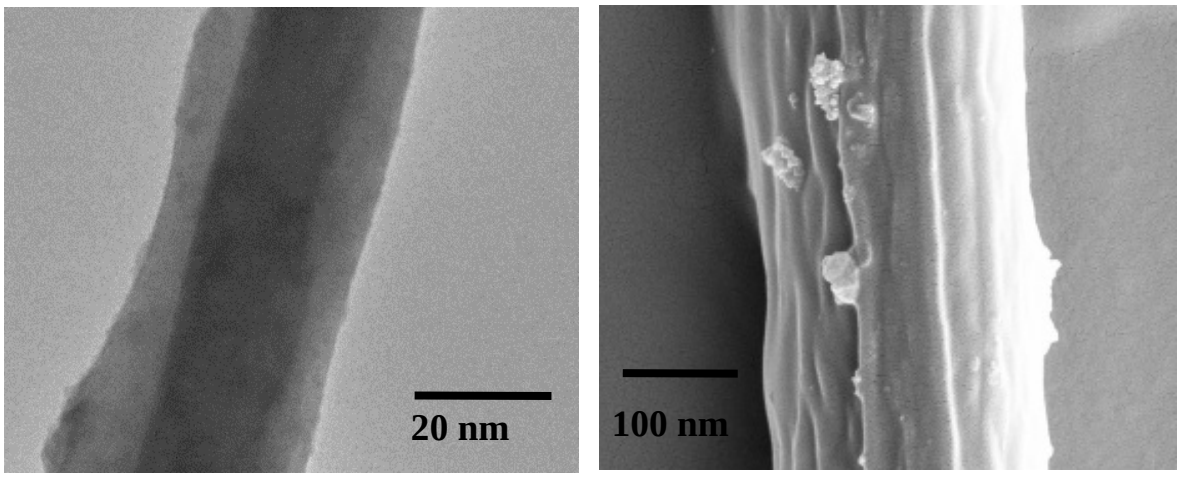

(a) (b)

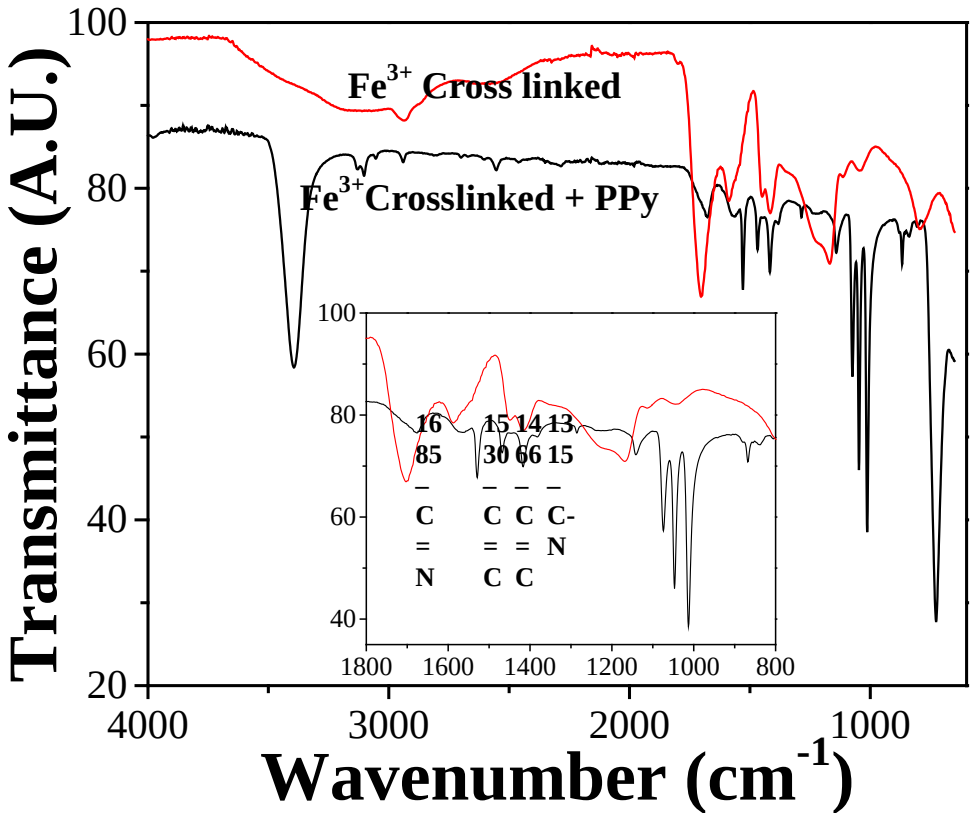

(c)

Figure 29: PAA-CS-Fe^{3+} fibers for in-situ polymerization of pyrrole. Morphology of the polypyrrol coated fibers: **(a)** TEM, **(b)** SEM images and **(c)** IR spectra showing the formation of PPy.

5.4.3 Biommimetic mineralization:

We propose that PAA-CS fibers can be used as scaffolds for biomimetic mineralization for bone and tissue regeneration. Hydroxyapatite (HaP) grown under biomimetic conditions is known to highly resemble the structure found in bone. Biomimetically mineralized fibers were obtained by incubating PAA-CS PCFs loaded with calcium ions in SBF at 37°C, for Hap nanocrystal formation.

It was observed that the Hap nanocrystals formed all over the surface of fibers. The crystals obtained were spherical or close to spherical in shape (and not rods) in shape, with an average diameter of 5 nm. The diffusion of calcium ions from the fibers into the solution is expected to be faster compared to the phosphate anions, suggesting that the reaction took place at the interface and Hap nanocrystals were found at the interface of fibers. Moreover the time of reaction leads to more diffusion of calcium ion from the fibers. The difference in shape can be attributed to the control of particle growth by polymer matrix.

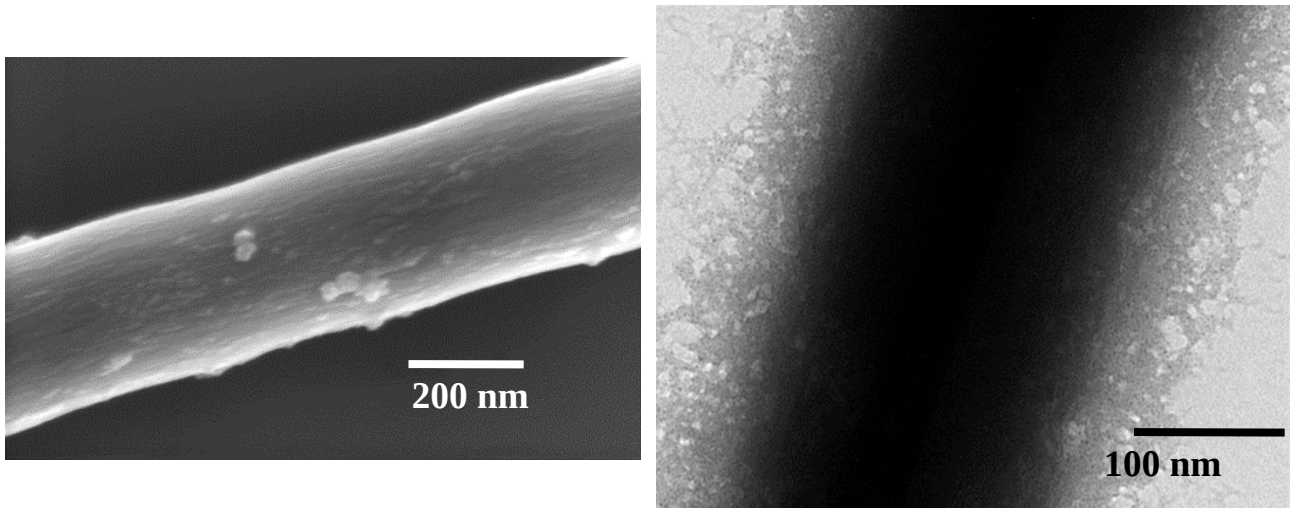

(a) (b)

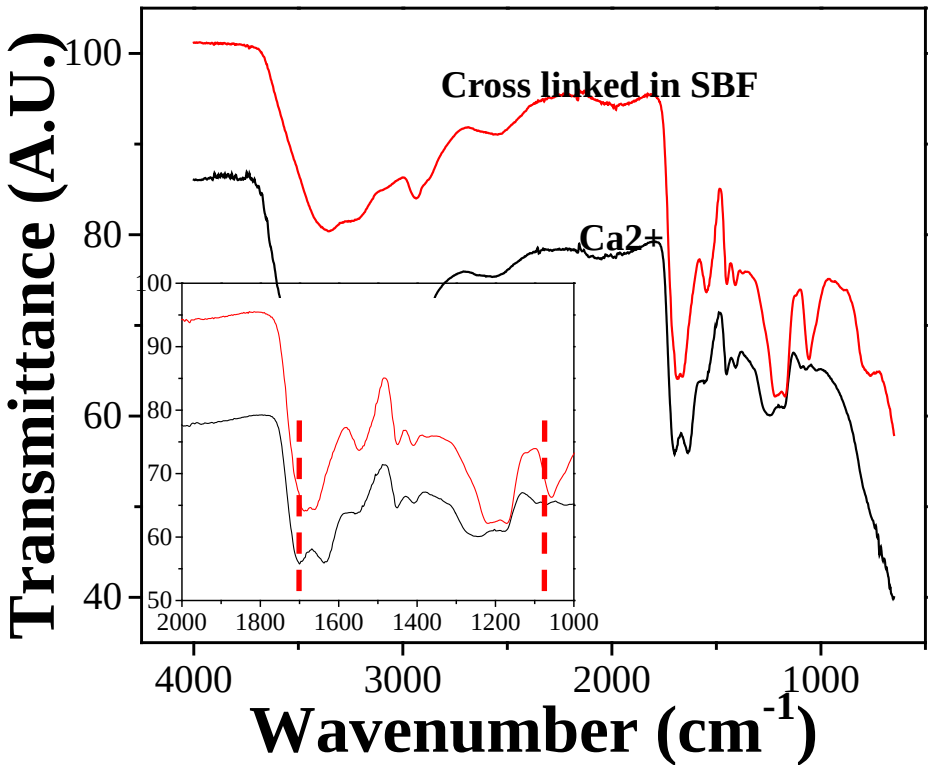

(c)

Figure 30: Calcium ions within the PAA-CS fibers can be further converted to HAP crystals: **(a)** TEM, **(b)** SEM and **(c)**IR spectra showing the formation of HAP.

Both PAA (carboxyl for Hap mineralization) and CS with its ability to control nucleation and growth during the mineralization process and prevent the interfacial mismatch. Confining and ordering the calcium cations onto a matrix prior to mineralization, ensures a more crystalline and ordered HaP. Due to the hydrogel nature of the fibers and controlled release of calcium, faster and more controlled growth of Hap nanocrystals occurs. The nanoscale structure and morphology of fibers (curved and cylinder) promotes the mineral orientation and length during the mineralization process similar to that of the bone and thus have immense potential for HaP mineralization and bone regeneration through a bottom-up scalable approach without the addition of any proteins.

Different reactions have different reaction conditions like pH or temperature and require the use of different solvents (organic, acids, bases). It is crucial for PCFs to withstand these reactions without degradation. It was observed that the PCFs were able to withstand all these conditions and there was no degradation or any other significant change in their morphology (other than swelling), as observed from SEM and TEM images.

5.5 Conclusion:

Functional nanofibers were electrospun from PAA-CS-M^{n+} complex using water as solvent. It was found that the metal ion identity and concentration in the salt greatly affects the morphology of electrospun nanostructures. The presence of metal ions and metal identity also influences the diffusion of molecules across the fibers. The potential of these PCFs as reservoirs for controlled release of ions in applications such as nanoreactor (nanoparticle synthesis), nanofabrication (mineralization, polymer coating), catalysis (polymerization), etc. has been demonstrated.

CHAPTER 6: DIFFUSION STUDIES

6.1 Introduction:

The diffusion through these fibers is due to random motions of the non-uniformly distributed molecules owing to concentration gradient across the fibers. Diffusion of molecules can be explained by Fick's first law where, the rate of diffusion per cross-section unit (flux) is directly proportional to a constant concentration gradient. However, in real, including diffusion through fiber, the concentration gradient changes with time. This situation can be explained by Fick's second law that describes diffusion as a function of time[131], corresponding to experimental conditions.

Typically, when dry, ion-loaded, polymer matrix is immersed in a releasing medium, the polymer starts to swell and relax[132]. Concurrently, ion diffusion will take place. Therefore, the difference between polymer relaxation rate and ion diffusion rate leads to ion diffusion profile across the fibers. If the rate of diffusion is much less than that of polymer relaxation, the diffusion will be the rate determining and the profile follows the Fickian mechanism: $M_t/M_\infty = kt^{0.5}$, where M_t and M_∞ are the accumulative and maximal amounts of ion diffused out, respectively, t is the releasing time and k is the diffusion coefficient. In contrast, if the rate of ion diffusion is much larger than that of polymer relaxation, the rate of interface movement is constant. Therefore, the amount is proportional to time: $M_t/M_\infty = kt$. When the rates of polymer relaxation and ion diffusion are about the same, the releasing is determined by both factors, leading to Ritger-Peppas' empirical equation: $M_t/M_\infty = kt^n$ $(0.5<n<1)$[133, 134].It should be kept

in mind that diffusion can both from outside to inside of the fibers and inside to outside of the fibers and depends on the size, shape and density of the specimen. Both the processes can take place at the same time and sometime at same orders of magnitudes.

Thus, the diffusion kinetics of metal ion loaded MPECS was investigated in two aspects: diffusion of ions out of the MPECs and the diffusion of dye from surroundings into the MPECS. The studies were performed with Arsenazo III (1, 8-dihydroxynaphthalene-3, 6-disulphonic acid-2, 7-bis [(azo-2) phenylarsenic acid]) a dye which forms highly colored complexes with metal ions (**Figure 31**). While uncomplexed Arsenazo is wine-red, the metal-Arsenazo complex ranges from green, blue or purple in color [135-137], depending on the metal ion and pH. It is hypothesized that the affinity and crosslinking of ions with PAA-CS will play a significant and contradictory role in diffusion and complexation of ions with dye.

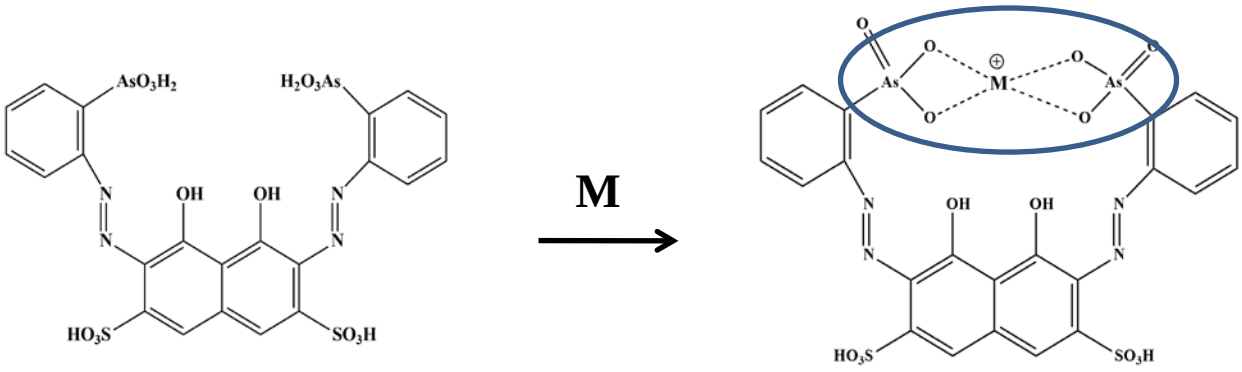

Figure 31: The molecular structure of the Arsenazo III dye before and after the complex formation with metal ions. The native dye solution has a absorption maxima at 538 nm; upon metal binding, either there is red shift in the absorption maxima or a new peak towards red appear, depending upon the metal ion.

The diffusion was monitored by tracking uncomplexed Arsenazo's absorbance peak at about 538 nm and the release of ions was monitored by absorbance of metal-ion Arsenazo complex around 600-650 nm. The complexation of dye with metal ions would result in decrease in the absorption of uncomplexed dye. However, a decrease in peak of uncomplexed dye may not be directly proportional to the complexation, as decrease can also be due to the uptake of dye in to the MPECs from the solution. Thus, decrease in dye is a combination of two processes (**Figure 32**).

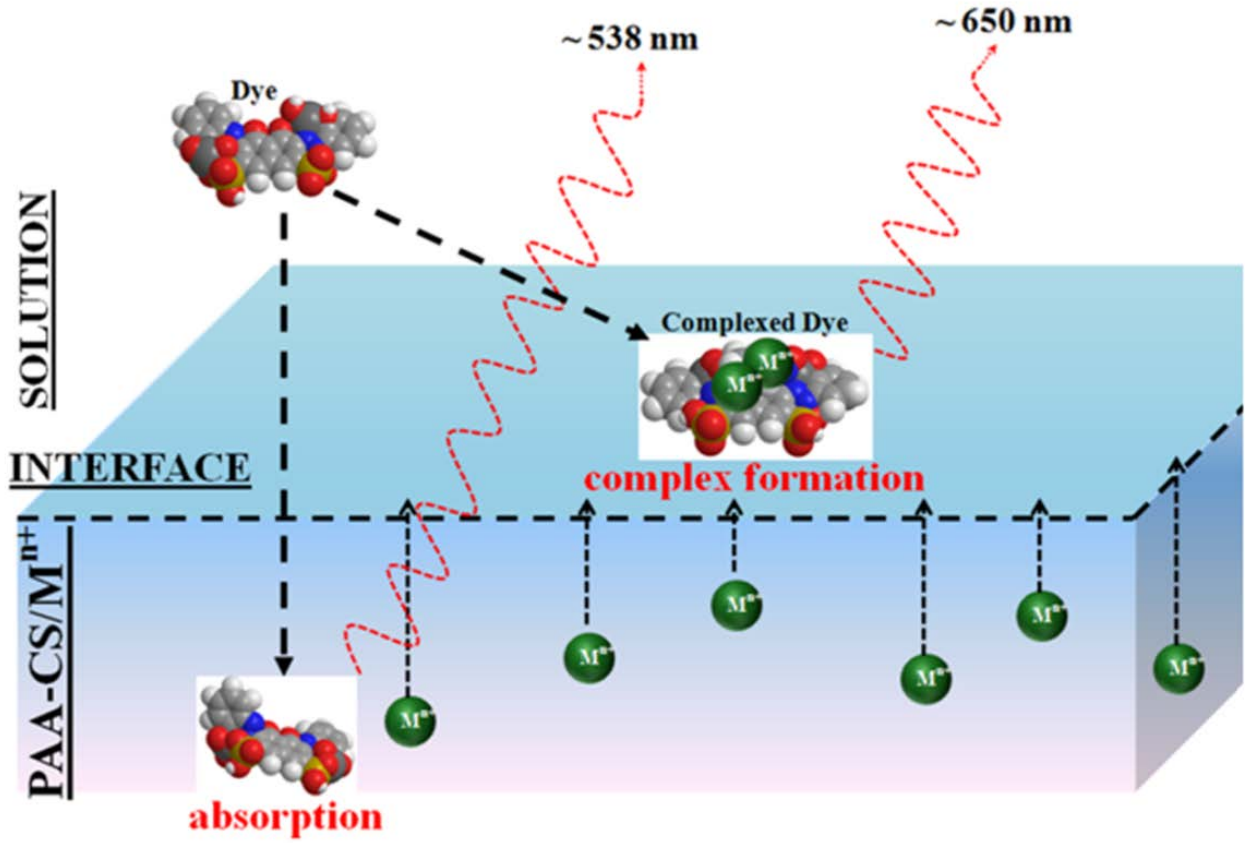

Figure 32: A schematic showing the diffusion of dye and metal ions happening simultaneously across the matrix and complex formation at matrix-solution interface.

6.2 Effect of PAA:CS ratio:

As a solvent diffuses into a network, the arrangement of the polymer chains will change as they adapt their conformation to the new concentration of penetrant. This rearrangement towards a new equilibrium state is unlikely occur instantaneously, especially when the rate of uptake is very high as in superabsorbent polymers. Two processes therefore influence the rate of swelling, the rate of diffusion of the penetrant molecules, and the response time for the network to relax towards its equilibrium conformation. Their relative rates determine the nature of diffusion, which may be deduced from observations of absorption with time.

The dye molecules are present in solution and diffuse inside the molecules, whereas the ions are present inside the fibers and diffuse out. This serves as an excellent model to study the role of diffusion in interfacial reactions. The rate of the two diffusion process determines the rate of reaction and whether the reaction will occur inside the fibers, in the solution or the interface. If the diffusion of ions is faster than the diffusion of dye inside the fibers, the reaction will take place in the solution. On the other hand, if dye diffuses faster than ions, reaction will occur inside the fibers. If the two diffusion rates are comparable then the reaction is more likely to happen at the interface. In general, diffusion of metal ions into the solution should be faster than the diffusion of dye molecules inside the fibers due to the small size of metal ions as compared to the metal ions.

The diffusion profile consisted of two sequential diffusion stages. The first stage of fast release/uptake ($t < 50$ min) follows the Fickian mechanism. In the second stage ($t > 40$ min), ion/ dye diffuses with a reduced rate probably due to the decreased concentration gradient.

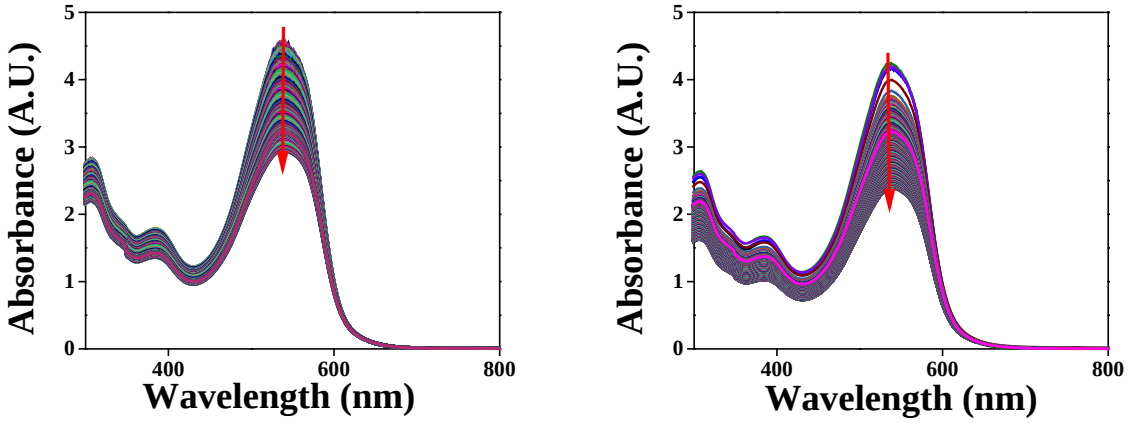

(a) (b)

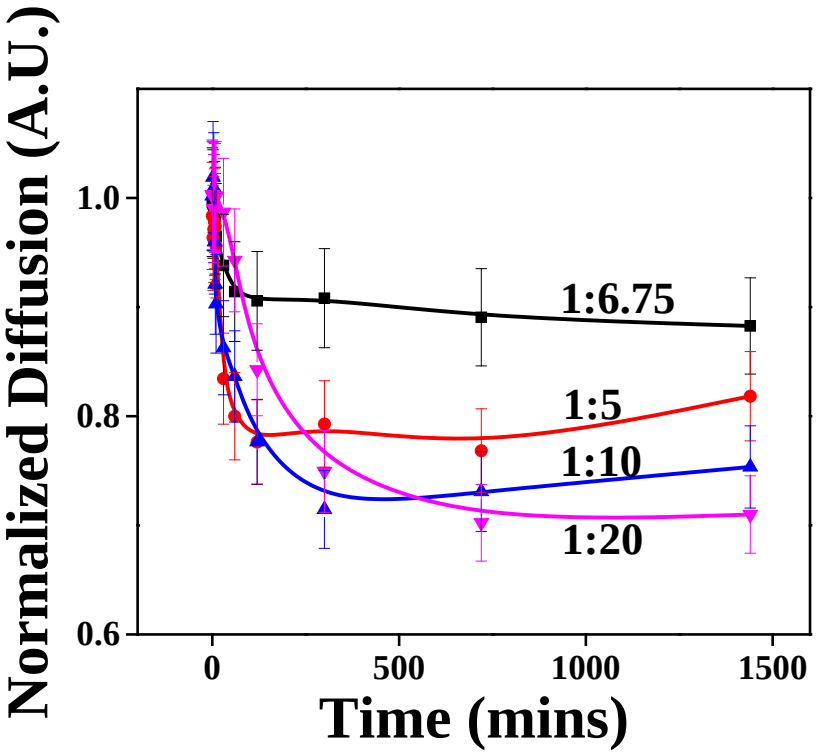

(c)

Figure 33: The effect of PAA:CS ratio on the diffusion of the dye in PAA-CS **gel**: the spectral change for the proportion **(a)** 1:6.75 and **(b)** 1:5; and **(c)** normalized diffusion of dye into the gels as a function of PAA: CS ratio.

6.3 Effect of metal ions:

It appears from the data that PAA-CS fibers exhibit the maximum decrease in dye, with pretty much no dye left in the solution, thus indicating the uptake of dye by fibers since there are no metal ions present, ruling out the possibility of complex formation (**Figure 35**). In case of PAA-CS-M^{n+} fibers, it was observed that the presence of metal ions and metal identity influence the diffusion of molecules across the fibers (**Figure 36**). There is a decrease in the dye; however, it is much lesser than the PAA-CS fibers, suggesting that presence of metal ions inhibit the dye uptake.

6.4 Effect of cross-linking:

As expected, the complex formation (as observed from absorbance at both 538 nm and 650nm) is affected by the crosslinking of ions with PAA-CS. The deviation of ferric ions is due to the acidification of ferric complexes to break strong interactions as mentioned above. We have also introduced diffusion studies with zirconium ions for comparison purposes.

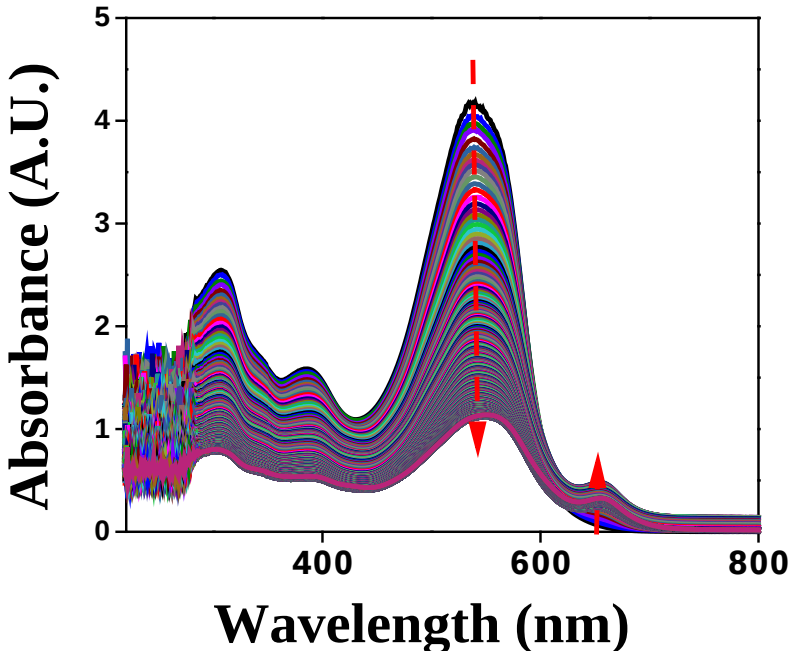

(a)

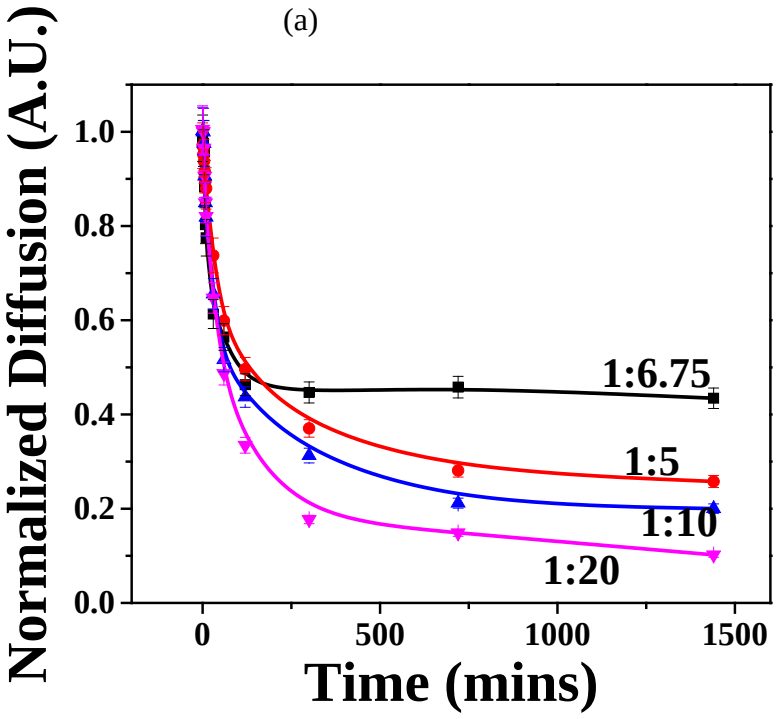

(b)

Figure 34: The diffusion kinetics of the Arsenazo dye in PAA-CS non cross-linked fibers: **(a)** The spectral change of the dye, **(b)** The change in 538 nm peak with time as a function of PAA:CS ratio.

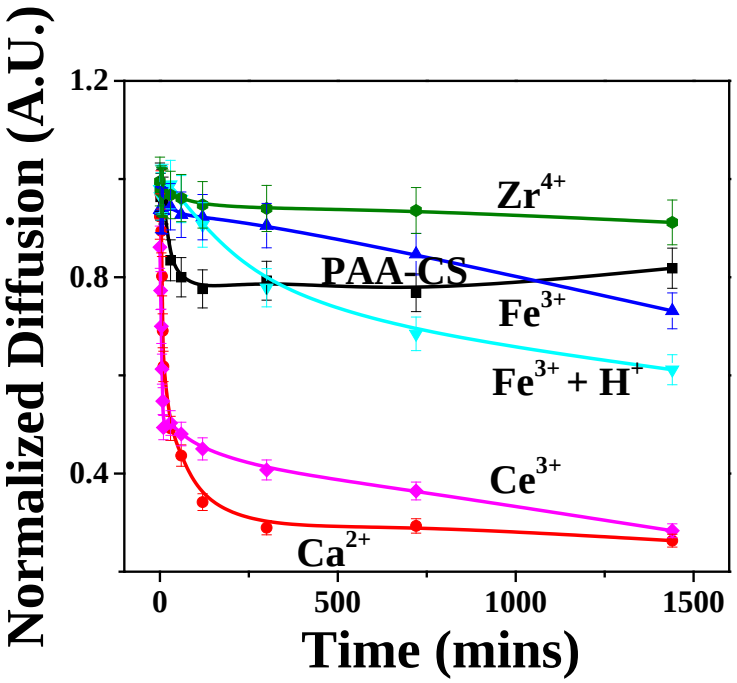

(a)

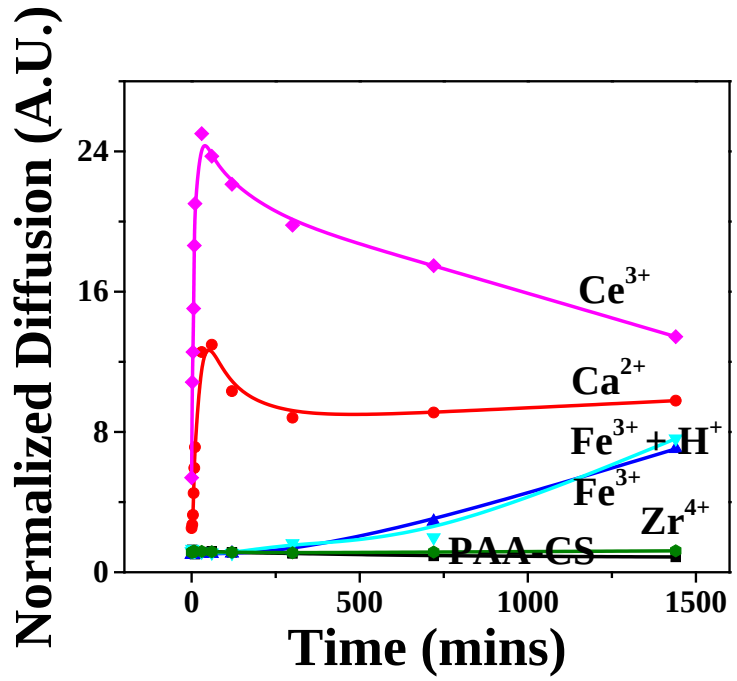

(b)

Figure 35: The effect of Metal ion on the diffusion for the PAA-CS **Gels**. **(a)** change in 538 nm absorption peak of dye and **(b)** complex formation peak at 650 nm with time as a function of different metal ions.

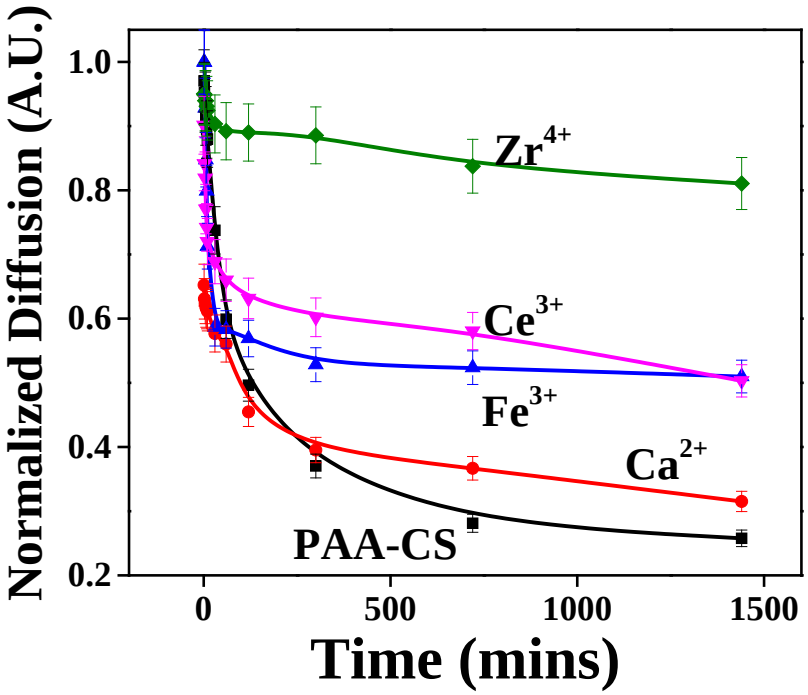

(a)

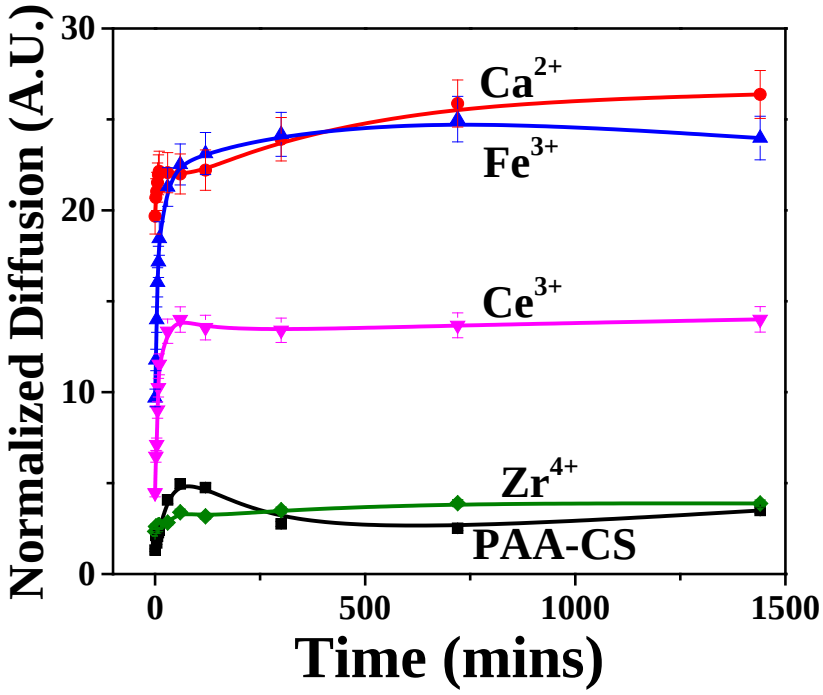

(b)

Figure 34: The effect of Metal ion on the diffusion of the dye: **(a)** spectra change in PAA-CS-Ce^{3+} ion fiber, **(b)** the change in 538 nm peak and **(c)** 650 nm with time as a function of different metal ions.

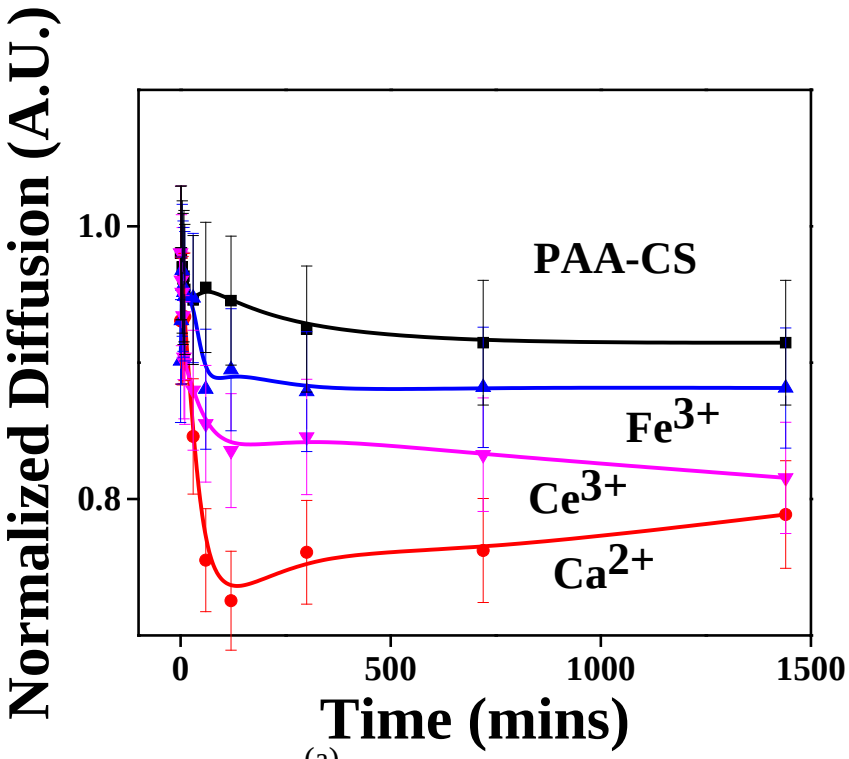

(a)

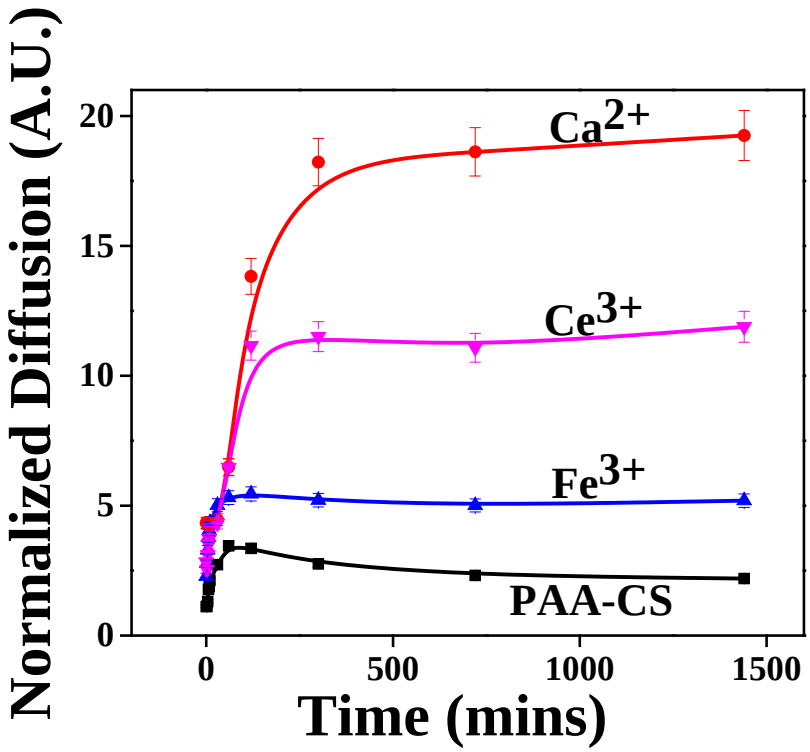

(b)

Figure 37: The effect of Metal ion on the diffusion for the PAA-CS thin films: **(a)** change in **(b)** 538 nm peak and **(b)** 650 nm with time as a function of different metal ions.

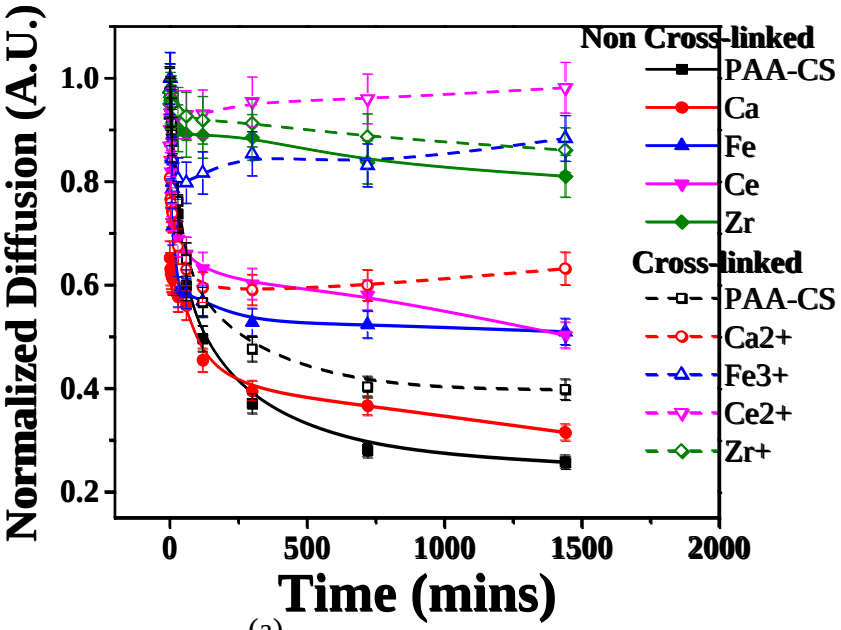

(a)

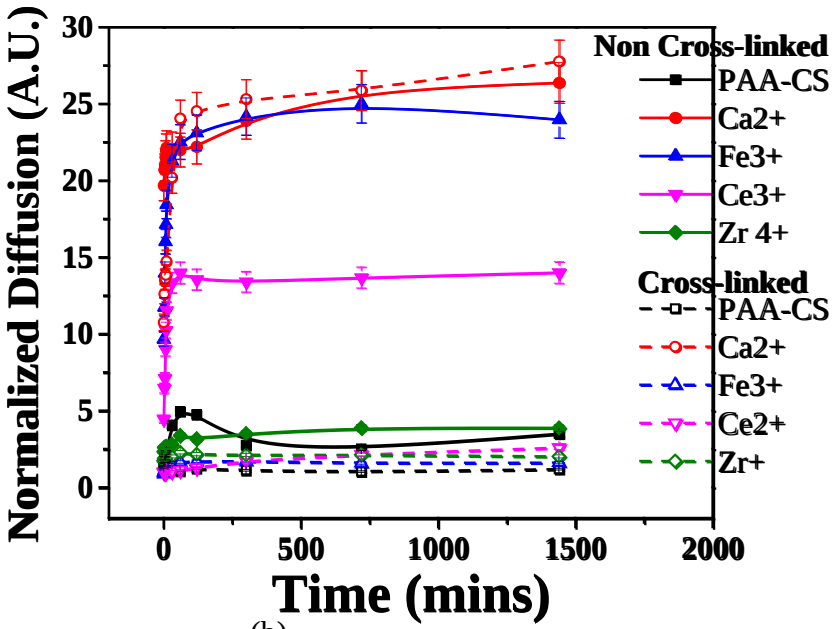

(b)

Figure 38: The effect of cross-linking on diffusion: comparison of both cross-linked and non cross-linked conditions together **(a)** at 538 nm and **(b)** 650 nm.

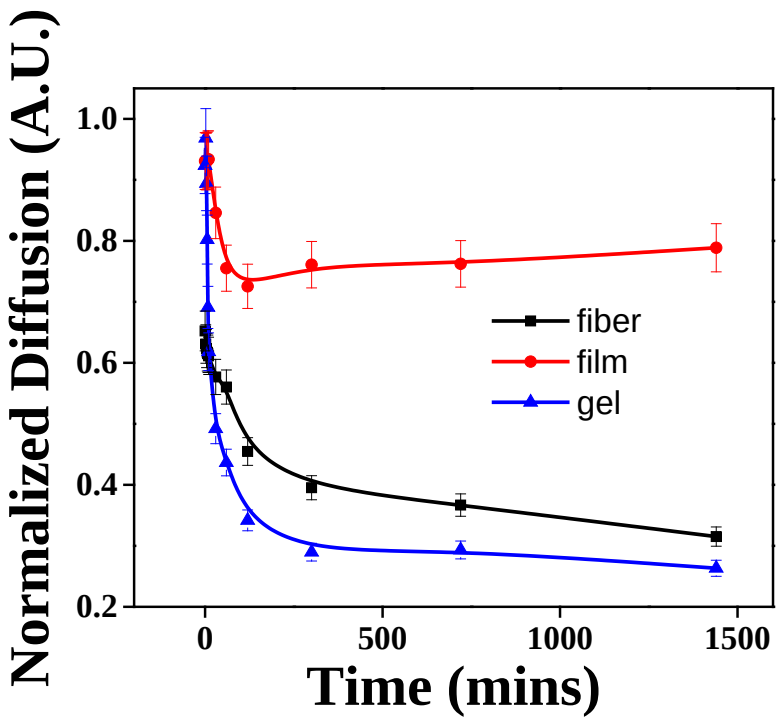

(a)

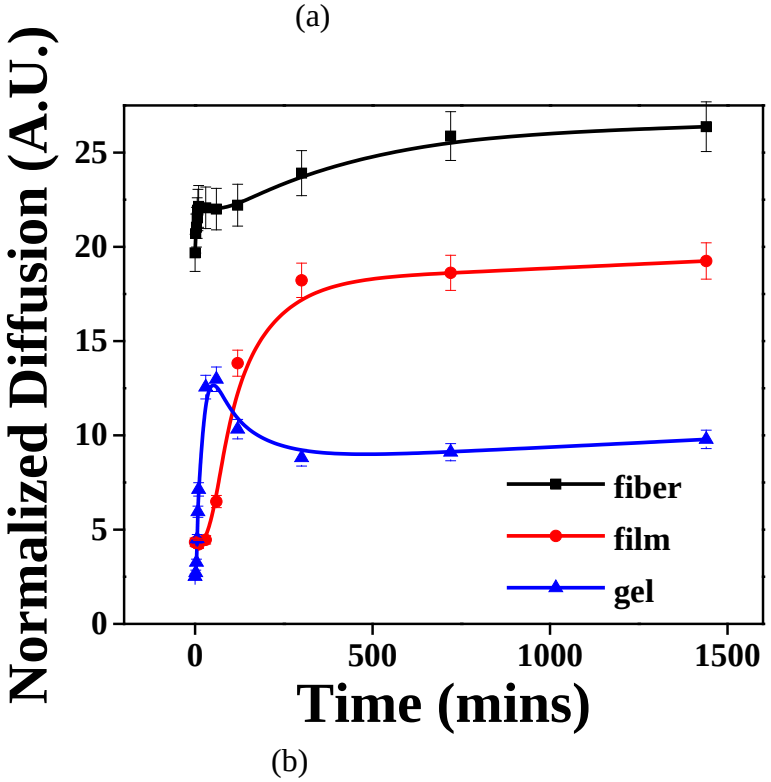

(b)

Figure 35: The effect of dimension, i.e. fiber (1D), thin film (2D) and gel (3D) on diffusion. The change in **(a)** 538 nm peak and **(b)** 650 nm with time.

6.5 Effect of dimension:

The most significant challenge to make efficient hydrogel devices is the slow response related to low diffusion coefficient. Because hydrogel swelling kinetics are inversely proportional to the square of the dimension, hydrogel fibers with reduced size and larger surface area offer more efficient material transport and faster response than hydrogels.

The polyelectrolyte fibers are expected to facilitate the diffusion of molecules from surrounding environment and stimulus with fast response, due to their nanoscale dimensions and high surface to volume ratio, high porosity and geometrical reasons. Hence, these fibers can be used for interfacial reactions. The reactions take place as a result of diffusion of molecules across the fibers.

6.6 Conclusion:

The diffusion of embedded metal ions from MPECs into aqueous solutions is affected by metal ion/polyelectrolyte interactions. It is expected that, transition metal ions will have a smaller diffusion rate than main group metal ions of the same valence because of stronger metal ion/polyelectrolyte interactions. The release or diffusion can be controlled by various parameters thus providing control over their properties and interfacial reactions on their surface.

CHAPTER 7: APPLICATION OF PAA-CS-M^{n+} COMPLEXES

7.1 Introduction:

Because of their porous structure, hydrogel nature, ease of chemical modification, biodegradability, biocompatibility and large surface area, PAA-CS-M^{n+} fibers and gels are promising candidates for biomedical applications. The good physicochemical and biological properties of PAA-CS, use of these biomaterials in tissue engineering and other applications show considerably very good physicochemical and biological properties.

7.2 Biodegradation:

It is known that in body chitosan is degraded enzymatically by lysozyme. In vitro degradation of scaffolds was investigated in physiological conditions in two different mediums PBS and Lysozyme solution (1mg/ml) as biomimetic fluids. Degradation was monitored at 37°C using weight loss method. During the degradation tests, the hydrogel samples steadily decreased in size. It is clearly observed that scaffolds degraded relatively faster in lysozyme solution than in PBS solution. The faster degradation is hypothesized due to the decreases stability of scaffolds because of decreased crosslinking due to degradation of chitosan. It was observed that scaffolds exhibited a decent degradability at physiochemical conditions, hence can be used for various applications.

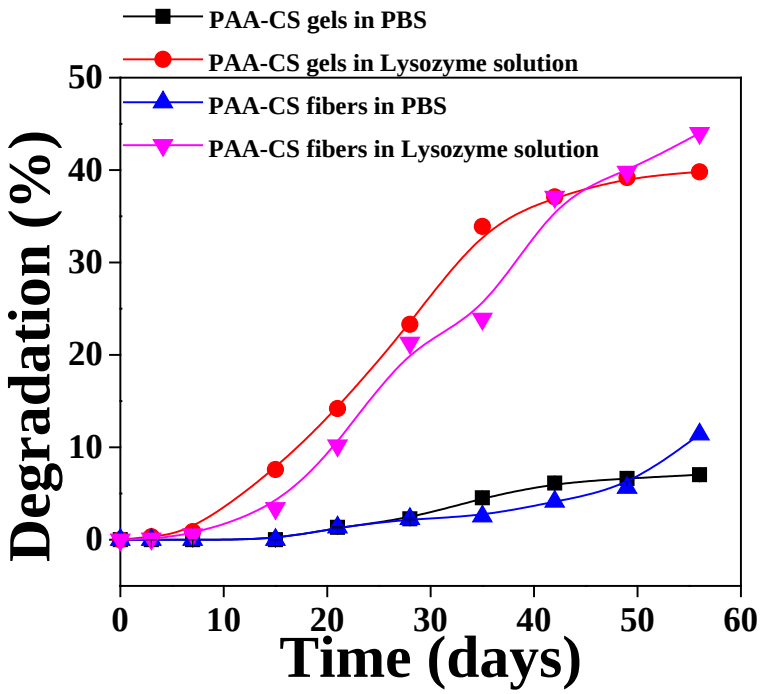

Figure 36: Biodegradation studied of PAA-CS gels and fibers in PBS and Lysozyme solution (1mg/mL).

7.3 Fibrous wound dressings:

Wound healing is a coordinated process for repairing damages tissues and protecting from further damage. The first step of healing is the inflammation of the tissue. This process is generally accompanied by increase in ROS for signaling and defense from pathogens. However, due to their high reactivity with biomolecules, excess ROS can be detrimental to wound repair resulting in cell dysfunction and death. Although free radicals are produced by all cells as part of normal metabolism and defense and signaling pathways, the inability to manage elevated levels of oxidative stress predictably leads to cell damage and an impaired wound healing. Thus, control of inflammation and ROS is important for faster and proper wound healing. Another problem in wound healing is infection of the wound leading slower recovery and further

complications. These problems are further heightened in patients with compromised immune system as in diabetes, where microbial infections and inflammation impairs the wound healing and leads to cell necrosis.

With free radical scavenging activity, neuroprotective, radio-protective and anti-inflammatory and antibacterial properties, lots of research has been devoted to study the antioxidant property of these ceria nanoparticles. Cerium ions exist in two oxidation states +3 and +4. The antioxidant activity is due to the interchange of these two states during a redox reaction. However, there is always a concern regarding the toxicity of these particles, especially when using for biomedical applications. For safer and wider use of ceria nanoparticles, a safe matrix is required. The synthesis of ceria nanoparticles in a solid matrix can meet such requirement. Ceria nanoparticles would be embedded in the matrix so that there is no direct contact between cells and nanoparticles.

Thus, PAA-CS-ceria nanofibers are ideal candidate for wound dressings. These fibers are hypothesized to have intrinsic antioxidant and antibacterial activity. Nanofibers assemble at the injury site, drawing the body's own growth factors to the injury site for wound healing. The ceria nanoparticles in the fibers ensure that the wound healing is faster and without any necrosis (due to inflammation and ROS) and infections.

The antibacterial properties of ceria nanoparticles embedded in PAA-CS fibers were tested on *E.coli* bacteria. It was observed that the cell suspension incubated with PAA-CS-ceria fibers resulted in less number of cell colonies when plated on agar, as compared to cells incubated with PAA-CS fibers or directly plated onto the agar.

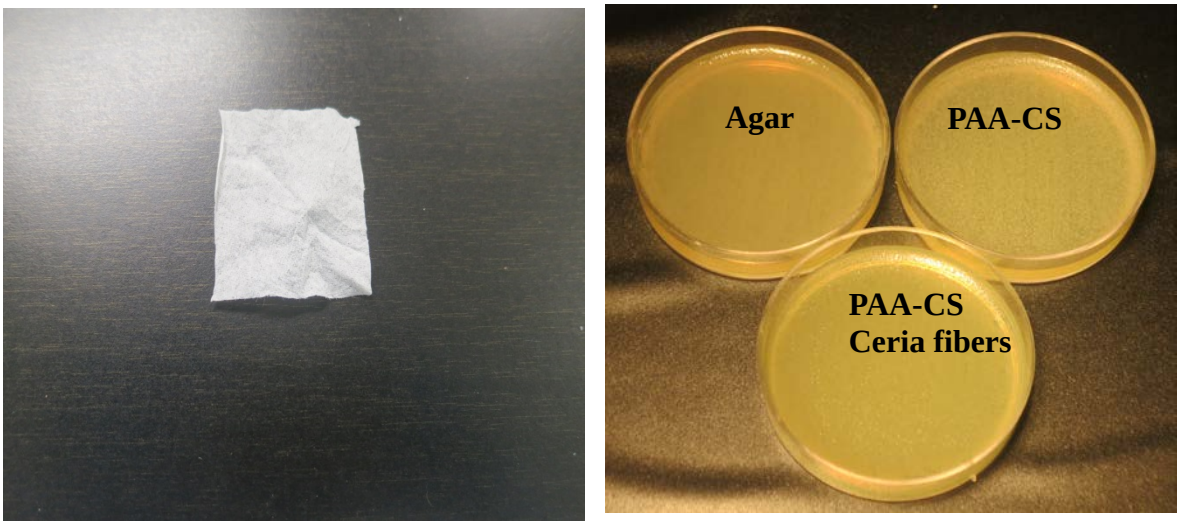

. (a) (b)

Figure 37: Antibacterial property of electrospun PAA-CS ceria fibers: (a) PAA-CS-ceria wound dressing and **(b)** Comparison of antibacterial of PAA-CS-ceria fibers with PAA-CS fibers.

There have been several studies on kinetics of reactive oxygen species (ROS) by ceria nanoparticles. The polyelectrolyte fibers are expected to facilitate the diffusion of molecules from surrounding environment and stimulus with fast response, due to their nanoscale dimensions and high surface to volume ratio, high porosity and geometrical reasons. Thus, it is hypothesized that embedding of ceria nanoparticles will not affect their antioxidant activity, as ROS can easily be diffused within fibers and ceria nanoparticles would be available to uptake them. The hypothesis is also based on the studies proving that the polymer coating on ceria

nanoparticles does not affect their antioxidant property. However, it would still be interesting to perform kinetic studies on the fibers to determine the diffusion of radicals from surroundings to the inside of the fibers and their uptake by nanoparticles and comparing it with free nanoparticles. The combination of electrospun polyelectrolyte fibers and ceria nanoparticles is a novel and promising approach for wound dressings with intrinsic anti oxidative and antimicrobial property.

To evaluate the efficiency of ceria nanoparticles in the scaffold for scavenging free radicals and protecting cell, a ROS uptake assay was performed. The task investigates the availability of ceria nanoparticles for radical scavenging since they are embedded inside the fibers. Reactive oxygen species are generally highly reactive and have short life time which makes them difficult to measure directly in biological systems. Therefore, indirect methods are employed to assess ROS levels. In general a non-fluorescent compound which can be oxidized to a fluorescent compound in the presence of ROS is used for ROS measurements. One such method using Amplex red dye was used in the present study to measure H_2O_2.*N*-acetyl-3,7-dihydroxyphenoxazine (Amplex Red) is oxidized by H_2O_2 in the presence of horse radish peroxidase (HRP), with 1:1 stoichiometry yielding the highly red fluorescent compound resorufin. This compound has an excitation maximum at 520 nm and emission maximum at 590 nm, and helps in detecting hydrogen peroxide at very low concentrations.

To test the antioxidant property of PAA-Cs scaffolds with embedded ceria nanoparticles, scaffolds were incubated with increasing concentrations of hydrogen peroxide and oxidation was

measured using an Amplex Red assay. PAA-CS scaffolds with embedded ceria nanoparticles effectively prevented the oxidation of the dye suggesting the ability of scaffolds with ceria nanoparticles to quench peroxide-induced oxidation reactions. In contrast, control scaffolds without ceria nanoparticles demonstrated oxidation with hydrogen peroxide exposure suggesting a weaker ability to quench free radicals. Together, these studies indicate that ceria nanoparticles embedded in scaffolds can act as antioxidant.

Figure 41 depicts the radical uptake by PAA-CS fibers with ceria nanoparticles. Different amounts of hydrogen peroxide were used to generate ROS. It was observed that fibers could uptake high amounts of hydrogen peroxide (5-200 μM). Cerium ions in ceria nanoparticles can convert from +3 to +4 oxidation state with the addition of H_2O_2, because of the peroxy radicals and ions. After all the H_2O_2 has been consumed, the cerium ions are converted back to +3 state and. Thus, the fibers inherit the antioxidant properties of the ceria nanoparticles and embedding ceria nanoparticles in fibers does not limit their ROS uptaking capacity.

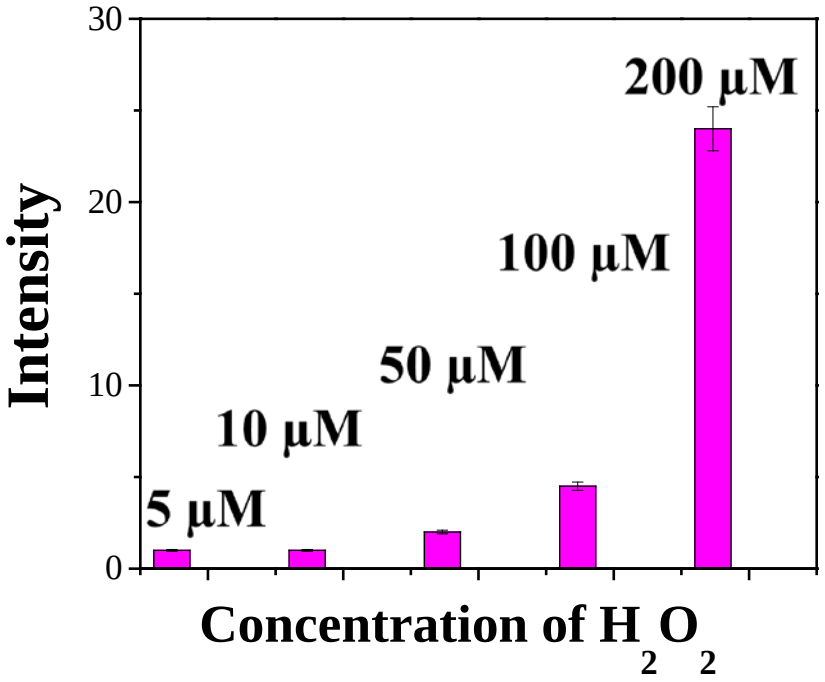

(a)

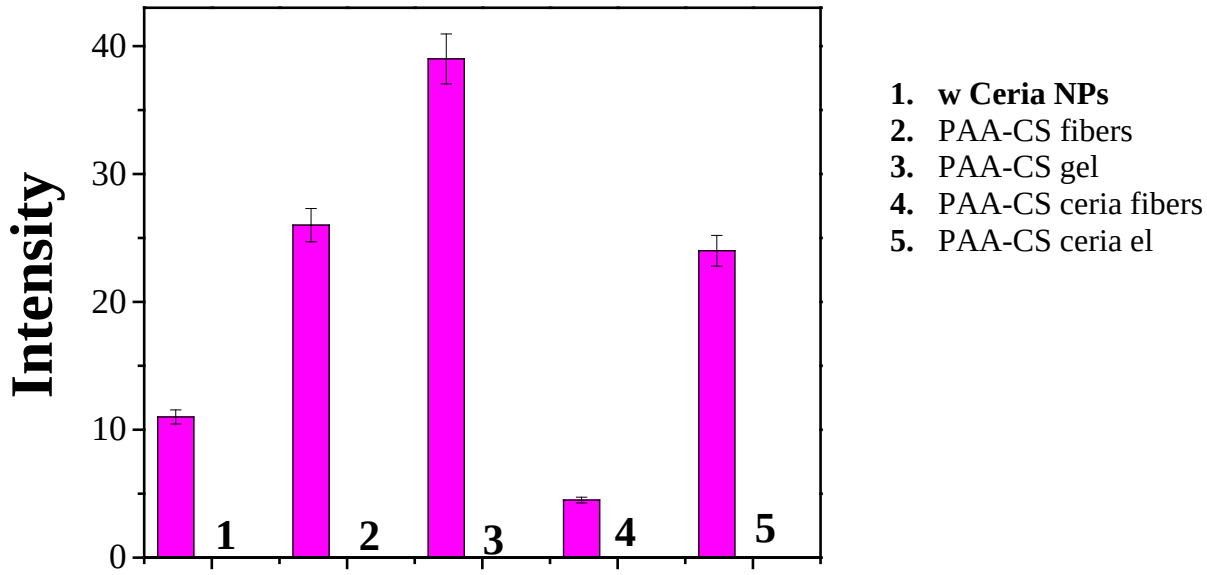

(b)

Figure 38: Antioxidant activities of scaffolds. **(a)** Antioxidant activity of PAA-CS fibers embedded with ceria nanoparticles assesses for different concentrations of H_2O_2 (5-200µM) using Amplex Red assay. **(b)** Comparison of antioxidant capacity of different scaffolds for 100 µM H_2O_2

7.4 Tissue engineering:

There are evidences that polyanion/polycations have similar properties as of extracellular matrix (ECM) of cells and nanofibers resemble the components of ECM and affect the cellular activity because of their nanometer size and geometrical reasons. Cells are able to organize around, attach and proliferate on these fibers as the scaffolds formed of such nanofibers are smaller than the size of the cell. Moreover, the bio and cytocompatibility of these fibers can also be modulated through post synthesis modification. Polymeric fibers can be used for providing a 3-D framework for in vitro attachment and growth of cells. These fibers with their mechanical and biological properties similar to extra cellular matrix can simulate an environment for tissue engineering both functionally and architecturally. These fibers should be biocompatible, biodegradable and porous with high surface to volume ratio and good mechanical strength for such applications. To investigate their potential as a scaffold and for further applications, in vitro cell assays are required. Most of the cells need to adhere to a surface for their growth and proliferation. The attachment of cells onto the surface depends on the compatibility of cells with the underlying substrate. If the cells are not attached properly to the scaffold, the cells become round in shape and start floating. Also, the compatibility can be assessed through the morphology of the cells and the number of cells (proliferation) and cell growth.

7.4.1 Fibers and gels with ceria nanoparticles for cell protection against oxidative damage:

The highly reactive radicals interact with cellular components such as DNA, lipids, proteins and damage them, leading to the loss of their function and eventually cell death. Due to their redox properties, ceria nanoparticles have the ability to uptake free radicals, behaving as antioxidants

and protecting the cell. The whole purpose of using fibers/gels embedded with ceria nanoparticles is to have a scaffold with intrinsic antioxidant activity for promoting cell growth and healing during tissue engineering applications.

Antioxidant studies were performed to evaluate the resistance of cells grown on scaffold with intrinsic anti oxidation property against oxidative damage by H_2O_2 as ROS species using Amplex Red assay. Since, Amplex red cannot permeate cell membrane; it can measure only extracellular H_2O_2.

Three cell lines fibroblasts (HDF), neuroblastoma (SHSYS5) and myoblasts (C2C12) were seeded on fibers and gels embedded with ceria nanoparticles. The attachment and morphology of the cells was observed by SEM. **Figure 43** depicts that all three cell line spreading on the scaffold surface within 24 hours of seeding, suggesting good of the cells adhesion to the scaffolds and their compatibility with the scaffolds.

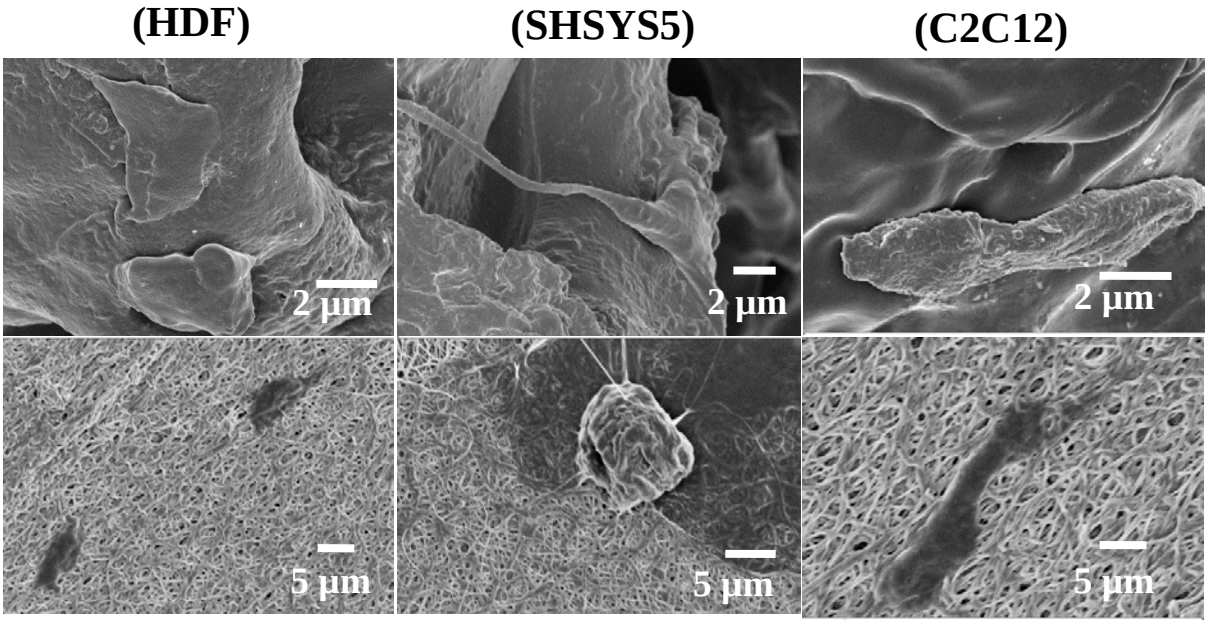

Figure 39: Cells attaching and spreading on PAA-CS fibers (bottom row) and gels (top row) embedded with ceria nanoparticles: (a) Fibroblasts (HDF), (b) Neuroblastoma (SHSYS5) and (c) Myoblasts (C2C12).

Since both cells and ceria nanoparticles can interact with radicals, it is expected that there would be a competition between the two and the one which is more easily available would interact more. In porous scaffolds like these fibers the interactions between the molecules is generally dependent on the diffusion of the molecules. It would be interesting to observe if radicals reach ceria nanoparticles or the cells first and if radicals will be able to reach ceria nanoparticles at all. The radicals should be up taken by the ceria nanoparticles preventing their interaction with the cells. This study was performed with gels and fibers with ceria nanoparticles. For control assays, cells treated with ceria nanoparticles, and cells grown on fibers without ceria nanoparticles and cells grown on normal polystyrene substrate was studied. **Figure 44** depicts the resistance of cells grown on different scaffolds to H_2O_2.

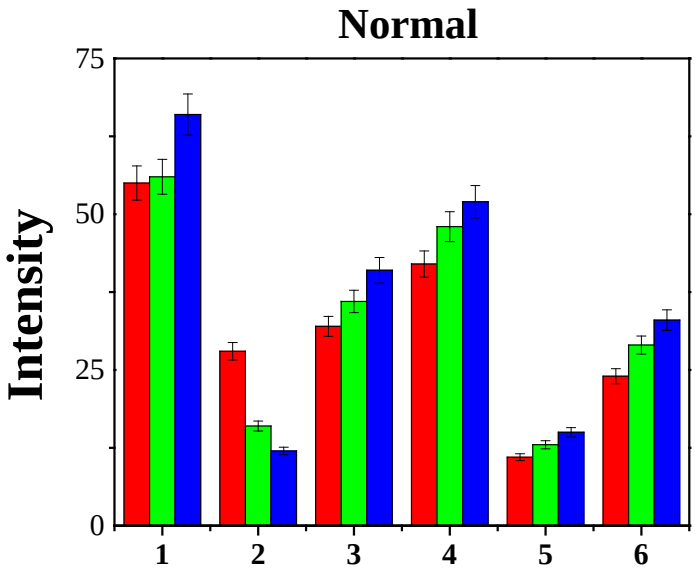

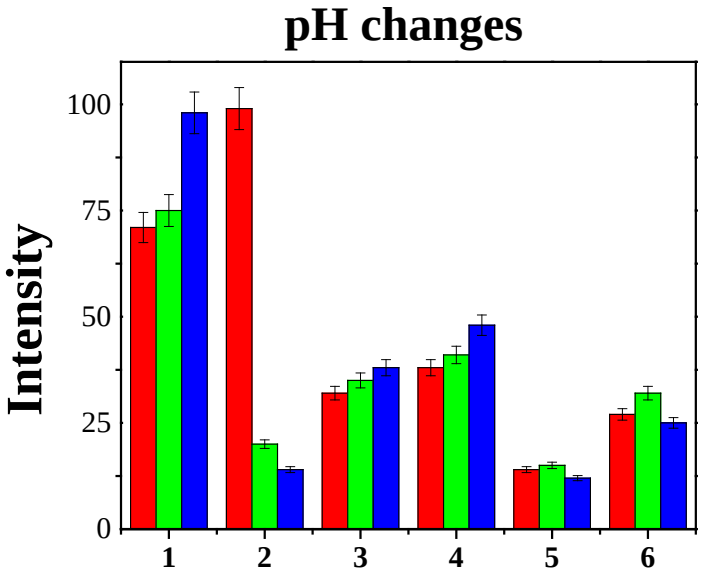

- hDF
- C2C12
- SHSY5Y

1. Plated
2. w Ceria NPs
3. PAA-CS Fibers
4. PAA-CS Gel
5. PAA-CS Ceria Fiber
6. PAA-CS Ceria Gel

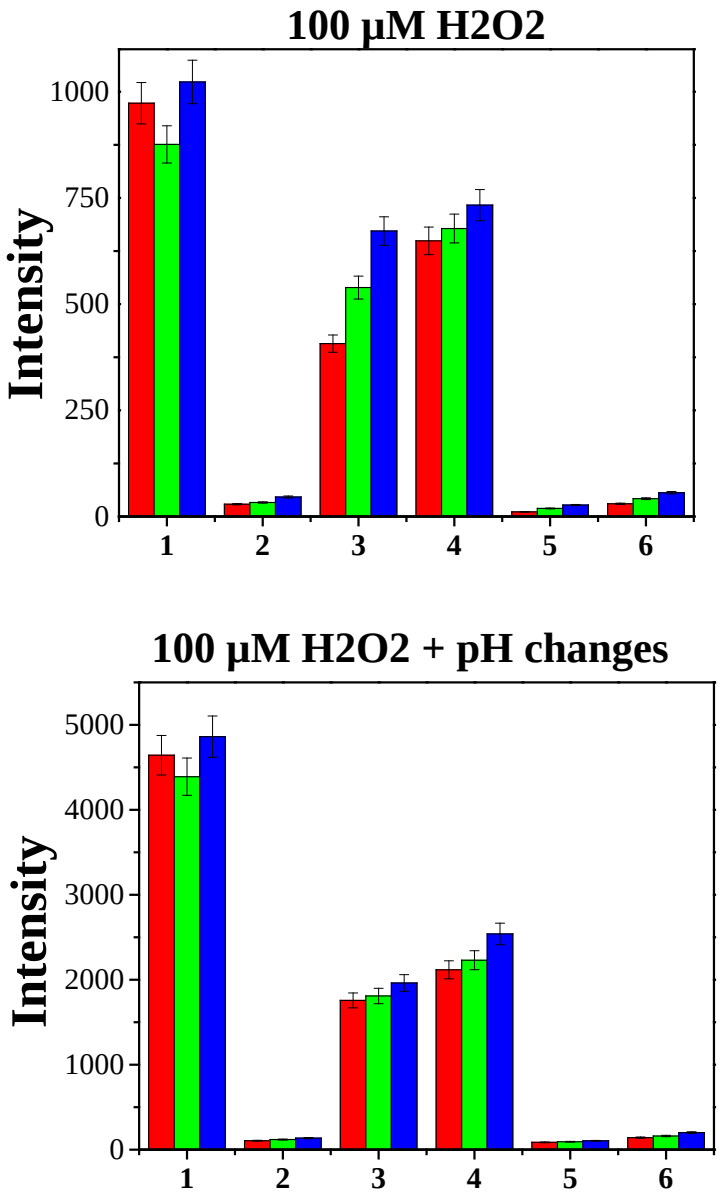

Figure 40: Resistance of cells grown on different scaffolds and polystyrene substrates (with and without ceria nanoparticles) to oxidative damage at **(a)** normal conditions, **(b)** stress generated due to pH change, **(c)**peroxide radicals generated by 100 µM $H_2O_2$and **(d)**combination of pH change and100 µM $H_2O_{2..}$

The scaffolds with ceria nanoparticles showed maximum antioxidant capacity. Interestingly, the antioxidant capacity of ceria nanoparticles embedded in scaffolds (fibers/gels) was found to be comparable to ceria nanoparticles. However, fibers with ceria nanoparticles showed enhanced resistance to H_2O_2compared to gels with ceria nanoparticles. This can be attributed to increased surface area and hence better diffusion of molecules across fibers than gels. These results indicate that the antioxidant capacity of scaffolds is embedded ceria nanoparticles.

For cell viability evaluation MTT assay was performed to see if the scaffold with embedded ceria nanoparticles is compatible or cytotoxic. In living cells, 3-(4,5-dimcthylthioazol-2-yl)-2,5-diphenyl-tetrazolium bromide (MTT) is reduced to purple formazan, with absorbance at 500 nm. The reduction of MTT to purple formazan takes place in the presence of active reductase enzymes, thus the formation of formazan is a measure of cell viability or cytotoxicity. The intensity of formazan absorbance provides the quantitative measure of the cell viability. Figure shows the cell viability of cells grown on different scaffolds in response to H_2O_2. The data corresponds to data obtained for cell resistance to H_2O_2.

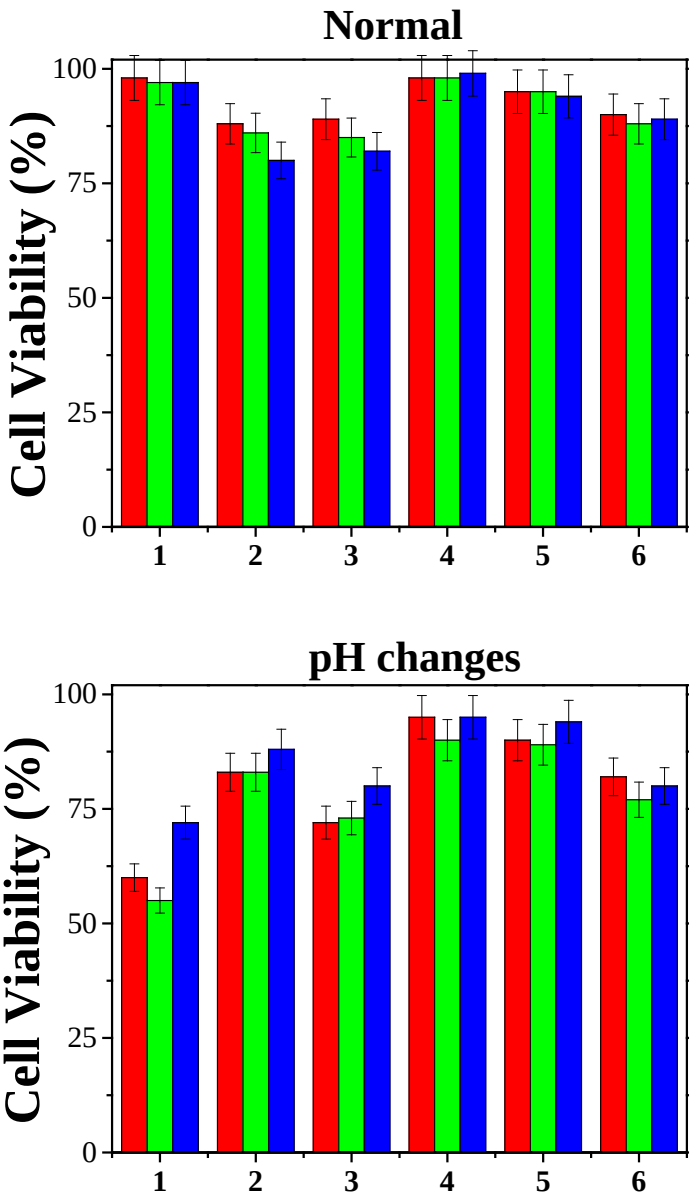
Normal
Cell Viability (%)
100
75
50
25
0
1
2
3
4
5
6
pH changes
Cell Viability (%)
100
75
50
25
0
1
2
3
4
5
6
- hDF
- C2C12
- SHSY5Y
1. Plated
2. w Ceria NPs
3. PAA-CS Fibers
4. PAA-CS Ceria Fiber
5. PAA-CS Ceria Gel
6. PAA-CS Gel

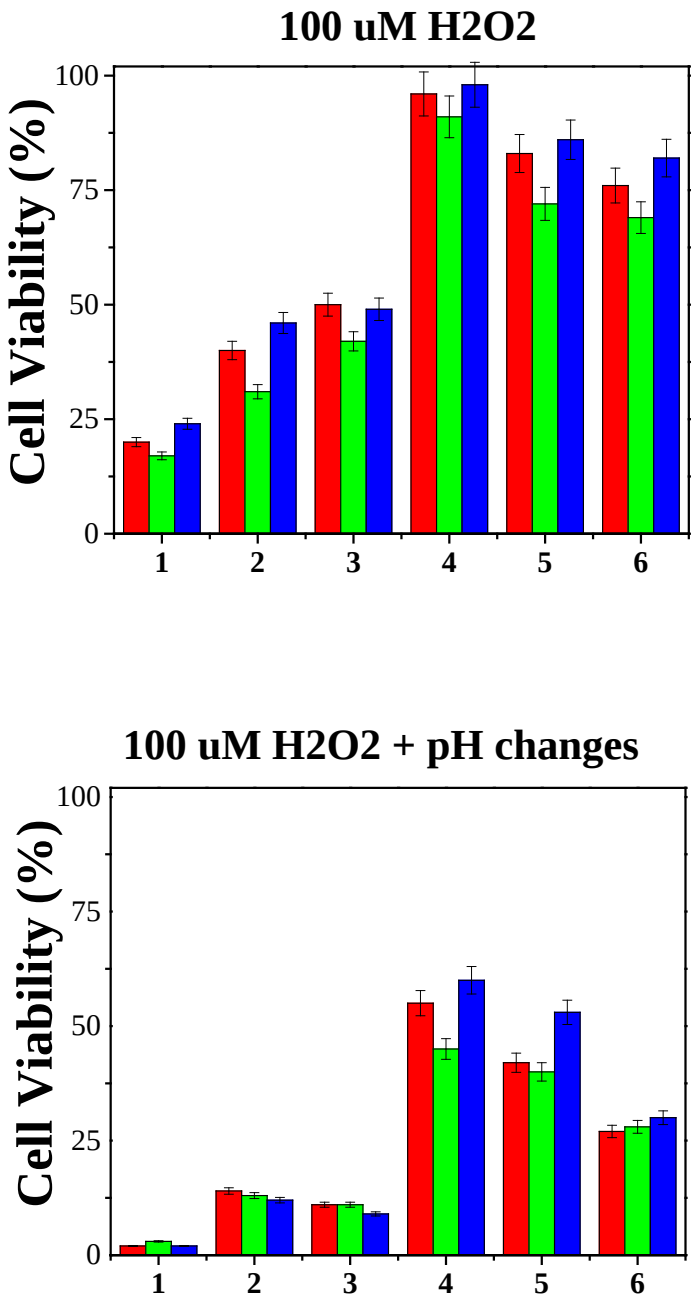

Figure 41**:**MTT assay for cell viability on different scaffolds and polystyrene substrates (with and without ceria nanoparticles) to oxidative damage at **(a)** normal conditions, **(b)** stress generated due to pH change, **(c)** peroxide radicals generated by 100 µM $H_2O_2$and **(d)**combination of pH change and100 µM H_2O_2.

Our results substantiate that our scaffolds with ceria nanoparticles have antioxidant activity protecting the cells from exogenous ROS generated in response to different stress conditions.

7.4.2 Hap mineralized gels and fibers for bone tissue engineering:

Hydroxyapatite (HaP) is a mineral found in human bones and teeth and HaP nanocrystals are grown for bone and dental tissue regeneration and as dental fillers. We propose that PAA-CS scaffolds can be used for biomimetic mineralization for bone and tissue regeneration. In this study, PAA-CS scaffolds loaded with calcium ions were incubated in SBF at room temperature, for Hap nanocrystals formation. It is expected that due to hydrogel nature and controlled release of calcium, faster and more controlled growth of Hap nanocrystals would occur. The crystallization of calcium in the form of HaP, rather than calcium phosphate is dependent on the presence and concentration of carboxyl groups.[109, 138]

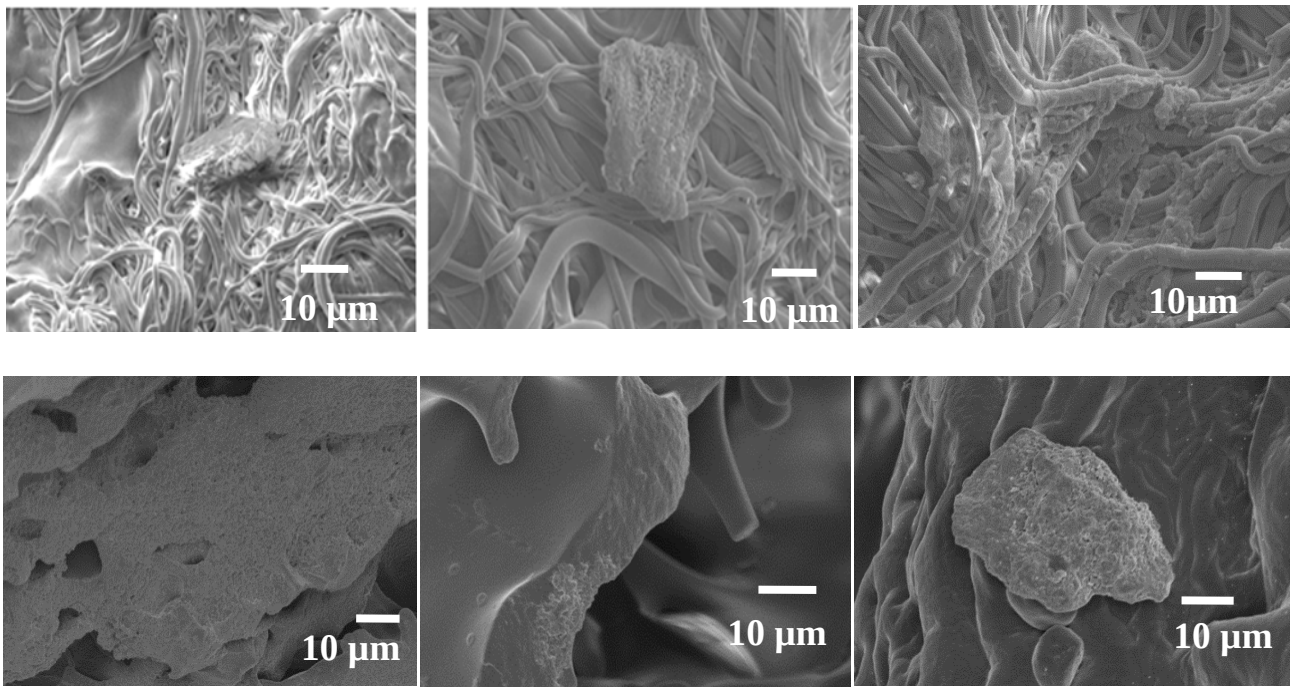

Figure 42: Bone sarcoma (MG-63) cells growing on Hap fibers and gels mineralizing matrix and forming nodules.

The attachment of bone sarcoma cells on Hap mineralized PAA-Cs scaffolds can be seen in **Figure 46**. It is observed that cell spread on the scaffolds, mineralizing the matrix. Formation of bone nodules can also been seen on both fibers and gels.

7.5 Calcium ion gels for artificial muscles:

Lot of research on engineered myoblasts for artificial muscles. Since, calcium ions are involved in several signaling pathways and also control muscle cell functioning, we studied the growth myoblast on calcium ion gels. Myoblast generally take a week to grow and fuse to form functioning units known as myotubes. In our studies, we found, good adhesion and spreading of myoblasts on the scaffold. Interestingly, within 24 hours we could see the formation of myotubes on the scaffolds.

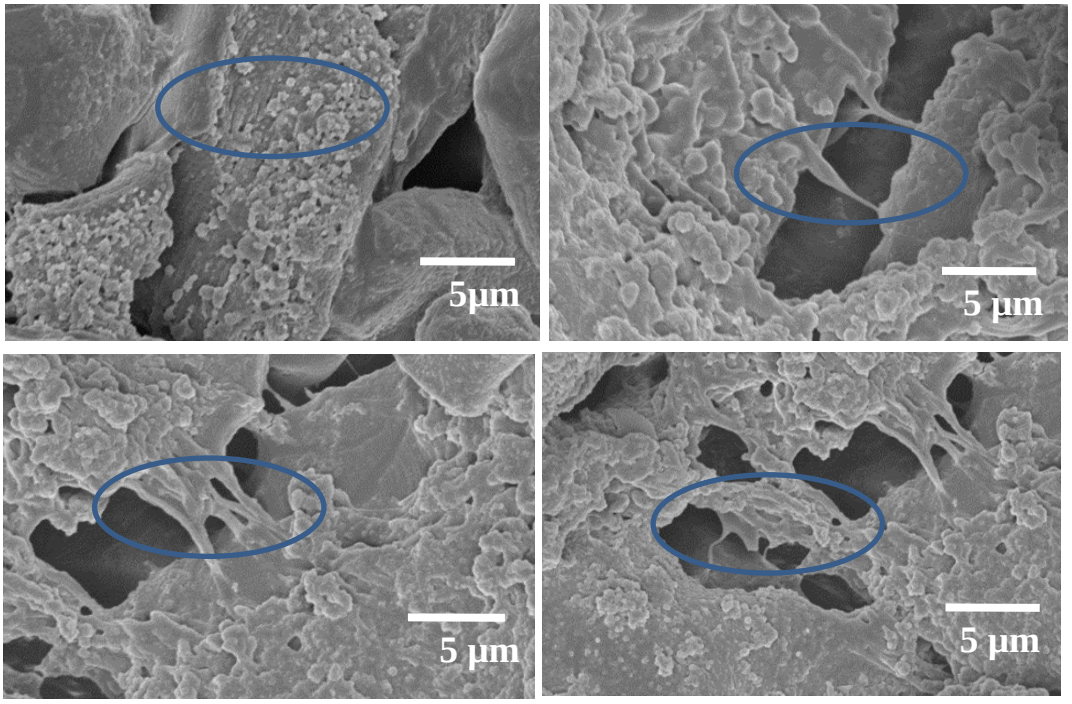

Figure 43: C2C12 cells growing and spreading on PAA-S-Ca^{2+} gels forming myotubes.

7.6 Conclusion:

In this chapter we demonstrated some applications of MPEC structures. The biocompatibility and biodegradability of these scaffolds was tested for their application in biomedical applications. The functionalized gels were examined for their potential in tissue engineering. The antioxidant activity of scaffolds with ceria nanoparticles were examined for their anti-inflammatory and antibacterial properties for wound dressings and protection of cells from ROS induced oxidation for tissue engineering applications. The HaP mineralized scaffolds also exhibited their potential for bone and dental tissue engineering application. The cell studies on gels with calcium ions showed interesting results of forming myotubes within 24 hours suggesting their application in artificial muscles.

CHAPTER 8: SUMMARY

This dissertation is focused on the synthesis of functional polyelectrolyte complexes and their multidirectional potential applications. The polyelectrolyte complexes cross-linked with metal ions were synthesized and tuned to develop functional structures with interesting diffusion and surface properties. The structure-property relationship of the polyelectrolyte complexes was thoroughly investigated and tuned during processing to achieve optimized properties for various applications. Electrospinning was to fabricate nanofibers followed by their functionalization to achieve desired applications. Diffusion characteristics of different structures and their effect on interfacial reactions and functionalization were analyzed. The potential of functionalized complexes for different applications was also investigated. The major findings from this research can be summarized as follow:

1. Incorporating metal ions of different valence into PECs introduces metal ion/polyelectrolyte interactions that can tune the morphology of MPECs. The metal ion-PAA interactions are more important than metal ion-CS interactions at low pH. Transition metal ions have much stronger interaction with PAA than main group metal ions due to the availability of d orbitals, which enables the manipulation of PEC morphology through the tuning of solution viscosity. The function of CS is improving the fiber stability is two-fold, forming electrostatic interactions with PAA and generating metal ion-CS interactions at increased pH.

The MPECs thus obtained have enhanced stability, are responsive to different stimuli and can be manipulated to obtain different structures like gels, fibers, films, nanoparticles etc.

2. MPECs form gels at room temperature. The gelation time depends upon the polymer concentration and PAA:CS ratio. For non-stoichiometric ratios (high PAA:CS ratio) complex can take days to month to gel. Addition of metal ions as cross linkers decreases the gelation time and also infers properties like stretching and self-healing. The ionic cross linking by metal ions is concentration dependent and varies with the metal ion type. Physiochemical parameters like temperature and pH can also induce gelation in these complexes. The gels thus obtained are stable over a wide range of pH.

3. Metal ion/polyelectrolyte interactions can be used to control the morphology of electrospun nanostructures and their swelling and stability in aqueous solutions. While metal ions have negligible interaction with CS during electrospinning, the protonated amine groups in fabricated PCFs will be deprotonated when the PCFs were immersed in aqueous solutions of higher pH. The function of CS is improving the fiber stability is two-fold, forming electrostatic interactions with PAA and generating metal ion-CS interactions at increased pH.

4. The release of embedded metal ions from MPECs into aqueous solutions is affected by metal ion/polyelectrolyte interactions. It is expected that, transition metal ions will have a smaller diffusion rate than main group metal ions of the same valence because of stronger metal ion/polyelectrolyte interactions. The release or diffusion can be controlled by various parameters thus providing control over their properties and interfacial reactions on their surface.

5. The embedded metal ions function as a reagent **reservoir** for various reactions to functionalize MPECs. The functionalized MPECs exhibit an immense potential for various applications as demonstrated.

REFERENCES

1. Thünemann, A., et al., *Polyelectrolyte Complexes*, in *Polyelectrolytes with Defined Molecular Architecture II*, M. Schmidt, Editor. 2004, Springer Berlin Heidelberg. p. 113-171.

2. Michaels, A.S., *POLYELECTROLYTE COMPLEXES.* Industrial & Engineering Chemistry, 1965. **57**(10): p. 32-40.

3. Gardlund, L., L. Wagberg, and M. Norgren, *New insights into the structure of polyelectrolyte complexes.* J Colloid Interface Sci, 2007. **312**(2): p. 237-46.

4. Nakajima, A., *Formation of polyelectrolyte complexes.* Journal of Macromolecular Science, Part B, 1980. **17**(4): p. 715-721.

5. Dautzenberg, H., et al., *Stoichiometry and structure of polyelectrolyte complex particles in diluted solutions.* Berichte der Bunsengesellschaft für physikalische Chemie, 1996. **100**(6): p. 1024-1032.

6. Chiappisi, L., I. Hoffmann, and M. Gradzielski, *Complexes of oppositely charged polyelectrolytes and surfactants - recent developments in the field of biologically derived polyelectrolytes.* Soft Matter, 2013. **9**(15): p. 3896-3909.

7. Yoshizawa, T., et al., *pH- and temperature-sensitive permeation through polyelectrolyte complex films composed of chitosan and polyalkyleneoxide–maleic acid copolymer.* Journal of Membrane Science, 2004. **241**(2): p. 347-354.

8. Porasso, R.D., J.C. Benegas, and M.A.G.T. Van den Hoop, *Chemical and Electrostatic Association of Various Metal Ions by Poly(acrylic acid) and Poly(methacrylic acid) As Studied by Potentiometry.* Journal of Physical Chemistry B, 1999. **103**(Copyright (C) 2014 American Chemical Society (ACS). All Rights Reserved.): p. 2361-2365.

9. van den Hoop, M.A.G.T., J.C. Benegas, and H.P. van Leeuwen, *Stripping voltammetry of heavy metal/polyelectrolyte complexes. Part 2. Analysis in terms of polyelectrolyte theory.* Analytica Chimica Acta, 1995. **317**(1–3): p. 327-334.

10. Tsuchida, E., *Formation of Polyelectrolyte Complexes and Their Structures.* Journal of Macromolecular Science, Part A, 1994. **31**(1): p. 1-15.

11. Billiet, T., et al., *A review of trends and limitations in hydrogel-rapid prototyping for tissue engineering.* Biomaterials, 2012. **33**(Copyright (C) 2014 American Chemical Society (ACS). All Rights Reserved.): p. 6020-6041.

12. Brandl, F., F. Sommer, and A. Goepferich, *Rational design of hydrogels for tissue engineering: Impact of physical factors on cell behavior.* Biomaterials, 2006. **28**(Copyright (C) 2014 American Chemical Society (ACS). All Rights Reserved.): p. 134-146.

13. Drury, J.L. and D.J. Mooney, *Hydrogels for tissue engineering: scaffold design variables and applications.* Biomaterials, 2003. **24**(Copyright (C) 2014 American Chemical Society (ACS). All Rights Reserved.): p. 4337-4351.

14. Ryan, D.M. and B.L. Nilsson, *Self-assembled amino acids and dipeptides as noncovalent hydrogels for tissue engineering.* Polym. Chem., 2012. **3**(Copyright (C) 2014 American Chemical Society (ACS). All Rights Reserved.): p. 18-33.

15. Place, E.S., N.D. Evans, and M.M. Stevens, *Complexity in biomaterials for tissue engineering.* Nature Materials, 2009. **8**(6): p. 457-470.

16. Moreira Teixeira, L.S., et al., *Enzyme-catalyzed crosslinkable hydrogels: Emerging strategies for tissue engineering.* Biomaterials, 2012. **33**(Copyright (C) 2014 American Chemical Society (ACS). All Rights Reserved.): p. 1281-1290.

17. Lee, K.Y. and D.J. Mooney, *Hydrogels for Tissue Engineering.* Chem. Rev. (Washington, D. C.), 2001. **101**(Copyright (C) 2014 American Chemical Society (ACS). All Rights Reserved.): p. 1869-1879.

18. Khademhosseini, A. and R. Langer, *Microengineered hydrogels for tissue engineering.* Biomaterials, 2007. **28**(Copyright (C) 2014 American Chemical Society (ACS). All Rights Reserved.): p. 5087-5092.

19. He, L., et al., *Surface modification of electrospun nanofibrous scaffolds via polysaccharide-protein assembly multilayer for neurite outgrowth.* Journal of Materials Chemistry, 2012. **22**(Copyright (C) 2014 American Chemical Society (ACS). All Rights Reserved.): p. 13187-13196.

20. Chung, B.G., et al., *Microfluidic fabrication of microengineered hydrogels and their application in tissue engineering.* Lab Chip, 2012. **12**(Copyright (C) 2014 American Chemical Society (ACS). All Rights Reserved.): p. 45-59.

21. Guiseppi-Elie, A., S.I. Brahim, and D. Narinesingh, *A Chemically Synthesized Artificial Pancreas: Release of Insulin from Glucose-Responsive Hydrogels.* Advanced Materials, 2002. **14**(10): p. 743-746.

22. Andrianov, A.K., et al., *Controlled release using ionotropic polyphosphazene hydrogels.* Journal of Controlled Release, 1993. **27**(1): p. 69-77.

23. Alarcon, C.d.l.H., S. Pennadam, and C. Alexander, *Stimuli responsive polymers for biomedical applications.* Chemical Society Reviews, 2005. **34**(3): p. 276-285.

24. Ji, C.-C., et al., *Self-assembly of three-dimensional interconnected graphene-based aerogels and its application in supercapacitors.* Journal of Colloid and Interface Science, 2013. **407**(Copyright (C) 2013 American Chemical Society (ACS). All Rights Reserved.): p. 416-424.

25. Gutiérrez, M.C., et al., *Hydrogel Scaffolds with Immobilized Bacteria for 3D Cultures.* Chemistry of Materials, 2007. **19**(8): p. 1968-1973.

26. Song, S.H., et al., *A wireless chemical sensor featuring iron oxide nanoparticle-embedded hydrogels.* Sensors and Actuators, B, 2014. **193**(Copyright (C) 2014 American Chemical Society (ACS). All Rights Reserved.): p. 925-930.

27. Peppas, N.A., et al., *Hydrogels in biology and medicine: from molecular principles to bionanotechnology.* Adv. Mater. (Weinheim, Ger.), 2006. **18**(Copyright (C) 2014 American Chemical Society (ACS). All Rights Reserved.): p. 1345-1360.

28. Nayak, S. and L.A. Lyon, *Soft nanotechnology with soft nanoparticles.* Angew. Chem., Int. Ed., 2005. **44**(Copyright (C) 2014 American Chemical Society (ACS). All Rights Reserved.): p. 7686-7708.

29. Lifson, M.A., D. Basu Roy, and B.L. Miller, *Enhancing the Detection Limit of Nanoscale Biosensors via Topographically Selective Functionalization.* Anal. Chem. (Washington, DC, U.

S.), 2014. **86**(Copyright (C) 2014 American Chemical Society (ACS). All Rights Reserved.): p. 1016-1022.

30. Hotz, N., L. Wilcke, and W. Weber, *Design, Synthesis, and Application of Stimulus-Sensing Biohybrid Hydrogels.* Macromolecular Rapid Communications, 2013. **34**(Copyright (C) 2014 American Chemical Society (ACS). All Rights Reserved.): p. 1594-1610.

31. Hendrickson, G.R. and L. Andrew Lyon, *Bioresponsive hydrogels for sensing applications.* Soft Matter, 2009. **5**(Copyright (C) 2014 American Chemical Society (ACS). All Rights Reserved.): p. 29-35.

32. Bai, W. and D.A. Spivak, *A Double-Imprinted Diffraction-Grating Sensor Based on a Virus-Responsive Super-Aptamer Hydrogel Derived from an Impure Extract.* Angew. Chem., Int. Ed., 2014. **53**(Copyright (C) 2014 American Chemical Society (ACS). All Rights Reserved.): p. 2095-2098.

33. Zinchenko, A., et al., *DNA Hydrogel as a Template for Synthesis of Ultrasmall Gold Nanoparticles for Catalytic Applications.* Acs Applied Materials & Interfaces, 2014(Copyright (C) 2014 American Chemical Society (ACS). All Rights Reserved.): p. Ahead of Print.

34. Sahiner, N., *Soft and flexible hydrogel templates of different sizes and various functionalities for metal nanoparticle preparation and their use in catalysis.* Progress in Polymer Science, 2013. **38**(Copyright (C) 2014 American Chemical Society (ACS). All Rights Reserved.): p. 1329-1356.

35. Bolisay, L.D., J.N. Culver, and P. Kofinas, *Molecularly imprinted polymers for tobacco mosaic virus recognition.* Biomaterials, 2006. **27**(22): p. 4165-4168.

36. Byrne, M.E., K. Park, and N.A. Peppas, *Molecular imprinting within hydrogels.* Adv. Drug Delivery Rev., 2002. **54**(Copyright (C) 2014 American Chemical Society (ACS). All Rights Reserved.): p. 149-161.

37. Gehrke, S., *Synthesis, equilibrium swelling, kinetics, permeability and applications of environmentally responsive gels*, in *Responsive Gels: Volume Transitions II*, K. Dušek, Editor. 1993, Springer Berlin Heidelberg. p. 81-144.

38. Zhang, Y.Z., et al., *Coaxial Electrospinning of (Fluorescein Isothiocyanate-Conjugated Bovine Serum Albumin)-Encapsulated Poly(ε-caprolactone) Nanofibers for Sustained Release.* Biomacromolecules, 2006. **7**(4): p. 1049-1057.

39. Luong-Van, E., et al., *Controlled release of heparin from poly(ε-caprolactone) electrospun fibers.* Biomaterials, 2006. **27**(9): p. 2042-2050.

40. Chew, S.Y., et al., *Sustained Release of Proteins from Electrospun Biodegradable Fibers.* Biomacromolecules, 2005. **6**(4): p. 2017-2024.

41. He, C.L., et al., *Coaxial Electrospun Poly(L‐Lactic Acid) Ultrafine Fibers for Sustained Drug Delivery.* Journal of Macromolecular Science, Part B, 2006. **45**(4): p. 515-524.

42. Verreck, G., et al., *Incorporation of drugs in an amorphous state into electrospun nanofibers composed of a water-insoluble, nonbiodegradable polymer.* Journal of Controlled Release, 2003. **92**(3): p. 349-360.

43. Katti, D.S., et al., *Bioresorbable nanofiber-based systems for wound healing and drug delivery: Optimization of fabrication parameters.* Journal of Biomedical Materials Research Part B: Applied Biomaterials, 2004. **70B**(2): p. 286-296.

44. Rho, K.S., et al., *Electrospinning of collagen nanofibers: Effects on the behavior of normal human keratinocytes and early-stage wound healing.* Biomaterials, 2006. **27**(8): p. 1452-1461.

45. Hsieh, A., et al., *Hydrogel/electrospun fiber composites influence neural stem/progenitor cell fate.* Soft Matter, 2010. **6**(10): p. 2227-2237.

46. Akbari, M., et al., *Composite living fibers for creating tissue constructs using textile techniques.* Advanced Functional Materials, 2014. **24**(Copyright (C) 2014 American Chemical Society (ACS). All Rights Reserved.): p. 4060-4067.

47. Du, C., et al., *Induced pluripotent stem cell-derived hepatocytes and endothelial cells in multi-component hydrogel fibers for liver tissue engineering.* Biomaterials, 2014. **35**(Copyright (C) 2014 American Chemical Society (ACS). All Rights Reserved.): p. 6006-6014.

48. Ekaputra, A.K., et al., *The three-dimensional vascularization of growth factor-releasing hybrid scaffold of poly (ϵ-caprolactone)/collagen fibers and hyaluronic acid hydrogel.* Biomaterials, 2011. **32**(Copyright (C) 2014 American Chemical Society (ACS). All Rights Reserved.): p. 8108-8117.

49. Lim, T.C., et al., *Follicular dermal papilla structures by organization of epithelial and mesenchymal cells in interfacial polyelectrolyte complex fibers.* Biomaterials, 2013. **34**(Copyright (C) 2014 American Chemical Society (ACS). All Rights Reserved.): p. 7064-7072.

50. Huang, C., et al., *Magnetic Electrospun Fibers for Cancer Therapy.* Advanced Functional Materials, 2012. **22**(Copyright (C) 2014 American Chemical Society (ACS). All Rights Reserved.): p. 2479-2486.

51. Lee, J.Y., et al., *Polypyrrole-coated electrospun PLGA nanofibers for neural tissue applications.* Biomaterials, 2009. **30**(26): p. 4325-4335.

52. Raghothaman, D., et al., *Engineering cell matrix interactions in assembled polyelectrolyte fiber hydrogels for mesenchymal stem cell chondrogenesis.* Biomaterials, 2014. **35**(Copyright (C) 2014 American Chemical Society (ACS). All Rights Reserved.): p. 2607-2616.

53. Lalani, R. and L. Liu, *Electrospun Zwitterionic Poly(Sulfobetaine Methacrylate) for Nonadherent, Superabsorbent, and Antimicrobial Wound Dressing Applications.* Biomacromolecules, 2012. **13**(Copyright (C) 2014 American Chemical Society (ACS). All Rights Reserved.): p. 1853-1863.

54. Munaweera, I., A. Aliev, and K.J. Balkus, Jr., *Electrospun Cellulose Acetate-Garnet Nanocomposite Magnetic Fibers for Bioseparations.* Acs Applied Materials & Interfaces, 2014. **6**(Copyright (C) 2014 American Chemical Society (ACS). All Rights Reserved.): p. 244-251.

55. Miao, Y.-E., et al., *High-Performance Supercapacitors Based on Hollow Polyaniline Nanofibers by Electrospinning.* Acs Applied Materials & Interfaces, 2013. **5**(10): p. 4423-4428.

56. Hsu, P.-C., et al., *Passivation Coating on Electrospun Copper Nanofibers for Stable Transparent Electrodes.* ACS Nano, 2012. **6**(6): p. 5150-5156.

57. Li, H.-Y. and Y.-L. Liu, *Polyelectrolyte composite membranes of polybenzimidazole and crosslinked polybenzimidazole-polybenzoxazine electrospun nanofibers for proton exchange membrane fuel cells.* J. Mater. Chem. A, 2013. **1**(Copyright (C) 2014 American Chemical Society (ACS). All Rights Reserved.): p. 1171-1178.

58. Kim, T., et al., *Preparation of PCDTBT nanofibers with a diameter of 20 nm and their application to air-processed organic solar cells.* Nanoscale, 2014. **6**(5): p. 2847-2854.

59. Hu, D., et al., *The assembly of dendrimer-stabilized gold nanoparticles onto electrospun polymer nanofibers for catalytic applications.* J. Mater. Chem. A, 2014. **2**(Copyright (C) 2014 American Chemical Society (ACS). All Rights Reserved.): p. 2323-2332.

60. Zhang, M., et al., *Hierarchical Nanostructures of Copper(II) Phthalocyanine on Electrospun TiO2 Nanofibers: Controllable Solvothermal-Fabrication and Enhanced Visible Photocatalytic Properties.* Acs Applied Materials & Interfaces, 2011. **3**(2): p. 369-377.

61. Haider, S. and S.-Y. Park, *Preparation of the electrospun chitosan nanofibers and their applications to the adsorption of Cu(II) and Pb(II) ions from an aqueous solution.* Journal of Membrane Science, 2009. **328**(1–2): p. 90-96.

62. Miao, Y.-E., et al., *Electrospun Self-Standing Membrane of Hierarchical SiO2@γ-AlOOH (Boehmite) Core/Sheath Fibers for Water Remediation.* Acs Applied Materials & Interfaces, 2012. **4**(10): p. 5353-5359.

63. Xiao, S.L., et al., *Fabrication of Water-Stable Electrospun Polyacrylic Acid-Based Nanofibrous Mats for Removal of Copper (II) Ions in Aqueous Solution.* Journal of Applied Polymer Science, 2010. **116**(4): p. 2409-2417.

64. Audrey Frenot, I.C., *Polymer nanofibers assembled by electrospinning.* Current Opinion in Colloid and Interface Science, 2003. **8**: p. 64-75.

65. Chen, S., Y. Li, and Y. Li, *Architecture of low dimensional nanostructures based on conjugated polymers.* Polym. Chem., 2013. **4**(Copyright (C) 2014 American Chemical Society (ACS). All Rights Reserved.): p. 5162-5180.

66. Coburn, J.M., et al., *Bioinspired nanofibers support chondrogenesis for articular cartilage repair.* Proc. Natl. Acad. Sci. U. S. A., 2012. **109**(Copyright (C) 2014 American Chemical Society (ACS). All Rights Reserved.): p. 10012-10017, S10012/1-S10012/4.

67. Darrell H Reneker , I.C., *Nanometre diameter fibres of polymer, produced by electrospinning.* Nanotechnology, 1996. **7**: p. 216-223.

68. Deitzel, J.M., et al., *The effect of processing variables on the morphology of electrospun nanofibers and textiles.* Polymer, 2001. **42**(1): p. 261-272.

69. Greiner, A. and J.H. Wendorff, *Electrospinning: a fascinating method for the preparation of ultrathin fibers.* Angew Chem Int Ed Engl, 2007. **46**(30): p. 5670-703.

70. H. Fong, I.C., D.H. Reneker, *Beaded nanofibers formed during electrospinning.* Polymer, 1999. **40**: p. 4585-4592.

71. Huang, Z.-M., et al., *A review on polymer nanofibers by electrospinning and their applications in nanocomposites.* Composites Science and Technology, 2003. **63**(15): p. 2223-2253.

72. Jo, S.B., et al., *Polymer blends with semiconducting nanowires for organic electronics.* Journal of Materials Chemistry, 2012. **22**(Copyright (C) 2013 American Chemical Society (ACS). All Rights Reserved.): p. 4244-4260.

73. Kalinov, K., et al., *Modification of electrospun poly(ε-caprolactone) mats by formation of a polyelectrolyte complex between poly(acrylic acid) and quaternized chitosan for tuning of their antibacterial properties.* European Polymer Journal, 2014. **50**(Copyright (C) 2014 American Chemical Society (ACS). All Rights Reserved.): p. 18-29.

74. Kim, I.L., et al., *Fibrous hyaluronic acid hydrogels that direct MSC chondrogenesis through mechanical and adhesive cues.* Biomaterials, 2013. **34**(Copyright (C) 2014 American Chemical Society (ACS). All Rights Reserved.): p. 5571-5580.

75. Laforgue, A. and L. Robitaille, *Production of Conductive PEDOT Nanofibers by the Combination of Electrospinning and Vapor-Phase Polymerization.* Macromolecules, 2010. **43**(9): p. 4194-4200.

76. Lee, C.H., et al., *Counterions-exchangeable, multifunctional polyelectrolyte fabrics.* Journal of Materials Chemistry, 2012. **22**(Copyright (C) 2014 American Chemical Society (ACS). All Rights Reserved.): p. 14656-14660.

77. Lee, H.J. and W.-G. Koh, *Hydrogel Micropattern-Incorporated Fibrous Scaffolds Capable of Sequential Growth Factor Delivery for Enhanced Osteogenesis of hMSCs.* Acs Applied Materials & Interfaces, 2014. **6**(Copyright (C) 2014 American Chemical Society (ACS). All Rights Reserved.): p. 9338-9348.

78. Lin, H.-Y., et al., *Pectin-chitosan-PVA nanofibrous scaffold made by electrospinning and its potential use as a skin tissue scaffold.* Journal of Biomaterials Science Polymer Edition, 2013. **24**(Copyright (C) 2014 American Chemical Society (ACS). All Rights Reserved.): p. 470-484.

79. Ma, G., et al., *Hyaluronic acid/chitosan polyelectrolyte complexes nanofibers prepared by electrospinning.* Materials Letters, 2012. **74**(0): p. 78-80.

80. Ner, Y., et al., *Electrospinning nanoribbons of a bioengineered silk-elastin-like protein (SELP) from water.* Polymer, 2009. **50**(24): p. 5828-5836.

81. Penchev, H., et al., *Novel Electrospun Nanofibers Composed of Polyelectrolyte Complexes.* Macromolecular Rapid Communications, 2008. **29**(8): p. 677-681.

82. Persano, L., et al., *Industrial Upscaling of Electrospinning and Applications of Polymer Nanofibers: A Review.* Macromolecular Materials and Engineering, 2013. **298**(5): p. 504-520.

83. Tan, S.H., et al., *Systematic parameter study for ultra-fine fiber fabrication via electrospinning process.* Polymer, 2005. **46**(16): p. 6128-6134.

84. Wang, X., et al., *Tuning hierarchically aligned structures for high-strength PMIA-MWCNT hybrid nanofibers.* Nanoscale, 2013. **5**(3): p. 886-889.

85. McKee, M.G., et al., *Solution Rheological Behavior and Electrospinning of Cationic Polyelectrolytes.* Macromolecules, 2006. **39**(Copyright (C) 2014 American Chemical Society (ACS). All Rights Reserved.): p. 575-583.

86. Schiffman, J.D., et al., *Crosslinking poly(allylamine) fibers electrospun from basic and acidic solutions.* J. Mater. Sci., 2013. **48**(Copyright (C) 2014 American Chemical Society (ACS). All Rights Reserved.): p. 7856-7862.

87. Subramanian, C., et al., *Chemical Cross-Linking of Highly Sulfonated Polystyrene Electrospun Fibers.* Macromolecules (Washington, DC, U. S.), 2012. **45**(Copyright (C) 2014 American Chemical Society (ACS). All Rights Reserved.): p. 3104-3111.

88. Chen, H., et al., *A Multifunctional Gold Nanoparticle/Polyelectrolyte Fibrous Nanocomposite Prepared from Electrospinning Process.* Materials Express, 2011. **1**(2): p. 154-159.

89. Gestos, A., et al., *Crosslinking neat ultrathin films and nanofibres of pH-responsive poly(acrylic acid) by UV radiation.* Soft Matter, 2010. **6**(Copyright (C) 2014 American Chemical Society (ACS). All Rights Reserved.): p. 1045-1052.

90. Katti, D.S., et al., *Bioresorbable nanofiber-based systems for wound healing and drug delivery: optimization of fabrication parameters.* J Biomed Mater Res B Appl Biomater, 2004. **70**(2): p. 286-96.

91. Lichtenegger, H.C., et al., *Zinc and mechanical prowess in the jaws of Nereis, a marine worm.* Proceedings of the National Academy of Sciences, 2003. **100**(16): p. 9144-9149.

92. Srivastava, A., et al., *Ragworm jaw-inspired metal ion cross-linking for improved mechanical properties of polymer blends.* Biomacromolecules, 2008. **9**(10): p. 2873-80.

93. Holten-Andersen, N., et al., *pH-induced metal-ligand cross-links inspired by mussel yield self-healing polymer networks with near-covalent elastic moduli.* Proceedings of the National Academy of Sciences, 2011. **108**(7): p. 2651-2655.

94. Monahan, J. and J.J. Wilker, *Specificity of metal ion cross-linking in marine mussel adhesives.* Chemical Communications, 2003(14): p. 1672-1673.

95. Smith, A.M., et al., *Robust cross-links in molluscan adhesive gels: testing for contributions from hydrophobic and electrostatic interactions.* Comp Biochem Physiol B Biochem Mol Biol, 2009. **152**(2): p. 110-7.

96. Werneke, S.W., et al., *The role of metals in molluscan adhesive gels.* J Exp Biol, 2007. **210**(Pt 12): p. 2137-45.

97. Braun, M., et al., *The relative contribution of calcium, zinc and oxidation-based cross-links to the stiffness of Arion subfuscus glue.* J Exp Biol, 2013. **216**(Pt 8): p. 1475-83.

98. Roma-Luciow, R., L. Sarraf, and M. Morcellet, *Concentration effects during the formation of poly (acrylic acid)-metal complexes in aqueous solutions.* Polym. Bull. (Berlin), 2000. **45**(Copyright (C) 2014 American Chemical Society (ACS). All Rights Reserved.): p. 411-418.

99. Roma-Luciow, R., L. Sarraf, and M. Morcellet, *Complexes of poly(acrylic acid) with some divalent, trivalent and tetravalent metal ions.* European Polymer Journal, 2001. **37**(Copyright (C) 2014 American Chemical Society (ACS). All Rights Reserved.): p. 1741-1745.

100. Pesonen, H., et al., *Density functional complexation study of metal ions with poly(carboxylic acid) ligands. Part 1. Poly(acrylic acid) and poly(α-hydroxy acrylic acid).* Polymer, 2005. **46**(Copyright (C) 2014 American Chemical Society (ACS). All Rights Reserved.): p. 12641-12652.

101. Guibal, E., T. Vincent, and R. Navarro, *Metal ion biosorption on chitosan for the synthesis of advanced materials.* J. Mater. Sci., 2014. **49**(Copyright (C) 2014 American Chemical Society (ACS). All Rights Reserved.): p. 5505-5518.

102. Roma, R., M. Morcellet, and L. Sarraf, *Elaboration of cerium oxide from polyacrylate–metal complexes.* Materials Letters, 2005. **59**(8–9): p. 889-893.

103. Mentbayeva, A., et al., *Polymer-Metal Complexes in Polyelectrolyte Multilayer Films as Catalysts for Oxidation of Toluene.* Langmuir, 2012. **28**(Copyright (C) 2014 American Chemical Society (ACS). All Rights Reserved.): p. 11948-11955.

104. Rahim, M.A., et al., *Metal Ion-Enriched Polyelectrolyte Complexes and Their Utilization in Multilayer Assembly and Catalytic Nanocomposite Films.* Langmuir, 2012. **28**(Copyright (C) 2014 American Chemical Society (ACS). All Rights Reserved.): p. 8486-8495.

105. Huang, X., et al., *Formation and Tunable Disassembly of Polyelectrolyte-Cu2+ Layer-by-Layer Complex Film.* Langmuir, 2013. **29**(Copyright (C) 2014 American Chemical Society (ACS). All Rights Reserved.): p. 12959-12968.

106. Huebsch, E., et al., *Multivalent Ion/Polyelectrolyte Exchange Processes in Exponentially Growing Multilayers.* Langmuir, 2005. **21**(Copyright (C) 2014 American Chemical Society (ACS). All Rights Reserved.): p. 3664-3669.

107. Ma, G., et al., *Freeze-dried chitosan-sodium hyaluronate polyelectrolyte complex fibers as tissue engineering scaffolds.* New Journal of Chemistry, 2014. **38**(3): p. 1211-1217.

108. Yancheva, E., et al., *Tuning of the Surface Biological Behavior of Poly(L-lactide)-Based Electrospun Materials by Polyelectrolyte Complex Formation.* Biomacromolecules, 2010. **11**(Copyright (C) 2014 American Chemical Society (ACS). All Rights Reserved.): p. 521-532.

109. Kawashita, M., et al., *Apatite-forming ability of carboxyl group-containing polymer gels in a simulated body fluid.* Biomaterials, 2003. **24**(14): p. 2477-84.

110. McCluskey, P.H., R.L. Snyder, and R.A. Condrate Sr, *Infrared spectral studies of various metal polyacrylates.* Journal of Solid State Chemistry, 1989. **83**(2): p. 332-339.

111. Guibal, E., *Interactions of metal ions with chitosan-based sorbents: a review.* Separation and Purification Technology, 2004. **38**(1): p. 43-74.

112. Guibal, E., E. Touraud, and J. Roussy, *Chitosan Interactions with Metal Ions and Dyes: Dissolved-state vs. Solid-state Application.* World Journal of Microbiology and Biotechnology, 2005. **21**(6-7): p. 913-920.

113. Trimukhe, K.D. and A.J. Varma, *Metal complexes of crosslinked chitosans: Correlations between metal ion complexation values and thermal properties.* Carbohydrate Polymers, 2009. **75**(1): p. 63-70.

114. Varma, A.J., S.V. Deshpande, and J.F. Kennedy, *Metal complexation by chitosan and its derivatives: a review.* Carbohydrate Polymers, 2004. **55**(1): p. 77-93.

115. Gliemann, G., *K. Nakamoto: Infrared and Raman Spectra of Inorganic and Coordination Compounds. John Wiley and Sons, New York, Chichester, Brisbane, Toronto 1978. 3. Aufl., XV, 448 Seiten mit 109 Abbildungen und 95 Tabellen. Preis: $ 31,15.* Berichte der Bunsengesellschaft für physikalische Chemie, 1978. **82**(11): p. 1263-1263.

116. Nickolov, Z., et al., *Raman and IR study of cobalt acetate dihydrate.* Journal of Molecular Structure, 1995. **354**(2): p. 119-125.

117. Konradi, R. and J. Rühe, *Interaction of Poly(methacrylic acid) Brushes with Metal Ions: An Infrared Investigation.* Macromolecules, 2004. **37**(18): p. 6954-6961.

118. Badawy, M.E.I. and A.F. El-Aswad, *Insecticidal activity of chitosans of different molecular weights and chitosan-metal complexes against cotton leafworm Spodoptera littoralis and oleander aphid Aphis nerii.* Plant Protection Science, 2012. **48**(3): p. 131-141.

119. Carneiro, J., et al., *Chitosan-based self-healing protective coatings doped with cerium nitrate for corrosion protection of aluminum alloy 2024.* Progress in Organic Coatings, 2012. **75**(1–2): p. 8-13.

120. Penchev, H., et al., *Novel electrospun nanofibers composed of polyelectrolyte complexes.* Macromolecular Rapid Communications, 2008. **29**(Copyright (C) 2014 American Chemical Society (ACS). All Rights Reserved.): p. 677-681.

121. Chunder, A., et al., *Fabrication of ultrathin polyelectrolyte fibers and their controlled release properties.* Colloids and Surfaces B: Biointerfaces, 2007. **58**(2): p. 172-179.

122. Jeong, S.I., et al., *Electrospun chitosan-alginate nanofibers with in situ polyelectrolyte complexation for use as tissue engineering scaffolds.* Tissue Eng Part A, 2011. **17**(1-2): p. 59-70.

123. Dong, F., et al., *Fabrication of semiconductor nanostructures on the outer surfaces of polyacrylonitrile nanofibers by in-situ electrospinning.* Materials Letters, 2007. **61**(11–12): p. 2556-2559.

124. Su, P., et al., *Electrospinning of chitosan nanofibers: The favorable effect of metal ions.* Carbohydrate Polymers, 2011. **84**(1): p. 239-246.

125. *Electrospinning of polyacrylonitrile (PAN) solution: Effect of conductive additive and filler on the process.* eXPRESS Polymer Letters, 2009.

126. Zhang, C.-L. and S.-H. Yu, *Nanoparticles meet electrospinning: recent advances and future prospects.* Chemical Society Reviews, 2014. **43**(13): p. 4423-4448.

127. Zhang, P.-p., et al., *Self-assembled core-shell Fe3O4@SiO2 nanoparticles from electrospun fibers.* Materials Research Bulletin, 2013. **48**(9): p. 3058-3064.

128. Ding, Q., Y.-E. Miao, and T. Liu, *Morphology and Photocatalytic Property of Hierarchical Polyimide/ZnO Fibers Prepared via a Direct Ion-exchange Process.* Acs Applied Materials & Interfaces, 2013. **5**(Copyright (C) 2014 American Chemical Society (ACS). All Rights Reserved.): p. 5617-5622.

129. Ren, T., et al., *Polyacrylonitrile/polybenzoxazine-based Fe3O4@carbon nanofibers: hierarchical porous structure and magnetic adsorption property.* Journal of Materials Chemistry, 2012. **22**(31): p. 15919-15927.

130. Zhang, D., et al., *Electrospun polyacrylonitrile nanocomposite fibers reinforced with Fe3O4 nanoparticles: Fabrication and property analysis.* Polymer, 2009. **50**(17): p. 4189-4198.

131. Chen, J., M. Liu, and S. Chen, *Synthesis and characterization of thermo- and pH-sensitive kappa-carrageenan-g-poly(methacrylic acid)/poly(N,N-diethylacrylamide) semi-IPN hydrogel.* Materials Chemistry and Physics, 2009. **115**(1): p. 339-346.

132. Yoshida, R., et al., *Positive thermosensitive pulsatile drug release using negative thermosensitive hydrogels.* Journal of Controlled Release, 1994. **32**(1): p. 97-102.

133. Ritger, P.L. and N.A. Peppas, *A simple equation for description of solute release II. Fickian and anomalous release from swellable devices.* Journal of Controlled Release, 1987. **5**(1): p. 37-42.

134. Higuchi, T., *Mechanism of sustained-action medication. Theoretical analysis of rate of release of solid drugs dispersed in solid matrices.* Journal of Pharmaceutical Sciences, 1963. **52**(12): p. 1145-1149.

135. Michaylova, V. and P. Ilkova, *Photometric determination of micro amounts of calcium with arsenazo III.* Analytica Chimica Acta, 1971. **53**(1): p. 194-198.

136. Onishi, H. and K. Sekine, *Spectrophotometric determination of zirconium, uranium, thorium and rare earths with arsenazo III after extractions with thenoyltrifluoroacetone and tri-n-octylamine.* Talanta, 1972. **19**(4): p. 473-8.

137. Savvin, S.B., *Analytical applications of arsenazo III—II: Determination of thorium, uranium, protactinium, neptunium, hafnium and scandium.* Talanta, 1964. **11**(1): p. 1-6.

138. Yokoi, T., M. Kawashita, and C. Ohtsuki, *Biomimetic mineralization of calcium phosphates in polymeric hydrogels containing carboxyl groups.* Journal of Asian Ceramic Societies, 2013. **1**(2): p. 155-162.